UNIVERSITAT POLITÈCNICA DE VALÈNCIA

Scenario-Based Model Predictive Control for Systems with Correlated Uncertainties

Doctoral Thesis

Author: Edwin Alonso González Querubín

Advisors: Prof. Javier Sanchis Sáez
Prof. José Vicente Salcedo Romero de Ávila

March 2024

A Dios.

A mamá, por darme tanto amor y por su infinita fe en mí.

My sincere gratitude to my advisors, Prof. Javier Sanchis and Prof. José Vicente Salcedo, for sharing their expertise with me, and even more for their encouragement and dedication during these years.

Abstract

The vast majority of real-world processes have inherent uncertainties, which, when considered in the modelling process, can provide a representation that most accurately describes the behaviour of the real process. Such uncertainties may be parametric, due to the nature of the process, and/or additive, due to external disturbances. In most practical cases, these are considered to have stochastic behaviour and their descriptions as probability distributions are known.

Stochastic model predictive control algorithms are developed to control processes with uncertainties of a stochastic nature, where the knowledge of the statistical properties of the uncertainties is exploited by including it in the optimal control problem (OCP) statement. Contrary to other model predictive control (MPC) schemes, hard constraints are relaxed by reformulating them as probabilistic constraints to reduce conservatism. That is, violations of the original hard constraints are allowed, but such violations must not exceed a permitted level of risk.

The non-convexity of such probabilistic constraints renders the optimisation problem computationally unmanageable, thus most stochastic MPC strategies in the literature differ in how they deal with such constraints and uncertainties to turn the problem computationally tractable. On the one hand, there are deterministic strategies that, offline, convert probabilistic constraints into new deterministic ones, using the propagation of uncertainties along the prediction horizon to tighten the original hard constraints.

Scenario-based approaches, on the other hand, use the uncertainty information to randomly generate, at each sampling instant, a set of possible evolutions of

uncertainties over the prediction horizon. In this fashion, they convert the probabilistic constraints into a set of deterministic constraints that must be fulfilled for all the scenarios generated. These strategies stand out for their ability to include real-time updated uncertainty information. However, this advantage comes with inconveniences such as computational effort, which grows as the number of scenarios does, and the undesired effect on the optimisation problem caused by scenarios with a low probability of occurrence when a small set of scenarios is used.

The aforementioned challenges steered this thesis toward stochastic scenario-based MPC approaches, and yielded three main contributions. The first one consists of a comparative study of an algorithm from the deterministic group with another one from the scenario-based group, where a special emphasis is made on how each of them deals with uncertainties, transforms the probabilistic constraints and on the structure of the optimisation problem, as well as pointing out their most outstanding aspects and challenges. Furthermore, the performances of these algorithms are analysed and compared by means of numerical examples, and their results provide the probabilistic feasibility of the optimisation problem, among others.

The second contribution is a new proposal for a MPC algorithm, which is based on conditional scenarios, developed for linear systems with parametric and/or additive uncertainties that are correlated. This scheme exploits the existence of such correlation to convert a large initial set of scenarios into a smaller one with their probabilities of occurrence, which preserves the characteristics of the initial set. The reduced set is used in an OCP in which the predictions of the system states and inputs are penalised according to the probabilities of the scenarios that compose them, giving less importance to the scenarios with lower probabilities of occurrence. Two OCP structures are proposed, the first one considers the whole reduced set, while the second one, in order to improve the cost index and reduce the computational expense, uses sampling and discarding approaches to exclude from the total set of constraints those related to scenarios with lower probability of occurrence.

The third contribution consists of a procedure for the implementation of the new MPC algorithm as an energy manager in a microgrid composed of the main electricity grid, renewable photovoltaic and wind energy sources, an energy storage system, and connected loads, in which the forecasts of renewables and loads are correlated.

Resumen

La gran mayoría de procesos del mundo real tienen incertidumbres inherentes, las cuales, al ser consideradas en el proceso de modelado, se puede obtener una representación que describa con la mayor precisión posible el comportamiento del proceso real. Tales incertidumbres pueden ser paramétricas, debido a la naturaleza del proceso, y/o aditivas, debido a perturbaciones externas. En la mayoría de casos prácticos, se considera que éstas tienen un comportamiento estocástico y sus descripciones como distribuciones de probabilidades son conocidas.

Las estrategias de control predictivo estocástico están desarrolladas para el control de procesos con incertidumbres de naturaleza estocástica, donde el conocimiento de las propiedades estadísticas de las incertidumbres es aprovechado al incluirlo en el planteamiento de un problema de control óptimo (OCP, del inglés Optimal Control Problem). En éste, y contrario a otros esquemas de control predictivo (MPC, del inglés Model Predictive Control), las restricciones duras son relajadas al reformularlas como restricciones de tipo probabilísticas con el fin de reducir el conservadurismo. Esto es, se permiten las violaciones de las restricciones duras originales, pero tales violaciones no deben exceder un nivel de riesgo permitido. La no-convexidad de tales restricciones probabilísticas hacen que el problema de optimización sea computacionalmente inmanejable, por lo que la mayoría de las estrategias de MPC estocástico en la literatura se diferencian en la forma en que abordan tales restricciones y las incertidumbres, para volver el problema computacionalmente manejable. Por un lado, están las estrategias deterministas que, fuera de línea, convierten las restricciones probabilísticas en unas nuevas de tipo deterministas, usando la propagación de las incertidumbres a lo largo del horizonte de predicción para ajustar las restricciones duras originales.

Por otra parte, las estrategias basadas en escenarios usan la información de las incertidumbres para, en cada instante de muestreo, generar de forma aleatoria un conjunto de posibles evoluciones de éstas a lo largo del horizonte de predicción. De esta manera, convierten las restricciones probabilísticas en un conjunto de restricciones deterministas que deben cumplirse para todos los escenarios gene-

rados. Estas estrategias se destacan por su capacidad de incluir en tiempo real información actualizada de las incertidumbres. No obstante, esta ventaja genera inconvenientes como su gasto computacional, el cual aumenta conforme lo hace el número de escenarios y; por otra parte, el efecto no deseado en el problema de optimización, causado por los escenarios con baja probabilidad de ocurrencia, cuando se usa un conjunto de escenarios pequeño.

Los retos mencionados anteriormente orientaron esta tesis hacia los enfoques de MPC estocástico basado en escenarios, produciendo tres contribuciones principales. La primera consiste en un estudio comparativo de un algoritmo del grupo determinista con otro del grupo basado en escenarios; en donde se hace un especial énfasis en cómo cada uno de estos aborda las incertidumbres, transforma las restricciones probabilísticas y en la estructura de su problema de optimización, además de señalar sus aspectos más destacados y desafíos. Asimismo, los desempeños de estos algoritmos son analizados y comparados por medio de ejemplos numéricos y en sus resultados se provee la factibilidad probabilística del problema de optimización, entre otros.

La segunda contribución es una nueva propuesta de algoritmo MPC, el cual se basa en escenarios condicionales, diseñado para sistemas lineales con incertidumbres paramétricas y/o aditivas que están correlacionadas. Este esquema aprovecha la existencia de tal correlación para convertir un conjunto de escenarios inicial de gran tamaño en un conjunto de escenarios más pequeño con sus probabilidades de ocurrencia, el cual conserva las características del conjunto inicial. El conjunto reducido es usado en un OCP en el que las predicciones de los estados y entradas del sistema son penalizadas de acuerdo con las probabilidades de los escenarios que las componen, dando menor importancia a los escenarios con menores probabilidades de ocurrencia. Se proponen dos estructuras de OCP, en la primera se considera todo el conjunto reducido, mientras que en la segunda, con el fin de mejorar el índice de coste y reducir el gasto computacional, se usan enfoques de muestreo y descarte para excluir del conjunto total de restricciones, las relacionadas con los escenarios con menor probabilidad de ocurrencia.

La tercera contribución consiste en un procedimiento para la implementación del nuevo algoritmo MPC como gestor de la energía en una microrred compuesta por la red eléctrica principal, fuentes de energía renovables fotovoltaica y eólica, un sistema de almacenamiento de energía, y cargas conectadas; en la que las previsiones de las energías renovables y las cargas están correlacionadas.

Resum

La gran majoria de processos del món real tenen incerteses inherents, les quals, en ser considerades en el procés de modelatge, es pot obtenir una representació que descriga amb la major precisió possible el comportament del procés real. Tals incerteses poden ser paramètriques, a causa de la naturalesa del procés, i/o additives, a causa de pertorbacions externes. En la majoria de casos pràctics, es considera que aquestes tenen un comportament estocàstic i les seues descripcions com a distribucions de probabilitats són conegudes.

Les estratègies de control predictiu estocàstic estan desenvolupades per al control de processos amb incerteses de naturalesa estocàstica, on el coneixement de les propietats estadístiques de les incerteses és aprofitat en incloure'l en el plantejament d'un problema de control òptim (OCP, de l'anglès Optimal Control Problem). En aquest, i contrari a altres esquemes de control predictiu (MPC, de l'anglès Model Predictive Control), les restriccions dures són relaxades en reformulades com a restriccions de tipus probabilístiques amb la finalitat de reduir el conservadorisme. Això és, es permeten les violacions de les restriccions dures originals, però tals violacions no han d'excedir un nivell de risc permès. La no-convexitat de tals restriccions probabilístiques fan que el problema d'optimització siga computacionalment immanejable, per la qual cosa la majoria de les estratègies de MPC estocàstic en la literatura es diferencien en la forma en què aborden tals restriccions i les incerteses, per a tornar el problema computacionalment manejable. D'una banda, estan les estratègies deterministes que, fora de línia, converteixen les restriccions probabilístiques en unes noves de tipus deterministes, usant la propagació de les incerteses al llarg de l'horitzó de predicció per a ajustar les restriccions dures originals.

D'altra banda, les estratègies basades en escenaris usen la informació de les incerteses per a, en cada instant de mostreig, generar de manera aleatòria un conjunt de possibles evolucions d'aquestes al llarg de l'horitzó de predicció. D'aquesta

manera, converteixen les restriccions probabilístiques en un conjunt de restriccions deterministes que s'han de complir per a tots els escenaris generats. Aquestes estratègies es destaquen per la seua capacitat d'incloure en temps real informació actualitzada de les incerteses. No obstant això, aquest avantatge genera inconvenients com la seua despesa computacional, el qual augmenta conforme ho fa el nombre d'escenaris i; d'altra banda, l'efecte no desitjat en el problema d'optimització, causat pels escenaris amb baixa probabilitat d'ocurrència, quan s'usa un conjunt d'escenaris xicotet.

Els reptes esmentats anteriorment van orientar aquesta tesi cap als enfocaments de MPC estocàstic basat en escenaris, produint tres contribucions principals. La primera consisteix en un estudi comparatiu d'un algorisme del grup determinista amb un altre del grup basat en escenaris; on es fa un especial èmfasi en com cadascun d'aquests aborda les incerteses, transforma les restriccions probabilístiques i en l'estructura del seu problema d'optimització, a més d'assenyalar els seus aspectes més destacats i desafiaments. Així mateix, els acompliments d'aquests algorismes són analitzats i comparats per mitjà d'exemples numèrics i en els seus resultats es proveeix la factibilitat probabilística del problema d'optimització, entre altres.

La segona contribució és una nova proposta d'algorisme MPC, el qual es basa en escenaris condicionals, dissenyat per a sistemes lineals amb incerteses paramètriques i/o additives que estan correlacionades. Aquest esquema aprofita l'existència de tal correlació per a convertir un conjunt d'escenaris inicial de gran grandària en un conjunt d'escenaris més xicotet amb les seues probabilitats d'ocurrència, el qual conserva les característiques del conjunt inicial. El conjunt reduït és usat en un OCP en el qual les prediccions dels estats i entrades del sistema són penalitzades d'acord amb les probabilitats dels escenaris que les componen, donant menor importància als escenaris amb menors probabilitats d'ocurrència. Es proposen dues estructures de OCP, en la primera es considera tot el conjunt reduït, mentre que en la segona, amb la finalitat de millorar l'índex de cost i reduir la despesa computacional, s'usen enfocaments de mostreig i descarte per a excloure del conjunt total de restriccions, les relacionades amb els escenaris amb menor probabilitat d'ocurrència.

La tercera contribució consisteix en un procediment per a la implementació del nou algorisme MPC com a gestor de l'energia en una microxarxa composta per la xarxa elèctrica principal, fonts d'energia renovables fotovoltaica i eòlica, un sistema d'emmagatzematge d'energia, i càrregues connectades; en la qual les previsions de les energies renovables i les càrregues estan correlacionades.

Abbreviations

BESS	Battery Energy Storage System
BNN	Bayesian Neural Network
CC	Chance Constraint
CC-MPC	Chance-Constrained MPC
CDF	Cumulative Distribution Function
CS	Conditional Scenario
CSB-MPC	Conditional Scenario-Based MPC
DER	Distributed Energy Resources
EMS	Energy Management System
ESS	Energy Storage System
EVP	Eigenvalue Problem
HVAC	Heating, Ventilation and Air Conditioning
i.i.d.	Independent and Identically Distributed
LMI	Linear Matrix Inequality
LQR	Linear-Quadratic Regulator
LTI	Linear Time-Invariant
MG	Microgrid
MHC	Moving Horizon Control
MILP	Mixed-Integer Linear Programming
MIQP	Mixed Integer Quadratic Program
MPC	Model Predictive Control
MPC n/c	Classic MPC without Constraints
MPC w/c	Classic MPC with Constraints
MPT	Multi-Parametric Toolbox

OCP	Optimal Control Problem
PRS	Probabilistic Reachable Set
PV	Photovoltaic
QP	Quadratic Programming
RES	Renewable Energy Source
RH	Receding Horizon
RHC	Receding Horizon Control
RMPC	Robust MPC
SAA	Sample Average Approximation
SCMPC	Scenario-Based MPC
SMILP	Stochastic Mixed-Integer Linear Programming
SOC	State of Charge
SRD	Scenario Reduction Based on Probability Distances
WT	Wind Turbine

Contents

Chapter 1

Introduction

This chapter presents an overview of the research conducted and how this led to the development of this thesis. In the first section, some of the potentialities of model predictive control (MPC) are briefly outlined, followed by how the uncertainties present in the system are addressed by some of its strategies, and how the research conducted to answer these questions motivated the choice of stochastic MPC, specifically scenario-based MPC, as the main topic of this thesis. The second section presents the objectives of this thesis. In the third section, a literature review of stochastic MPC approaches, and some applications as energy managers in the microgrids field. In the fourth section, the main contributions of this thesis and their importance are discussed.

1.1 Motivation

Model Predictive Control (MPC) is widely used to control industrial processes [1]–[3]; in fields such as automation and robotics [4]–[8], energy management in buildings and renewable energies [9]–[14], and in many other areas [15]–[17]. This is because of its main feature of predicting, using a mathematical model of the process, the future behaviour of the real process, as well as the simplicity of its application and its robustness in controlling various complex processes, with many inputs and outputs, and with the possibility of taking into account their constraints.

Based on updated information on process variables and the process model, at each sampling time, the MPC makes predictions of future process behaviour over a time window referred to as the prediction horizon [18]–[20]. These predictions, depending on future controls (decision variables), are included in a cost function to solve a constrained open-loop Optimal Control Problem (OCP); providing the sequence of optimal controls that minimise this function as a solution. Then, using the Receding Horizon principle (RH) [21], the first element, corresponding to the input calculated for the current instant, of the sequence of future controls is applied to the process, and the rest of the elements are discarded. This is because once a sample period has elapsed, the OCP is solved again with updated information, and the RH concept is applied again.

One significant issue when using a deterministic MPC is its need for an accurate model of the process to be controlled. The complexity of the dynamics of most real-life processes does not allow them to be represented by a fixed mathematical model since various types of uncertainties are always present. This can be problematic, as using an inaccurate model can lead to erroneous predictions that are far from the actual behaviour of the process, thus affecting its performance and, more importantly, the stability and feasibility of the control system [18], [22]. Robust MPC and stochastic MPC approaches take into account process uncertainties by incorporating them into the model used for prediction. Thus, they are more appropriate strategies for uncertain systems.

Robust MPC (RMPC) approaches [22]–[25] are developed to control systems with uncertainties, which are unknown but are bounded, and their limits are known. Under this premise, a family of models is constructed, in which one of them is an approximate representation of the real process; thereby forming a polytopic system that contains the nominal one. Thus, an OCP is formulated for all vertices of the polytope, whose predicted trajectories form a band around that of the nominal model. The sequence of optimal controls is computed by minimising the worst-case (*minimax* problem), subject to constraints that must be met for all

cases. Implementing these algorithms is computationally demanding, and in some cases prohibitive, due to worst-case online optimisation, which does not always occur, thus making them conservative.

On the other hand, stochastic MPC strategies [20], [24], [26]–[29] consider that the uncertainties, that are not required to be bounded, are of a stochastic nature and the information about how they are distributed is considered as known. This statistical information knowledge is exploited to solve an OCP, with an expected value cost function, and where hard constraints on states and inputs, commonly the former, are reformulated as probabilistic constraints, so that they must be satisfied at least at a desired probability level. Such constraints relaxation, in probabilistic terms, reduces the worst-case conservatism, as a transgression of the constraints is allowed within a permitted probability level.

During the early stage of this research, it was noted that in the topic related to stochastic MPC, most algorithms are categorised into two major groups: the deterministic group and the scenario-based group. This led to carrying out a comparative study of two MPCs, each from one group, pointing out the advantages and challenges of each. The scenario-based MPC, has outstanding aspects such as the possibility to include online the updated statistical information related to the uncertainties, and the ability to consider uncertainties historical data, in case the analytical expressions of their probabilities distributions are unavailable. Challenges include, on the one side, the computational burden that grows as the number of scenarios employed to solve the OCP does and, on the other side, the effect that unlikely scenarios have on the quality of the optimal solution when a reduced number of scenarios are considered in the OCP.

In most practical applications the uncertainties are considered stochastic and their probabilistic characteristics are known. It is considered, therefore, that this information can be exploited in the formulation of the OCP. The above motivated to focus this thesis on the area of stochastic MPC, specifically the scenario-based MPC, in view of its highlights and improvement opportunities mentioned above.

Consequently, this thesis explores how the stochastic MPC works, how it addresses the uncertainties information and what are its strengths and weaknesses; how a scenario-based MPC can take into account the knowledge of system uncertainties when there is a correlation between some of them, in order to enhance the probability of constraint satisfaction; and how to use a scenario-based MPC for energy management in a microgrid where some power generation and demand forecasts are correlated.

1.2 Thesis Objectives

The main objective of this thesis is to propose a scenario-based model predictive control approach suitable for systems with correlated uncertainties, which leverages the knowledge of these features to enhance the probability of satisfying the constraints.

The defined specific objectives for the general objective fulfilment are listed below:

1. Conduct a comparative study between two stochastic MPC techniques of the deterministic and scenario-based groups to determine the most salient aspects of these strategies and their possible improvement opportunities.
2. Propose a new scenario-based MPC algorithm that considers the correlation between system uncertainties to improve constraint satisfaction.
3. Develop a procedure to adapt the proposed MPC algorithm as a solution to energy management in the field of microgrids.
4. Conduct a case study of a microgrid including photovoltaic and wind generation, and energy storage system, with correlation between generation and demand, to validate the effectiveness of the proposed MPC as an energy management system.

1.3 Literature Review

As mentioned in section 1.1, stochastic model predictive control strategies [26]–[29] were conceived for systems in which their uncertainties are considered to be stochastic in nature, and whose features such as the distribution types of these random variables are considered to be known. Such uncertainties can be either parametric [30], [31], due to external disturbances [28], [32]–[34] or both [35]–[38], and may be bounded [35], [38], [39] (necessary in most strategies to ensure the feasibility of the OCP and the stability of the system [27], [40]) or not [32], [34], [41], [42], and features as their probability distributions shapes are usually considered Gaussian type, and their sequences in time are generally supposed to be independent and identically distributed (i.i.d.).

The stochastic MPC uses this statistical information to solve an optimal control problem (OCP) whose cost function to be minimised is a quadratic cost based on the expected value. In this function, the predictions of the states, control actions and the terminal state, the latter related to system stability [40], are penalised.

Hard constraints on system states and inputs, usually the first, are reformulated as probabilistic constraints (chance constraints) where they are required to be satisfied at least with a user-defined minimum desired probability level. Considering such detailed information on uncertainties in the formulation of this OCP provides it robustness, and, on the other side, relaxing the constraints in probabilistic terms reduces the conservatism [24], [43] of the worst-case, in relation to the robust MPC, by allowing its transgression within a permitted probability level.

Most stochastic MPC approaches in the literature can be classified into two groups [29], [41] depending on how the information related to the uncertainties is addressed in the OCP formulation. These are, the deterministic group strategies [39], [42], [44], [45] and; on the other side, the group of scenario-based (or randomised) strategies [35], [36], [41], [46].

The deterministic approaches adopt an OCP in which state constraints are formulated as chance or probabilistic constraints (CC), where it is required that the probability of constraint fulfilment in the states must not be lower than a desired level. Due to the non-convexity of these chance constraints, they can render the problem computationally intractable, and therefore, they are generally converted into equivalent deterministic and convex ones. For this purpose, the first two statistical moments knowledge of uncertainties (random variables) is exploited to calculate their propagation over the prediction horizon and use them for tightening of the original hard constraints, this offline. Thus, the chance-constrained OCP, it becomes a deterministic one, in which the cost function, based on the expected value, is replaced by one that only contains the predictions of the nominal trajectories of the states and inputs, and which is subject to the new deterministic constraints, which are functions of these states and inputs. As a result, the OCP is similar to a classical MPC in both structure and computational effort.

The scenario-based approaches, conversely, make use of statistical data on uncertainties and a random number generator to online, i.e., at each sampling interval, generate a set of possible evolutions, so-called scenarios [47], [48], of the uncertainties along the prediction horizon. In this way, these scenarios are incorporated into a conventional convex OCP, where the expected value of the cost function is approximated to the sample average of all states and inputs predicted trajectories, obtained from all the generated scenarios. The probabilistic constraints are substituted by the original hard constraints, that must be fulfilled for all of these predicted states and inputs. The number of realisations to be employed to solve the OCP determines the quality of the solution or its closeness to the original stochastic MPC problem. This number can be computed as a function [36], [47],

[48] of a defined desired probability level of constraint satisfaction and the number of decision variables of the OCP, among others.

Some successful practical applications involving scenario-based schemes include the control of processes such as comfort or thermal management in buildings [13], autonomous vehicles [49], water resources management [16], [17] and management of microgrids [14], [50], among others. The online scenario generation provides these schemes with the flexibility to include new information or changes in uncertainties, as well as using historical data when their probability distributions are unknown or do not have classical distribution shapes.

However, as discussed in [29], [36], the mentioned advantages of scenario-based MPCs lead to, on one side, a larger computational overhead due to the time it takes for the OCP to be solved, increasing or decreasing in line with the number of scenarios for which all constraints must be fulfilled, and that for very large values may become intractable. On the other side, there is the impact that the unlikely scenarios have on the OCP solution if few scenarios are employed. This is due to the possibility that, given the *randomness* in the scenarios selection, many of them may be far from the system reality and, as a result, the calculated optimal controls may lead to a wrong closed-loop system behaviour.

In random convex programs [51], [52], the number of scenarios required such that the optimal solutions obtained by the OCP meet the original probabilistic constraints is calculated regarding the desired probability of satisfying the constraints, the number of decision variables in the OCP, and a defined very low probability of a *catastrophic* event occurring, i.e. the probability that such probabilistic constraints are not satisfied. Such an undesired event may occur if for a limited number of scenarios most of them are improbable, but a reduction in this level of risk leads to an increase in the number of scenarios.

Sampling and discarding approaches [52] improve the cost function while maintaining a minimum allowable level of constraint satisfaction. This is achieved for a reasonably large number of generated scenarios, of which some are discarded from the OCP constraints. Both the numbers of scenarios to be considered and discarded from the OCP constraints are calculated as a function of the desired probability level of constraints satisfaction, the probability level of a bad event occurring and the number of decision variables. In [36], a reduced sample-removal pair is proposed for MPC where the probabilistic constraints are interpreted as the average-in-time probability of constraint violations. By defining an acceptable level of risk of constraint violation and a parameter associated with the dimension of the unconstrained subspace of the search space, a given pair consisting of the minimum number of scenarios to consider in the cost function and a maximum

number of scenarios to discard from the constraints in the states is calculated. Nevertheless, these sampling-discarding approaches can lead to an increase in the time taken to solve the problem as they first require a large number of scenarios to maintain the level of constraint satisfaction in the absence of the discarded scenarios. Secondly, the unlikely scenarios to be excluded from the constraints must be identified, so a suitable algorithm [52] is also required to identify them, which, depending on their level of greed, could lead to a computationally prohibitive OCP to solve.

Others approaches are the scenario tree-based MPC [53]–[57], which are based on multistage stochastic optimisation, in which a tree-shaped scenario structure is constructed, through a set of realisations of uncertainties. Each branch or node in the tree depicts a specific future instant, having the associated state, control action and the probability of being reached, given the uncertainty. Starting from the current state and time, and following the temporal order, each possible path in this tree is referred to as a scenario, in which each has its own control actions, thereby augmenting the number of decision variables. In [57], one these approaches is integrated together with the sampling-discarding [36] to improve solution time by considering only a small number of scenarios that correspond to those with the highest probability of occurrence. In [55] presents an approach that uses the Gaussian regression process to learn the uncertainty of the system, dependent on the state-input relationship, and is adapted to a scenario tree algorithm. In [56] an adaptive scenario tree approach is introduced for nonlinear systems where, both, state and input-dependent uncertainties are assumed, where a Bayesian neural network (BNN) is required to model the uncertain dynamics of the system by using historical data on its trajectory.

A combination of deterministic and scenario-based approaches are considered in [32], [34], [38], [41], for systems with purely additive uncertainties in [32], [34], [41], where the sequences of uncertainties are assumed to be generally correlated in time, and not independent and identically distributed (i.i.d.) in time as in most stochastic algorithms. In [41], features such as the time correlation of uncertainties and the concept of scenarios are leveraged to, offline, calculate so-called probabilistic reachable sets (PRS) [58] for constraints tightening, which, applying the concept of error tubes in MPC [21], are used to formulate the OCP. In [32], both the mean and the covariance of the uncertainty vector are assumed to be bounded; thereby such considerations are used to tighten the constraints by calculating PRSs applying the concept of the correlation bound. A state initialisation technique is proposed in [34] to, according to a specified probability level, enforce that the actual state remains within a PRS and close to the nominal state. The varied presumptions about the uncertainties used offline to perform

the constraint tightening by the above techniques improve the online computational effort, giving them similar characteristics to those of the MPCs from the first group. However, the potential of scenario-based approaches, such as the online inclusion of updated uncertainty information, would be wasted, besides their implementation is only possible for systems with additive uncertainties.

A field in which the characteristics of MPCs, such as their prediction capability and robustness, have been most successfully exploited is that of microgrids; in particular stochastic MPC approaches, given the inherent uncertainties in these systems. The growing energy demand [59], whether due to the use of new technologies by consumers, population growth, economic expansion or climate change impacts increasingly on the supply capacity of the main network, resulting in poor service quality, sudden power outages, and increased electricity prices, with high fluctuation associated with existing demand or drought periods. These factors have generated the need for users of the electricity service to explore other energy sources, either to mitigate such technical issues and/or to reduce energy consumption from the main grid for electricity cost savings or reduce dependence on the distribution network [60]. Some examples of these energy types are renewable energy sources (RES) such as photovoltaic (PV) generators and wind turbines (WT), and controllable generators like fuel cells and diesel engines. The integration of these technologies together with technologies as energy storage systems (ESS) [61]–[63], such as battery systems, supercapacitors or flywheels among others, is referred to as distributed energy resources (DER) [60], [64].

A microgrid (MG) [64], [65] of small or large size can generally be defined as a system consisting of several DERs and multiple loads, which extracts or sends (to generate economic benefits) energy if connected to the main grid, or is self-sufficient if not connected (isolated). The choice of the MG energy management system (EMS) is essential since it is responsible for managing demand autonomously in real-time by coordinating its DERs.

Compared to conventional controllers, an EMS based on a MPC strategy [66], [67] considerably improves the efficiency of the MG due to its robustness and the fact that in each control period, it uses a model of the MG which can incorporate updated RES and demand forecasts to predict its future behaviour within a time window in the range of minutes up to months. These predictions are considered in a constrained OCP, in which the cost of energy to be consumed from the main grid is generally minimised, yielding the necessary future controls for optimal MG operation; where obeying the receding horizon principle, only the first element of the sequence of controls is applied, executing the OCP again at the next instant.

As mentioned in section 1.1, an important issue when using a deterministic MPC [68], [69] is the accuracy of the employed MG model. RES and demand forecasts, which are related to fluctuating weather conditions, have inherent uncertainties [70] that might produce predictions far from the actual behaviour of the MG, leading to inefficient use of DERs and affecting the cost benefits. Consequently, energy management in a MG with stochastic MPC schemes is more suitable, given the above factors.

Some works related to applications of stochastic MPC approaches from both stochastic groups to the context of EMS in a MG include [71]–[78], which addresses problems such as thermal comfort in buildings, demand response, fault detection, isolated MG and coordination of multiple RES, EMS and households. For example, [71] addresses the thermal comfort of a household while providing a demand response, taking into account uncertainties in PV power and outdoor temperature forecasts. In [75], is applied to the control of a heating, ventilating and air conditioning (HVAC) system for maintain indoor thermal comfort in buildings, taking into account the occupancy status of its zones; all this is coordinated with an ESS and with PV penetration, considering the presence of uncertainties in temperature and in the PV forecasts.

In [76], an EMS is proposed for a MG consisting of PV generators, wind turbines, controllable generators and a ESS, as well as the classification of demand into critical, curtailable and shiftable loads; considering the presence of uncertainties in the forecasts of demand, electricity prices, PV and wind generation. The OCP consists of a mixed integer quadratic program (MIQP), which considers the scenarios obtained from reducing a primary set of scenarios through a two-stage reduction technique. In [77] proposes the EMS for a microgrid consisting of several ESS, houses, and PV generators with forecast uncertainties. The OCP objectives are maintaining the ESS state of charge (SOC) at certain levels in case of unexpected events, lower purchased energy costs and increasing profits from the sale of the energy produced. Based on the tightest constraint of the set of scenarios, the OCP is reformulated into a computationally more tractable one incorporating slack variables. In [78], a two-stage scenario-based MPC is proposed for the energy management of ESSs. The upper stage is run hourly to forecast PV generation and demand, while the lower stage is run on a minute scale and focuses on maintaining the power balance. The scenarios are generated using a proposed methodology, considering the presence of uncertainties in PV generation and demand.

1.4 Main Contributions

The work conducted in order to answer the research questions outlined in section 1.1 produced outcomes such as a comparative study of two stochastic MPCs belonging to the deterministic and scenario-based groups, which researchers interested in studying these control strategies will find very useful; a scenario-based MPC approach for linear systems with correlated uncertainties, where exploiting these uncertainty characteristics leads to an OCP with a higher probability of constraint satisfaction; and the implementation of this approach as an energy management system in the framework of a microgrid with correlated forecasts.

Comparison of a stochastic MPC from the deterministic group with one from the scenario-based group

There are limited works comparing the techniques of deterministic and scenario-based MPC groups, discussing in detail the approach to the control problem, retaining their core structures, and validating the probabilistic feasibility of each OCP by means of examples. Some works on such comparisons can be found in [17], [57], [79]. In [79], several stochastic MPC proposals are outlined and compared with the deterministic counterpart. However, these approaches differ from the general formulation, so the conventional way of converting probabilistic constraints into their deterministic equivalents is not addressed. In [57], a strategy from the first group is compared with two from the second group for the control of a hydrogen-based microgrid. The nature of this process requires a cost function that differs from the general formulation, while the inputs are taken as the decision variables, in contrast to most algorithms, which obey the dual paradigm [18], [40], where the inputs consist of a state feedback [35], [38], [39], [80] or state error feedback [32], [34], [41], [44], [45] parameterisation. Also, the results do not present an analysis of constraint satisfaction, in probabilistic form, for each OCP. Another comparison is made in [17] applied to applied to drinkingwater network, where, as in the previous work, a strategy from the first group is also compared with two from the second group. Also, as in the previous case, the structures of OCPs differ from those generally proposed. The results analyse different performance indices but do not include any index indicating the probability with which the obtained optimal solutions satisfy the constraints.

Consequently, such a classification of stochastic MPC algorithms led to the first contribution of this thesis, consisting of a comparative study of two stochastic MPC algorithms, one from the deterministic group and the other from the scenario-based group, also a classic MPC as a baseline, focused on linear systems with parametric and additive uncertainties. This is in order, on the one

side, to obtain a detailed description of the theoretical background of each strategy, comparing the way they address the uncertainties, their prediction models, cost functions, the transformation of the probabilistic constraints into deterministic ones, and the OCP structures they set out. On the other side, to analyse their computational feasibility and constraint satisfaction, among others, through numerical examples, besides highlighting the most outstanding aspects of these strategies and their possible enhancement opportunities.

The numerical examples results demonstrate that the two stochastic MPC approaches have better probabilities of satisfying the constraints than a classical MPC. Due to the offline constraints tightening, the deterministic group MPC has a similar computational effort to the classic MPC, but with a considerable increase in the probability of satisfaction. Nevertheless, if the characteristics of the uncertainties change due to the nature of the system [46], [55], [56], [81], in that case, their new information could not be considered during online operation, so affecting the control performance.

On the other hand, scenario-based schemes, in addition to providing better probabilities of constraint satisfaction, have an inherent flexibility by enabling the addition of this new information online to generate the scenarios since, unlike the deterministic approaches, they do not require offline constraint adjustment. Besides, these techniques are widely used when there is no model of the uncertainties or when they do not obey any known distribution type, because if a large amount of empirical information on uncertainty values is available, scenarios can be selected from these and, therefore, it is not necessary to know the distribution of the random variables. However, this requires a higher computational effort due to the generation of scenarios online and the inclusion of these in the OCP constraints.

A proposal for a scenario-based MPC algorithm for systems with correlated uncertainties

The challenges of a scenario-based MPC discussed above, such as enhancing its probability of constraint satisfaction, as well as reducing its computational tractability; were addressed and led to the second significant contribution of this dissertation, consisting of a scenario-based MPC algorithm called conditional scenario-based model predictive control (CSB-MPC). This was developed for discrete-time linear systems influenced by either parametric uncertainties or exogenous disturbances, or both, and which are correlated and bounded.

Most stochastic MPC approaches are oriented to systems with largely strictly additive or, to a lesser extent, strictly parametric uncertainties; and whose realisations are either independent or correlated in time. In addition to the above systems, this proposal also considers systems that include both types of uncertainties, which are considered bounded and feature a correlation between all random variables or between some of them.

This strategy adapts a reduction method based on conditional scenarios (CS) [82], proposed as an approximation to the two-stage stochastic mixed-integer linear programming problems, to the MPC framework. The purpose of this is to approximate a large primary set of equiprobable scenarios of uncertainties realisations to a new reduced one of CSs with their probabilities of occurrence, retaining the main features of this primary set; where updated uncertainties information, such as probability distributions or historical data, can be included since the scenario generation-reduction process is performed online. The probabilities of occurrence of the uncertainties are utilised in the proposed cost function as penalising weights for the states and inputs related to these realisations. The above is to mitigate the effect of unlikely scenarios in the OCP, whereby more emphasis is given to states and inputs with higher probabilities of occurrence.

The results in this contribution showed that a CSB-MPC has a higher probability of satisfying the constraints than a standard scenario-based MPC for the same number of scenarios and offers a similar, sometimes shorter, solution time when using a smaller primary set.

A procedure for adapting the proposed MPC algorithm as an energy management system in a microgrid with correlated forecasts

In the works mentioned section 1.3 and in most of the literature, uncertainties in a microgrids are assumed to be either uncorrelated or each is correlated in time, but no consideration is given to the correlation that may exist between them. There are cases, due to working hours, off-hours, activity in a household, etc., where there is a high correlation between powers [83]–[87], either between the output powers of RES generators, PV-wind, PV-demand, wind-demand, or between various loads on the demand side. Moreover, photovoltaic and wind power generation forecasts, and possibly demand forecast, are strongly influenced by meteorological conditions that can be highly fluctuating, which can also affect the type or distribution of uncertainties. Therefore, a energy management based on a scenario-based MPC is desirable, given its possibility to include updated statistical information in real-time, to make better decisions consistent with the actual situation of the system.

The issues above, inherent in a MG were addressed in the development of the third important contribution of this thesis, which consists of the adaptation of the proposed conditional scenario-based MPC (CSB-MPC) to manage energy in a microgrid with correlated forecasts. First, a mathematical model of a standard microgrid that includes uncertainties in power generation and demand forecasts, with the possibility of being correlated to improve EMS performance in a microgrid with these characteristics is established. Secondly, a procedure is established to adapt a CSB-MPC to the EMS framework in a MG with, where these correlation features are exploited in the solution of a OCP with guaranteed numerical and probabilistic feasibilities, that assigns greater importance to predictions with a higher probability of occurrence.

The results of a case study comparing the performance of the CSB-MPC with that of a deterministic MPC, a stochastic MPC from the first group, and a stochastic MPC from the second group demonstrated that a CSB-MPC has better probabilities of constraint satisfaction. Also, the CSB-MPC showed similar solution times and lower operating costs than those of the MPC of the second group. ■

The contributions outlined in this section also yielded the following products:

Journal articles:

- E. A. González, J. Sanchis, S. García-Nieto, J. V. Salcedo, "A Comparative Study of Stochastic Model Predictive Controllers", *Electronics* (dec. 2020), doi: 10.3390/electronics9122078.
- E. A. González, J. Sanchis, J. V. Salcedo, M. A. Martínez, "Conditional Scenario-Based Model Predictive Control", *Journal of the Franklin Institute* (may 2023), doi: 10.1016/j.jfranklin.2023.05.012.
- E. A. González, J. Sanchis, J. V. Salcedo, M. A. Martínez, "Conditional Scenario-Based Energy Management Algorithm with Uncertain Correlated Forecasts", *Journal of Energy Storage* (mar. 2024), doi: 10.1016/j.est.2024.111177.

Software toolboxes:

- E. A. González, "Stochastic Model Predictive Control Toolbox", Version 1.0.8, 2021, url: MATLAB Central.
- E. A. González, "Conditional Scenario-Based MPC", Version 1.0.2, 2023, url: MATLAB Central.

Chapter 2

A Comparative Study of Stochastic Model Predictive Controllers

This chapter presents an overview of the main concepts of the stochastic MPC; starting from the structure of a classical MPC and continuing with those of stochastic MPCs of the deterministic (CC-MPC) and scenario-based (SCMPC) groups. On the one hand, the CC-MPC is based on analytical methods and solves an optimal control problem (OCP) similar to a classic MPC with constraints. This defines probabilistic constraints on the states, which are transformed into equivalent deterministic ones. On the other hand, SCMPC solves an OCP for a specified number of random realisations of uncertainties, also called scenarios. The first section presents the scope of this chapter. The second section presents a review of classic MPC. The third section shows stochastic MPC approaches of both groups for the control of linear systems. In the fourth section, two numerical examples comparing the performance of stochastic MPCs and classic MPC are presented, using simulations to control mechanical and liquid level systems. For comparison purposes, a set of indicators related to control performance, constraint violations and computational cost, among others, was calculated for both examples. Finally, the fifth section presents the conclusions of this chapter.

2.1 Introduction

This chapter addresses an overview of the main concepts of the stochastic model predictive control. Also, a comparative study of two stochastic model predictive controllers for linear systems with parametric and additive uncertainties, belonging to the deterministic and scenario-based groups is made. The main aspects to be highlighted are

- A detailed description of the theoretical background of the stochastic model predictive control strategy is presented. Emphasis is made on the formulation of the optimal control problem and how uncertainties are addressed. In addition, the SCMPC formulation for worst case OCP is analysed.
- The ways in which OCPs are stated in each strategy are compared with respect to the cost function and constraints on the states according to the statistical information. The structural similarity between the CC-MPC approach and classic MPC is shown by transforming probabilistic constraints into deterministic ones.
- The viability of these two control strategies is analysed through two numerical examples: a two-mass spring SISO system with parametric and additive uncertainties and a nonlinear quadruple-tank system with additive uncertainties. The controllers comparison is made by using performance indices such as number of successful runs, number of times the constraints are violated, mean value of the integral absolute error and the computational cost. The results show that the two stochastic schemes have higher probability of success than the classic MPC. The SCMPC presents the highest probability of success, but with the highest computational cost. The CC-MPC has similar computational cost to the classic MPC, but with a considerable increase in the probability of success.

2.2 Model Predictive Control Strategy

Consider the discrete linear system (2.1a) with constraints in states and inputs (2.1b) and (2.1c), respectively

$$x_{i+1} = Ax_i + Bu_i \tag{2.1a}$$

$$x \in \mathbb{X} \tag{2.1b}$$

$$u \in \mathbb{U}. \tag{2.1c}$$

where variables $x \in \mathbb{R}^{n_x}$ and $u \in \mathbb{R}^{n_u}$ represent the state and system inputs vectors at the instant $i \in \mathbb{N}$; $A \in \mathbb{R}^{n_x \times n_x}$ is the state matrix and $B \in \mathbb{R}^{n_x \times n_u}$ is the system input matrix. $\mathbb{X}$ and $\mathbb{U}$ are convex sets that contain the origin in their interiors

MPC is a strategy that uses an explicit model of the process where, at each sampling time and with the current information of the process variables, predictions of process future behaviour along a horizon are managed. Such predictions are incorporated into a cost index to solve an open loop Optimal Control Problem (OCP) subject to constraints, which results in the sequence of future optimal controls.

With the above in mind, given the current instant k and with the availability of the current state of the plant $\hat{x}_k$, based on (2.1a), predictions are made for the states $x_{i+1|k}$, along a prediction horizon N

$$\begin{aligned} x_{i+1|k} &= Ax_{i|k} + Bu_{i|k} \\ \forall i &\in \{0, 1, \ldots, N-1\} \end{aligned} \tag{2.2}$$

where, the terms $x_{i|k}$ and $u_{i|k}$ indicate the predicted value of such a variable for instant i ahead of k, based on the information available at time k, such that $x_{0|k} = \hat{x}_k$.

Predictions (2.2) are included in the quadratic cost index (2.3), where, the decision variables are the future controls $\boldsymbol{u}_k = \{u_{0|k}, u_{1|k}, \ldots, u_{N-1|k}\}$. Matrices $Q \in \mathbb{R}^{n_x \times n_x}$ and $R \in \mathbb{R}^{n_u \times n_u}$ are weighting matrices that penalise the first N predicted states and predicted inputs, respectively, and are defined by the designer such that Q be a positive semi-defined symmetric matrix ($Q \geq 0$) and R a positive defined symmetric matrix ($R > 0$)

$$J(\hat{x}_k, \boldsymbol{u}_k) = \sum_{i=0}^{N-1} \left(x_{i|k}^\top Q x_{i|k} + u_{i|k}^\top R u_{i|k} \right). \tag{2.3}$$

The optimal decision variables $\boldsymbol{u}_k^* = \{u_{0|k}^*, u_{1|k}^*, \ldots, u_{N-1|k}^*\}$ that lead the states of the system to a desired operating point [88], or as a regulator towards the origin, are calculated by minimising $J(\hat{x}_k, \boldsymbol{u}_k)$ in OCP (2.4a) with constraints (2.4b)-(2.4f). This strategy is also known as Moving Horizon Control (MHC) or Receding Horizon Control (RHC), in the sense that only the first element $u_{0|k}^*$ of the optimal controls sequence $\boldsymbol{u}_k^*$, which corresponds to the input for the current instant k, is applied to the system; so that OCP (2.4) is performed again at time

$k+1$.

$$\min_{u_{0|k},u_{1|k},\ldots,u_{N-1|k}} J(\hat{x}_k, \boldsymbol{u}_k) \tag{2.4a}$$

s.t.

$$x_{i+1|k} = Ax_{i|k} + Bu_{i|k} \tag{2.4b}$$
$$x_{i+1|k} \in \mathbb{X} \tag{2.4c}$$
$$u_{i|k} \in \mathbb{U} \tag{2.4d}$$
$$x_{0|k} = \hat{x}_k \tag{2.4e}$$
$$\forall i \in \{0, 1, \ldots, N-1\}. \tag{2.4f}$$

The cost index $J(\hat{x}_k, \boldsymbol{u}_k)$ has drawbacks [19], [22] in the sense of stability (all the trajectories of the states converge towards an equilibrium point) and feasibility (the OCP always finds a feasible solution) since for small prediction horizons the computational cost is low, but it may cause a deviation between trajectories of the open-loop predictions and the closed-loop system, or not find a feasible solution; while for very large horizons it improves stability and feasibility but increases the computational load.

Dual Mode Paradigm

Dual mode prediction paradigm [18], [19], [22] seeks to ensure stability for an appropriate (or long enough) horizon N, incorporating in (2.3) the terminal cost $x_{N|k}^\top P x_{N|k}$ that penalizes the terminal state $x_{N|k}$ with matrix $P \in \mathbb{R}^{n_x \times n_x}$, which is a positive defined symmetric matrix $P > 0$

$$J_N(\hat{x}_k, \boldsymbol{v}_k) = \sum_{i=0}^{N-1} \left(x_{i|k}^\top Q x_{i|k} + u_{i|k}^\top R u_{i|k} \right) + x_{N|k}^\top P x_{N|k}. \tag{2.5}$$

The sequence of inputs $\boldsymbol{u}_k$ obey the state feedback control law (2.6), where $K \in \mathbb{R}^{n_u \times n_x}$ is a gain or feedback matrix that stabilizes the system, and $v_k \in \mathbb{R}^{n_u}$ are the new decision variables such that $\boldsymbol{v}_k = \{v_{0|k}, v_{1|k}, \ldots, v_{N-1|k}\}$

$$u_{i|k} = Kx_{i|k} + v_{i|k}. \tag{2.6}$$

Therefore, the solution of the OCP (2.4) using (2.5) is divided into two parts $J_N(\hat{x}_k, \boldsymbol{v}_k) = J_1 + J_2$. In mode one,

$$J_1 = \sum_{i=0}^{N-1} \left(x_{i|k}^\top Q x_{i|k} + u_{i|k}^\top R u_{i|k} \right)$$

the OCP is solved, subject to constraints (2.4c)–(2.4d), where the future control sequences (2.7) are calculated for the first N instants

$$u_{i|k} = Kx_{i|k} + v_{i|k}, \qquad \forall i \in \{0, 1, \ldots, N-1\} \tag{2.7}$$

in mode 2,

$$J_2 = \sum_{i=N}^{\infty} \left(x_{i|k}^{\top} Q x_{i|k} + u_{i|k}^{\top} R u_{i|k} \right) = x_{N|k}^{\top} P x_{N|k}$$

for the following instants, the optimization is carried out assuming that there are no constraints, through a terminal feedback law (2.8) that stabilizes the system

$$u_{i|k} = Kx_{i|k}, \qquad \forall i \in \{N, N+1, \ldots, \infty\}. \tag{2.8}$$

By parameterizing the inputs through the state feedback law (2.6), it is sought to make the closed-loop system obey a quadratic stability criterion [89]. For LTI systems such as (2.1a), assuming that matrix $A + BK$ is strictly stable, matrices K and P are obtained from solving a Quadratic Optimal Control Problem (LQR) [90]; where K is given by (2.9a), P is calculated by the convergence of the discrete Riccati equation (2.9b), $\forall k \in \{0, 1, \ldots\}$

$$K = -(R + B^{\top} P B)^{-1} B^{\top} P A \tag{2.9a}$$

$$P_{k+1} = Q + A^{\top} P_k A - A^{\top} P_k B (R + B^{\top} P_k B)^{-1} B^{\top} P_k A, \qquad P_0 = Q. \tag{2.9b}$$

Based on this paradigm, and for a long enough horizon, the system will be stable in the Lyapunov's sense as long as two conditions are met. The first condition requires the existence of a solution for P such that $P > 0$. The second condition requires that the predicted inputs and states satisfy the constraints along a finite horizon, which is achieved by ensuring that $J_N(\hat{x}_k, \boldsymbol{v}_k)$ is decreasing from time k.

Another condition also used to ensure closed-loop stability, is to complement the dual mode by adding the terminal constraint $x_{N|k} \in \mathbb{X}_T$ [18], [20] to the OCP, with $\mathbb{X}$ being the set of allowed values for the states. The purpose of this is to force the terminal state $x_{N|k}$ and the following states to remain within a safe zone or terminal set $\mathbb{X}_T$, positively invariant [89]–[91], under the terminal control law (2.8); such that $\mathbb{X}_T \subset \mathbb{X}$. ■

Given the current state $x_{0|k} = \hat{x}_k$ and incorporating the model (2.2) and control law(2.6) in the cost function (2.5), the equivalent of OCP (2.4) is as follows

$$\min_{v_{0|k}, v_{1|k}, \ldots, v_{N-1|k}} J_N(\hat{x}_k, \boldsymbol{v}_k) \tag{2.10a}$$

s.t.

$$x_{i+1|k} = Ax_{i|k} + Bu_{i|k} \tag{2.10b}$$
$$u_{i|k} = Kx_{i|k} + v_{i|k} \tag{2.10c}$$
$$Hx_{i+1|k} \leq h \tag{2.10d}$$
$$Du_{i|k} \leq d \tag{2.10e}$$
$$x_{0|k} = \hat{x}_k \tag{2.10f}$$
$$\forall i \in \{0, 1, \ldots, N-1\} \tag{2.10g}$$

where constraints for the predicted states (2.1b) and input (2.1c) trajectories are expressed as linear inequalities (2.10d) and (2.10e), respectively; with $H \in \mathbb{R}^{c_x \times n_x}$ and $D \in \mathbb{R}^{c_u \times n_u}$; vectors $h \in \mathbb{R}^{c_x}$ and $d \in \mathbb{R}^{c_u}$ represent the constraint limits; and c_x and c_u are the number of state constraints and input constraints, respectively.

Given the quadratic and convex nature of (2.5), the linear model (2.2) and the type of constraints (2.10d) and (2.10e), a finite horizon OCP stated as in (2.10) can be solved at each control period. This OCP is a quadratic programming problem (QP) with a global optimum whose solution results in the optimal control vector $\boldsymbol{v}_k^* = \{v_{0|k}^*, v_{1|k}^*, \ldots, v_{N-1|k}^*\}$, where only the first element $v_{0|k}^*$ is applied to the input at that instant. This is $u_{0|k} = K\hat{x}_k + v_{0|k}^*$.

2.3 Stochastic MPC

Consider the dynamics of an uncertain system defined by

$$x_{i+1} = A(\delta_i)x_i + B(\delta_i)u_i + G(\delta_i)w_i \tag{2.11}$$

where $w \in \mathbb{R}^{n_w}$ are additive disturbances, $G \in \mathbb{R}^{n_x \times n_w}$ is a matrix that relates the influence of w on system states, and δ are parametric uncertainties.

Stochastic model predictive control approaches were inspired by this type of systems, in which δ and w are stochastic in nature, independent and with known probability distributions. Since this statistical information is taken into account in the solution of the OCP [26]–[29], stochastic predictive control has been widely accepted and has been applied in different areas such as building air conditioning

[13], [75], [92], renewable energy management [93], [94], process control [3], [95], robotics and automotive [5], [41], [96]–[98]. A more extensive review of these and other applications is presented in [26], [27], [29], [45], [46], where network control systems, air traffic, finance, path planning and training control are discussed.

Most stochastic model predictive control strategies can be classified into two groups: those based on analytical methods (CC-MPC) [39], [44], [45], [80], which solve an OCP based on the expected value of a cost index, subject to probabilistic constraints (usually on the predicted states); and those based on random scenarios (SCMPC) [35], [36], [41], which solve an OCP for a determined number of random realisations of uncertainties also called scenarios.

2.3.1 Chance-Constrained MPC (CC-MPC)

Consider (2.12a) an uncertain system with additive uncertainties, and with state feedback input (2.12b)

$$x_{i+1|k} = Ax_{i|k} + Bu_{i|k} + Gw_{i|k} \tag{2.12a}$$
$$u_{i|k} = Kx_{i|k} + v_{i|k} \tag{2.12b}$$
$$\forall i \in \{0, 1, \ldots, N-1\} \tag{2.12c}$$

where w, which is not necessarily bounded [29], [42], [44], has a distribution P_w and any sequence $\{w_0, w_1, \ldots, w_{N-1}\}$ has zero mean ($\mathbb{E}[w_i] = 0$) with its values independent and identically distributed (i.i.d.).

In the CC-MPC approach, the cost index $J_S(\hat{x}_k, \boldsymbol{v}_k)$ is expressed as the expected value of the quadratic index (2.5)

$$J_S(\hat{x}_k, \boldsymbol{v}_k) = \mathbb{E}_k \left[\sum_{i=0}^{N-1} \left(x_{i|k}^\top Q x_{i|k} + u_{i|k}^\top R u_{i|k} \right) + x_{N|k}^\top P x_{N|k} \right] \tag{2.13}$$

where matrices K and P are obtained using (2.9). Also, the hard constraints in the states $Hx_{i+1|k} \leq h$ are replaced by probabilistic constraints [29], [42] (2.14), with the aim that the probability of constraint satisfaction in the state is above a desired level $p \in [0, 1]$, or does not exceed a permitted level of risk $1 - p$

$$\mathbb{P}_k[Hx_{i+1|k} \leq h] \geq p. \tag{2.14}$$

According to the above, the analogous OCP of (2.10) to be solved for the uncertain system (2.12) is the following stochastic OCP

$$\min_{v_{0|k},v_{1|k},\ldots,v_{N-1|k}} \quad J_S(\hat{x}_k, \boldsymbol{v}_k) \tag{2.15a}$$

s.t.

$$x_{i+1|k} = Ax_{i|k} + Bu_{i|k} + Gw_{i|k} \tag{2.15b}$$
$$u_{i|k} = Kx_{i|k} + v_{i|k} \tag{2.15c}$$
$$\mathbb{P}_k[Hx_{i+1|k} \leq h] \geq p \tag{2.15d}$$
$$Du_{i|k} \leq d \tag{2.15e}$$
$$x_{0|k} = \hat{x}_k \tag{2.15f}$$
$$\forall i \in \{0, 1, \ldots, N-1\}. \tag{2.15g}$$

Defining the prediction $x_{i|k}$ as the sum of two variables, a deterministic variable $z_{i|k} = \mathbb{E}_k[x_{i|k}]$ which represents the predicted nominal value of $x_{i|k}$, and a stochastic variable $e_{i|k} = x_{i|k} - z_{i|k}$ which comprises the effect of the perturbation and whose mean is zero, that is

$$x_{i|k} = z_{i|k} + e_{i|k} \tag{2.16}$$

substituting (2.16) in (2.12b), the following state feedback control law is obtained

$$u_{i|k} = K(z_{i|k} + e_{i|k}) + v_{i|k}. \tag{2.17}$$

a common alternative to (2.17) is based on feedback of the deviation $e_{i|k}$ [44], [45] as $u_{i|k} = Ke_{i|k} + v_{i|k}$. Hence, replacing (2.17) and (2.16) in (2.12a), predictions $\forall i \in \{0, 1, \ldots, N-1\}$ are given in (2.18), where $z_{0|k} = \hat{x}_k$, $e_{0|k} = 0$, and $A_{cl} = A + BK$

$$z_{i+1|k} + e_{i+1|k} = A_{cl}z_{i|k} + Bv_{i|k} + A_{cl}e_{i|k} + Gw_{i|k}. \tag{2.18}$$

The above expression can be divided into two parts. Predictions of the nominal state (2.19a), and predictions of the deviation (2.19b)

$$z_{i+1|k} = A_{cl}z_{i|k} + Bv_{i|k}, \qquad z_{0|k} = \hat{x}_k \tag{2.19a}$$
$$e_{i+1|k} = A_{cl}e_{i|k} + Gw_{i|k}, \qquad e_{0|k} = 0. \tag{2.19b}$$

Replacing (2.16) and (2.17) in (2.13), and remembering that the expected value of a product involving $e_{i|k}$ is zero (since $e_{i|k}$ is zero mean), a new cost index

containing the nominal trajectories of the predicted states $z_{i|k}$ is obtained

$$\hat{J}_S(\hat{x}_k, \boldsymbol{v}_k) = \sum_{i=0}^{N-1} \left(z_{i|k}^\top Q_{zz} z_{i|k} + z_{i|k}^\top Q_{zv} v_{i|k} + v_{i|k}^\top R v_{i|k} \right) + z_{N|k}^\top P z_{N|k} + c \quad (2.20)$$

where $Q_{zz} = Q + K^\top R K$, $Q_{zv} = 2K^\top R$, and $c = \mathbb{E}_k[\sum_{i=0}^{N-1}(e_{i|k}^\top Q_{xx} e_{i|k}) + e_{N|k}^\top P e_{N|k}]$ is a constant term that can be excluded from the cost index, since it does not depend on the decision variables $v_{i|k}$ and does not influence the optimum.

Constraints Tightening

The nonconvexity of constraints (2.15d) can make the OCP (2.15) computationally unmanageable. For this reason, such probabilistic constraints are converted into deterministic and convex equivalents [44], [45] using the knowledge of the first two statistical moments of the random variable w, by tightening the hard constraints $Hx_{i+1|k} \leq h$ offline. This results in an OCP similar to (2.10) in structure and computational tractability.

Defining the constraints (2.14) as a set of single chance-constraints (2.21), can be interpreted as the probability that a predicted state does not violate the jth constraint must be greater than or equal to the jth desired probability level p_j

$$\mathbb{P}_k[H_j x_{i+1|k} \leq h_j] \geq p_j, \qquad \forall j \in \{1, 2, \ldots, c_x\}. \quad (2.21)$$

Substituting (2.16) into (2.21), separating the deterministic part $H_j z_{i+1|k}$ from the stochastic one, $h_j - H_j e_{i+1|k}$, and setting a new bound $\eta_{j\,i+1|k}$ calculated in such a way that $H_j z_{i+1|k} \leq \eta_{j\,i+1|k}$ then

$$\mathbb{P}_k[\eta_{j\,i+1|k} \leq h_j - H_j e_{i+1|k}] \geq p_j. \quad (2.22)$$

The bound $\eta_{j\,i+1|k}$, that is the new tightened bound for h_j, can be obtained from solving a chance-constrained optimization problem stated as in (2.23), whose decision variable is η

$$\eta_{j\,i+1|k} = \max_{\eta} \ \eta \quad (2.23a)$$

s.t.

$$\mathbb{P}_k[\eta \leq h_j - H_j e_{i+1|k}] \geq p_j \quad (2.23b)$$

$$\forall i \in \{0, 1, \ldots, N-1\}, \qquad \forall j \in \{1, 2, \ldots, c_x\} \quad (2.23c)$$

where the left-hand side of inequality (2.23b) is expressed in terms of the integral of the probability density function of $h_j - H_j e_{i+1|k}$.

As an alternative to solve (2.23), let us assume that probability distribution of w is known and is of Gaussian type $w \sim \mathcal{N}(0, \Sigma_w)$, with zero mean and covariance Σ_w. This assumption implies that the error $e_{i+1|k}$ in (2.19b) also has a known normal distribution $e_{i+1|k} \sim \mathcal{N}(0, \Sigma_{e_{i+1|k}})$ with zero mean ($\mathbb{E}[e_{i+1|k}] = 0$), and covariance $\Sigma_{e_{i+1|k}}$, whose evolution can be obtained by applying the covariance formula of a random variable, i.e. $\Sigma_Y = \mathbb{E}[(Y - \mathbb{E}[Y])^2]$

$$\begin{aligned}
\Sigma_{e_{i+1|k}} =& \mathbb{E}\left[\left(e_{i+1|k} - \mathbb{E}\left[e_{i+1|k}\right]\right)\left(e_{i+1|k} - \mathbb{E}\left[e_{i+1|k}\right]\right)^\top\right] \\
=& \mathbb{E}[(A_{cl} e_{i|k} + G w_{i|k})(A_{cl} e_{i|k} + G w_{i|k})^\top] \\
=& A_{cl}\mathbb{E}[e_{i|k} e_{i|k}^\top] A_{cl}^\top + 2A_{cl}\mathbb{E}[e_{i|k} w_{i|k}^\top] G^\top + G\mathbb{E}[w_{i|k} w_{i|k}^\top] G^\top \\
=& A_{cl}\Sigma_{e_{i|k}} A_{cl}^\top + 2A_{cl}\Sigma_{e_{i|k}, w_{i|k}} G^\top + G\Sigma_w G^\top
\end{aligned}$$

due to the independence between the random variables $e_{i|k}$ and $w_{i|k}$, it follows that $\Sigma_{e_{i|k}, w_{i|k}} = 0$, so that

$$\Sigma_{e_{i+1|k}} = A_{cl}\Sigma_{e_{i|k}} A_{cl}^\top + G\Sigma_w G^\top, \qquad \Sigma_{e_{0|k}} = 0. \tag{2.24}$$

Now, reordering Equation (2.22)

$$\mathbb{P}_k[H_j e_{i+1|k} \leq h_j - \eta_{j\,i+1|k}] \geq p_j \tag{2.25}$$

random variable $H_j e_{i+1|k}$ in (2.25) has zero mean $\mu = 0$ and covariance $\sigma_{j\,i+1|k}^2 = H_j \Sigma_{e_{i+1|k}} H_j^\top$, and its cumulative distribution function (CDF) F_{He} is

$$F_{He}(h_j - \eta_{j\,i+1|k}) = \frac{1}{2}\left[1 + \operatorname{erf}\left(\frac{(h_j - \eta_{j\,i+1|k}) - \mu}{\sigma_{j\,i+1|k}\sqrt{2}}\right)\right] \tag{2.26}$$

where $\operatorname{erf}(\cdot)$ is the error function. Given that(2.26) is the left-hand side of (2.25), it is required to satisfy

$$\frac{1}{2}\left[1 + \operatorname{erf}\left(\frac{h_j - \eta_{j\,i+1|k}}{\sigma_{j\,i+1|k}\sqrt{2}}\right)\right] = p_j.$$

From the above equation, an expression can be obtained for the $\eta_{j\,i+1|k}$ bound, where $\text{erf}^{-1}(\cdot)$ is the inverse error function

$$\eta_{j\,i+1|k} = h_j - \sigma_{j\,i+1|k} f(p_j) \tag{2.27a}$$

$$f(p_j) = \sqrt{2}\text{erf}^{-1}(2p_j - 1). \tag{2.27b}$$

Note that the constraints are tightened for values of p_j within the range $0.5 \leq p_j \leq 1$, where for $p_j = 0.5$ the bound $\eta_{j\,i+1|k}$ corresponds to the original h_j, while for larger values this bound is further reduced.

For unknown distributions of w, by means of Chebyshev-Cantelli inequality [29], [45], it is also possible to find $\eta_{j\,i+1|k}$, where only the first two statistical moments of state $x_{i+1|k}$ are required. This inequality is given by the expression

$$\mathbb{P}[Y - \mathbb{E}[Y] < \lambda] \geq 1 - \frac{\sigma^2}{\sigma^2 + \lambda^2}, \qquad \lambda > 0 \tag{2.28}$$

where Y is the random variable, $\mathbb{E}[Y]$ its mean, σ^2 is the covariance and λ is an upper bound. The left-hand side term of the inequality (2.25) in the (2.28) form will be

$$\mathbb{P}_k[H_j e_{i+1|k} - \mu < h_j - \eta_{j\,i+1|k}] \geq 1 - \frac{\sigma_{j\,i+1|k}^2}{\sigma_{j\,i+1|k}^2 + (h_j - \eta_{j\,i+1|k})^2}. \tag{2.29}$$

Based on (2.25) and (2.29) as its left-hand side, the following must be fulfilled

$$1 - \frac{\sigma_{j\,i+1|k}^2}{\sigma_{j\,i+1|k}^2 + (h_j - \eta_{j\,i+1|k})^2} = p_j. \tag{2.30}$$

Finally, an expression for $\eta_{j\,i+1|k}$ can be obtained

$$\eta_{j\,i+1|k} = h_j - \sigma_{j\,i+1|k} f(p_j) \tag{2.31a}$$

$$f(p_j) = \sqrt{\frac{p_j}{1 - p_j}}. \tag{2.31b}$$

It should be noted that the calculation of $\eta_{j\,i+1|k}$, through either (2.23), (2.27) or (2.31), presents an advantage in computational terms when it is performed offline since the random variable $e_{i+1|k}$ does not depend on the state $x_{i|k}$ or the decision

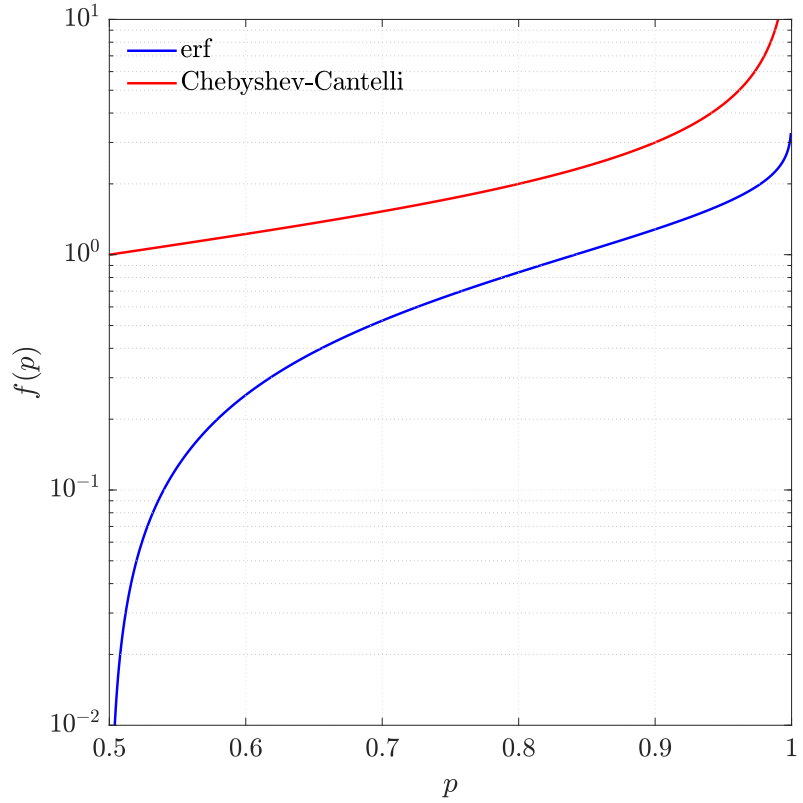

Figure 2.1: Comparison of obtained distances $\sigma f(p)$, based on the error function erf (2.27) and based on the Chebyshev-Cantelli inequality (2.31), for various values of p and with $\sigma = 1$.

variable $v_{i|k}$ (see (2.19b)). Therefore, the deterministic equivalent of the chance constraints (2.25) is

$$H_j z_{i+1|k} \leq \eta_{j\,i+1|k}. \tag{2.32}$$

Furthermore, note that in equations (2.27a) and (2.31a), the term $\sigma_{i+1|k} f(p_j)$ determines the minimum distance at which the nominal state $z_{i+1|k}$ can approach the original limit h_j to account for uncertainties and thus, a lower probability of violation of h_j.

Figure 2.1 compares the minimum distances $\sigma f(p)$ obtained with (2.27b) and (2.31b), for various values of p and with $\sigma = 1$, i.e., $1f(p)$. There it can be seen that in both cases, this distance increases as the desired probability of constraints

satisfaction p increases. Besides, the distance calculated using the Chebyshev-Cantelli inequality is larger than the one obtained based on the error function erf, which makes it more conservative. ■

Based on the nominal index (2.20) and deterministic constraints (2.32), the deterministic equivalent of the CC-MPC (2.15) with finite prediction horizon N can be stated as

$$\min_{v_{0|k}, v_{1|k}, \ldots, v_{N-1|k}} \quad \hat{J}_S(\hat{x}_k, \boldsymbol{v}_k) \tag{2.33a}$$

s.t.

$$z_{i+1|k} = A_{cl} z_{i|k} + B v_{i|k} \tag{2.33b}$$
$$u_{i|k} = K z_{i|k} + v_{i|k} \tag{2.33c}$$
$$H_j z_{i+1|k} \leq \eta_{j\, i+1|k} \tag{2.33d}$$
$$D u_{i|k} \leq d \tag{2.33e}$$
$$z_{0|k} = \hat{x}_k \tag{2.33f}$$
$$\forall i \in \{0, 1, \ldots, N-1\}, \qquad \forall j \in \{1, 2, \ldots, c_x\}. \tag{2.33g}$$

This OCP, as well as (2.10), can be solved using quadratic programming, where at each sampling time only the first element $v^*_{0|k}$ of the optimal sequence $\boldsymbol{v}^*_k$ is applied to the system, that is $u_{k|k} = K\hat{x}_k + v^*_{0|k}$.

2.3.2 Scenario-Based MPC (SCMPC)

The aim of SCMCP is to solve a convex OCP whose cost index for a prediction horizon N is composed not by a single trajectory of the states, but by the average of a set of C trajectories generated due to random realisations of the disturbances also known as scenarios [35], [36]. The optimal controls $\boldsymbol{u}^*_k = \{u^*_{0|k}, u^*_{1|k}, \ldots, u^*_{N-1|k}\}$ are those that minimise such an index satisfying the constraints for each scenario. For this reason, the selection of the number of scenarios, C, requires special attention in order to guarantee a defined minimum level of confidence or non-violation of constraints.

Consider the uncertain system defined in (2.11), where for a given instant k, the state predictions $x_{i+1|k}$ and future control inputs $u_{i|k}$ are given by

$$x_{i+1|k} = A(\delta_{i|k}) x_{i|k} + B(\delta_{i|k}) u_{i|k} + G(\delta_{i|k}) w_{i|k} \tag{2.34a}$$
$$u_{i|k} = K x_{i|k} + v_{i|k} \tag{2.34b}$$
$$\forall i \in \{0, 1, \ldots, N-1\} \tag{2.34c}$$

where δ is associated with bounded parametric uncertainties [47] with probability distribution P_δ, while w (which is not necessarily bounded [29], [42], [44]) has a distribution P_w. Any sequence $\{w_0, w_1, \ldots, w_{N-1}\}$ and $\{\delta_0, \delta_1, \ldots, \delta_{N-1}\}$ has zero mean ($\mathbb{E}[\delta_i] = 0, \mathbb{E}[w_i] = 0$) with its values independent and identically distributed (i.i.d.).

In the following, the notation $X^{[j]}_{i|k}$ is interpreted as the predicted value of the variable X of scenario j, for the time step i ahead of the current time instant k. With this in mind, for a given instant k, let us define the jth scenario denoted by

$$\gamma^{[j]}_k = \{\boldsymbol{\delta}^{[j]}_k, \boldsymbol{w}^{[j]}_k\}$$

where $\boldsymbol{\delta}^{[j]}_k$ and $\boldsymbol{w}^{[j]}_k$ are random and known realisations of the parametric and additive uncertainties along N, respectively

$$\begin{aligned}\boldsymbol{\delta}^{[j]}_k &= \{\delta^{[j]}_{0|k}\ \delta^{[j]}_{1|k}\ \ldots\ \delta^{[j]}_{N-1|k}\},\\ \boldsymbol{w}^{[j]}_k &= \{w^{[j]}_{0|k}\ w^{[j]}_{1|k}\ \ldots\ w^{[j]}_{N-1|k}\}.\end{aligned}$$

Thus, the set $\boldsymbol{\Gamma}_k$ of C random and independent scenarios for the instant k is given by

$$\begin{gathered}\boldsymbol{\Gamma}_k = \{\gamma^{[1]}_k, \gamma^{[2]}_k, \ldots, \gamma^{[C]}_k\},\\ \forall j \in \{1, 2, \ldots, C\}.\end{gathered}$$

With knowledge of the probability distributions P_δ and P_w, the realisations $\boldsymbol{\delta}^{[j]}_k$ and $\boldsymbol{w}^{[j]}_k$ can be obtained by means of a random number generator. On the other hand, if there is no knowledge of the probability distributions, $\boldsymbol{\delta}^{[j]}_k$ and $\boldsymbol{w}^{[j]}_k$ can be extracted from experimental data.

Therefore, predictions (2.34a) and (2.34b) for the jth scenario are given by (2.35a) and (2.35b), where it is fulfilled that the initial condition $x^{[j]}_{0|k} = \hat{x}_k$ and the decision variables $\{v_{0|k}, v_{1|k}, \ldots, v_{N-1|k}\}$ are the same for each j

$$x^{[j]}_{i+1|k} = A(\delta^{[j]}_{i|k})x^{[j]}_{i|k} + B(\delta^{[j]}_{i|k})u_{i|k} + G(\delta^{[j]}_{i|k})w^{[j]}_{i|k}, \qquad x^{[j]}_{0|k} = \hat{x}_k \tag{2.35a}$$

$$u^{[j]}_{i|k} = Kx^{[j]}_{i|k} + v_{i|k} \tag{2.35b}$$

$$\forall i \in \{0, 1, \ldots, N-1\}, \qquad \forall j \in \{1, 2, \ldots, C\}. \tag{2.35c}$$

Then, based in (2.5), the cost index in which the evolutions of the states (2.35a) and inputs (2.35b) of scenario j are penalised is given by

$$J_N^{[j]}(\hat{x}_k, \boldsymbol{v}_k) = \sum_{i=0}^{N-1} \left(x_{i|k}^{[j]\top} Q x_{i|k}^{[j]} + u_{i|k}^{[j]\top} R u_{i|k}^{[j]} \right) + x_{N|k}^{[j]\top} P x_{N|k}^{[j]}. \tag{2.36}$$

From (2.36), a global cost index $J_{Sc}(\hat{x}_k, \boldsymbol{v}_k)$ is defined as the average of the C trajectories generated, which conform a band around a nominal trajectory

$$J_{Sc}(\hat{x}_k, \boldsymbol{v}_k) = \frac{1}{C} \sum_{j=1}^{C} J_N^{[j]}(\hat{x}_k, \boldsymbol{v}_k) \tag{2.37}$$

Note that in the scenario framework, (2.37) represents the sample average of the cost function based on the expected value (2.13). Under (2.37), a scenario-based optimal control problem is stated as

$$\min_{v_{0|k}, v_{1|k}, \ldots, v_{N-1|k}} \quad J_{Sc}(\hat{x}_k, \boldsymbol{v}_k) \tag{2.38a}$$

s.t.

$$x_{i+1|k}^{[j]} = A(\delta_{i|k}^{[j]}) x_{i|k}^{[j]} + B(\delta_{i|k}^{[j]}) u_{i|k} + G(\delta_{i|k}^{[j]}) w_{i|k}^{[j]} \tag{2.38b}$$

$$u_{i|k}^{[j]} = K x_{i|k}^{[j]} + v_{i|k} \tag{2.38c}$$

$$H x_{i+1|k}^{[j]} \leq h \tag{2.38d}$$

$$D u_{i|k}^{[j]} \leq d \tag{2.38e}$$

$$x_{0|k}^{[j]} = \hat{x}_k \tag{2.38f}$$

$$\forall i \in \{0, 1, \ldots, N-1\}, \qquad \forall j \in \{1, 2, \ldots, C\} \tag{2.38g}$$

where constraints (2.38d) and (2.38e), whose matrices are the same as in (2.10d) and (2.10e), indicate that they must be met for each scenario j. OCP (2.38) can be solved by quadratic programming where, the solution at time k yields the optimal controls

$$\boldsymbol{v}_k^* = \{v_{0|k}^*, v_{k+1|k}^*, \ldots, v_{k+N-1|k}^*\}$$

and only the first element $v_{0|k}^*$ is applied to the process in that time, i.e., $u_{0|k} = K\hat{x}_k + v_{0|k}^*$.

A robust SCMPC approach is achieved by replacing (2.38a) with (2.39), so that the sequence $\boldsymbol{v}_k$ that minimises the worst case (min-max optimisation) [29], [35]

of the C realisations is calculated, as opposed to (2.38a), in which a nominal trajectory is minimised

$$\min_{v_{0|k},v_{1|k},\ldots,v_{N-1|k}} \max_{j=1,2,\ldots,C} J_N^{[j]}(\hat{x}_k, \boldsymbol{v}_k). \tag{2.39}$$

This robust approach is expensive computationally, because the worst case of all the scenarios is obtained first, to subsequently perform a minimisation on it. Another drawback is that the worst case does not always correspond to reality at that moment, so an optimum applied to the real process could lead to poor behaviour.

Number of Scenarios

The number of scenarios C demands special attention in order to guarantee compliance with the constraints in the states with at least a specified probability level [26], [27], [35], [51]. Consider the chance-constrained optimisation problem (2.40), where x is the vector of decision variables of dimension d, γ is the vector of random variables; and $p \in [0, 1]$ is a desired probability level of satisfaction of the constraints $f(x, \gamma) \leq 0$, with $f(x, \gamma)$ convex in x

$$\min_x c^\top x \tag{2.40a}$$

s.t.

$$\mathbb{P}[f(x, \gamma) \leq 0] \geq p. \tag{2.40b}$$

In random convex programs [51], the problem (2.40) is approximated to (2.41) by considering C samples $\left\{\gamma^{[1]}, \gamma^{[2]}, \ldots, \gamma^{[C]}\right\}$ of the random vector γ, whereby the probabilistic constraints (2.40b) are converted into C convex constraints (2.41b)

$$\min_x c^\top x \tag{2.41a}$$

s.t.

$$f(x, \gamma^{[j]}) \leq 0, \qquad \forall j \in \{1, 2, \ldots, C\}. \tag{2.41b}$$

Let $x^* = x^*\left(\left\{\gamma^{[1]}, \gamma^{[2]}, \ldots, \gamma^{[C]}\right\}\right)$ be an optimal solution of (2.41), and $V(x)$ the probability violation of constraint $f(x, \gamma) \leq 0$, i.e., $V(x) = \mathbb{P}[f(x, \gamma) > 0]$. Then, the probability the optimal solution x^* does not meet the constraints, at least with probability level p, is expressed by

$$\mathbb{P}[V(x^*) > 1 - p] \tag{2.42}$$

the expression (2.42) can be understood as the probability of a bad event occurring, since x^* does not satisfy (2.40b). By setting $\beta \in [0, 1]$ as a very small pessimistic probability level (e.g., $\beta = 10^{-9}$), it is intended that for (2.42) the following is satisfied

$$\mathbb{P}[V(x^*) > 1 - p] \leq \beta$$

the left part of the above expression is reformulated in terms of the number of decision variables d, the number of scenarios C and the probability p, through the binomial cumulative probability function which represents the probability of having no more than $d - 1$ successes in C Bernoulli trials with a probability of success $1 - p$

$$\sum_{j=0}^{d-1} \binom{C}{j} (1-p)^j p^{C-j} \leq \beta \tag{2.43}$$

hence, the number of scenarios C can be obtained as the minimum value that satisfies the condition (2.43), or by its approximation using the Chernoff bound for the Binomial tail

$$C \geq \frac{2}{1-p}\left(\ln\left(\frac{1}{\beta}\right) + d\right)$$

where, according to Theorem 3.1 in [51], it holds that any optimal solution x^*, feasible or not, obtained by the scenario program (2.41) has a guaranteed feasibility level $1-\beta$ of satisfying the constraints (2.41b), or the probabilistic constraints (2.40b).

Also, in [29] provides another straightforward way to calculate C that is the following inequality

$$C \geq \frac{d + 1 + \ln\left(\frac{1}{\beta}\right) + \sqrt{2(d+1)\ln\left(\frac{1}{\beta}\right)}}{1-p}. \tag{2.44}$$

Note that in both (2.43) and (2.44), the computation of C only depends on the probability levels set and the number of decision variables; and its value grows as p does or β diminishes. The latter can be seen in Figure 2.2, which shows the scenarios obtained using (2.43), with a fixed $d = 5$ and for various values of p and β.

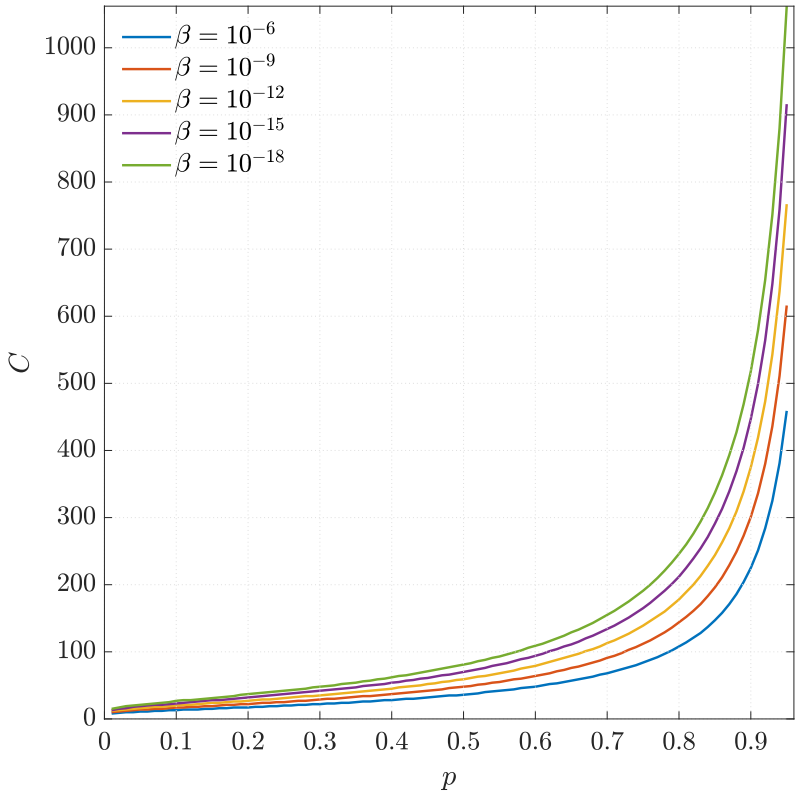

Figure 2.2: Number of computed scenarios C using inequality (2.43), with a fixed $d = 5$ and various values of p and β.

Finally, in the context of the SCMPC (2.38), by establishing a desired probability of constraints satisfaction p, a very low confidence level β, and with the number of decision variables given by $d = n_u N$, the probabilistic constraints (2.14) $\mathbb{P}_k[x_{i+1|k} \in \mathbb{X}] \geq p$ can be transformed into C deterministic constraints, where the number of C scenarios to be used is determined using either (2.43) or (2.44).

Matrices K and P

For systems such as (2.34a), such matrices are obtained from a quadratic stability analysis from Lyapunov's approach [19], [90], [99]. For example, consider the polytopic system (2.45a) and the control law (2.45b), where the pairs $[A_k, B_k]$ form the polytope of uncertainty Ω, $[A_k, B_k] \in \Omega$ and whose convex hull Co of L vertices is given by $\Omega = Co\{[A_1, B_1], [A_2, B_2], \ldots, [A_L, B_L]\}$

$$x_{i+1} = A_k x_i + B_k u_i \tag{2.45a}$$
$$u_i = K x_i \tag{2.45b}$$
$$\forall i \in \{0, 1, \ldots\}, \qquad \forall k \in \{1, 2, \ldots, L\}. \tag{2.45c}$$

Replacing (2.45b) in (2.45a) yields the following autonomous system

$$x_{i+1} = (A_k + B_k K) x_i \tag{2.46}$$

where the matrix $A_k + B_k K$ will be strictly stable, i.e., its eigenvalues lie inside the unit circle or all trajectories of (2.46) converge to zero $x_\infty = 0$, only if there exists a positive definite hermitian P matrix ($P > 0$) such that for the quadratic Lyapunov function $V(x_i)$ it holds that

$$V(x_i) = x_i^\top P x_i \tag{2.47a}$$
$$\Delta V(x_i) \leq 0 \tag{2.47b}$$

with $\Delta V(x_i) = V(x_{i+1}) - V(x_i)$, using (2.46) can be expressed as

$$\Delta V(x_i) = x_i^\top \left[(A_k + B_k K)^\top P (A_k + B_k K) - P \right] x_i.$$

Let $J(x_i)$ be a desired quadratic performance index for the system (2.45a) with input (2.45b)

$$\begin{aligned} J(x_i) &= \sum_{i=0}^{\infty} (x_i^\top Q x_i + u_i^\top R u_i) \\ &= \sum_{i=0}^{\infty} x_i^\top (Q + K^\top R K) x_i \end{aligned} \tag{2.48}$$

where, in order to achieve asymptotic stability for (2.45a), it must be satisfied that (2.47a) is the upper bound of (2.48) $J(x_i) \leq V(x_i)$ (see section 8.4 in [19]

for more details). Since $x_\infty = 0$ (hence $V(x_\infty) = 0$), such an inequality can be expressed in terms of $\Delta V(x_i)$, that is

$$J(x_i) \leq -\sum_{i=0}^{\infty} \Delta V(x_i),$$

$$\sum_{i=0}^{\infty} x_i^\top (Q + K^\top R K) x_i \leq -\sum_{i=0}^{\infty} x_i^\top \left[(A_k + B_k K)^\top P (A_k + B_k K) - P \right] x_i,$$

$$\sum_{i=0}^{\infty} x_i^\top \left[(A_k + B_k K)^\top P (A_k + B_k K) - P \right] x_i + \sum_{i=0}^{\infty} x_i^\top (Q + K^\top R K) x_i \leq 0,$$

$$\sum_{i=0}^{\infty} x_i^\top \left[(A_k + B_k K)^\top P (A_k + B_k K) - P + Q + K^\top R K \right] x_i \leq 0$$

which is true for any x_i if it holds that

$$(A_k + B_k K)^\top P (A_k + B_k K) - P + Q + K^\top R K \leq 0. \tag{2.49}$$

The expression (2.49) represents the so-called discrete Lyapunov inequality. Making the change of variables $K = Y X^{-1}$ and $P = X^{-1}$, and premultiplying and postmultiplying (2.49) by X

$$X - (A_k X + B_k Y)^\top X^{-1} (A_k X + B_k Y) - X Q X - Y^\top R Y \geq 0. \tag{2.50}$$

Via (2.50), Y and X can be obtained by solving the problem of eigenvalues (EVP) (2.51a) [19], [99]; subject to constraint (2.51b), which represents a linear matrix inequality (LMI) in terms of the vertices of Ω

$$\max_{X,Y} \ \operatorname{tr}(X) \tag{2.51a}$$

s.t.

$$\begin{bmatrix} X & 0 & 0 & A_k X + B_k Y \\ 0 & Q^{-1} & 0 & X \\ 0 & 0 & R^{-1} & Y \\ (A_k X + B_k Y)^\top & X^\top & Y^\top & X \end{bmatrix} \geq 0 \tag{2.51b}$$

$$\forall k \in \{1, 2, \ldots, L\} \tag{2.51c}$$

where $\operatorname{tr}(X)$ is the trace of X. With the solution of (2.51), finally

$$K = Y X^{-1} \tag{2.52a}$$

$$P = X^{-1}. \tag{2.52b}$$

2.4 Comparison of Stochastic MPCs Through Numerical Examples

In this section, two examples are presented in which various MPCs were evaluated by performing N_r Monte Carlo simulations for each control scheme, always starting from the same initial state $x_{0|0}$ and assuming that the state measurements are accurate. The performances of the MPCs were analysed through the following performance indices

- N_s: number of simulations from N_r where no constraints were violated.
- p_s: probability of success of a simulation, $p_\mathrm{s} = N_\mathrm{s}/N_\mathrm{r}$.
- N_v: number of constraints violated in all N_r simulations.
- $\mathrm{IAE}_\mathrm{avg}$: mean value of the integral absolute error of the states, based on the closed-loop system responses of the N_r simulations.
- $\mathrm{IAU}_\mathrm{avg}$: mean value of the integral of the absolute value of the applied inputs of all N_r.
- t_avg: average time taken for the algorithm to obtain a solution.
- σ_max: maximum standard deviation of the states with constraints.
- PO_avg: average percentage overshoot of constraints in the violated states.
- C_OCP: number of OCP constraints.

A 64-bit Windows 10 computer, 16 GB of RAM and 2.5 GHz Intel Core i7 processor was used. Simulations were run in Matlab R2018b; control actions for classic MPC, CC-MPC and SCMPC were calculated using the quadprog toolbox of the Mosek 9.2 optimisation software and Matlab fminimax function for the Robust SCMPC.

Furthermore, for reproducible results, the specialised *Stochastic Model Predictive Control Toolbox* software was developed in Matlab for the realisation of a part of the simulations in this section. This software allows simulating (Matlab's quadprog solver is used for optimisation) a CC-MPC or SCMPC to control multivariable systems with additive disturbances and is available at MATLAB Central [100] so that the reader can reproduce the results of this section or use it in other systems.

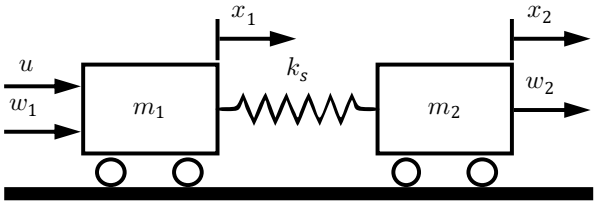

Figure 2.3: Two-mass spring system.

2.4.1 Example 1: Two-Mass Spring System

Consider the two-mass spring system [23], [101] with friction-less sliding of Figure 2.3 where the masses m_1 with position x_1 and m_2 with position x_2 are linked by a spring with elastic constant k_s. The control input u is a force acting on m_1 and w_1 and w_2 are external disturbances acting on m_1 and m_2, respectively.

The system's equations of motion using x_3 as the linear velocity of m_1 and x_4 as the linear velocity of m_2 are

$$\begin{aligned}\dot{x}_1 &= x_3\\ \dot{x}_2 &= x_4\\ m_1\dot{x}_3 &= -k_s(x_1 - x_2) + u + w_1\\ m_2\dot{x}_4 &= k_s(x_1 - x_2) + w_2.\end{aligned}$$

Setting the state vectors as $x = [x_1\ x_2\ x_3\ x_4]^\top$ and additive disturbances as $w = [w_1\ w_2]^\top$; its representation in the discrete state space by Euler's approximation method, for a sampling time T_s is

$$x_{k+1} = Ax_k + Bu_k + Gw_k$$

$$A = \begin{bmatrix} 1 & 0 & T_\mathrm{s} & 0\\ 0 & 1 & 0 & T_\mathrm{s}\\ -\frac{k_s T_\mathrm{s}}{m_1} & \frac{k_s T_\mathrm{s}}{m_1} & 1 & 0\\ \frac{k_s T_\mathrm{s}}{m_2} & -\frac{k_s T_\mathrm{s}}{m_2} & 0 & 1 \end{bmatrix},\quad B = \begin{bmatrix} 0\\ 0\\ \frac{T_\mathrm{s}}{m_1}\\ 0 \end{bmatrix},\quad G = \begin{bmatrix} 0 & 0\\ 0 & 0\\ \frac{T_\mathrm{s}}{m_1} & 0\\ 0 & \frac{T_\mathrm{s}}{m_2} \end{bmatrix}$$

where $m_1,\ m_2 = 1$ kg are constant, $T_\mathrm{s} = 0.1$ s (this was selected fulfilling the Nyquist–Shannon sampling theorem, taking the highest frequency of the poles of the system) and the constraints $|x_3|, |x_4| \leq 0.12$m/s must be satisfied.

The elastic constant k_s is associated with parametric uncertainties δ and it has a uniform probability distribution $k_s \sim \mathcal{U}([0.5, 2.0])$N/m. The additive disturbances

w have a normal distribution $w \sim \mathcal{N}(0, \Sigma_w)$N with zero mean and covariance matrix $\Sigma_w = \text{diag}(0.022^2, 0.022^2)$.

For all controllers $Q = \text{diag}(1, 1, 4, 6)$, $R = 1$, where $N = 6$, hence 6 decision variables given a single input. The probability level of constraint satisfaction for CC-MPC and SCMPC is $p = 0.95$ for both. Setting $\beta = 10^{-9}$ and replacing together with p in (2.44), produces $C = 896$ scenarios for the SCMPC.

Three cases were established based on the parameter k_s to evaluate the performance of five MPCs. classic without constraints (MPC n/c), classic with constraints (MPC w/c), CC-MPC, SCMPC and Robust SCMPC:

- Case 1: k_s is known, constant and it is set to its nominal value $k_s = 1.25$.
- Case 2: k_s is unknown and varies according to its probability distribution at every control period.
- Case 3: k_s is unknown and remains constant for all instants along each simulation. The k_s value varies according to its probability distribution in each simulation.

For each case, $N_{\text{r}} = 100$ simulations with $N_{T_{\text{s}}} = 100$ sampling times of duration were performed, starting from the initial state $x_{0|0} = \hat{x}_0 = [0.5\ 0.5\ 0\ 0]^\top$ towards the origin as the desired state.

For Case 1, the feedback matrix K and the terminal state weighting P are obtained from solving a Quadratic Optimal Control Problem (LQR) [19], [28]

$$K = \begin{bmatrix} -2.876 \\ 1.683 \\ -3.187 \\ -0.904 \end{bmatrix}^\top, \qquad P = \begin{bmatrix} 155.739 & -102.335 & 43.512 & 77.451 \\ -102.335 & 117.489 & -26.755 & -30.134 \\ 43.512 & -26.755 & 40.392 & 15.371 \\ 77.451 & -30.134 & 15.371 & 126.794 \end{bmatrix}.$$

For Cases 2 and 3, they are obtained by solving an eigenvalues problem (EVP); through a stability analysis of Lyapunov's approach [19], [90], [99], such matrices are

$$K = \begin{bmatrix} -56.563 \\ 41.356 \\ -15.171 \\ -45.156 \end{bmatrix}^\top, \qquad P = \begin{bmatrix} 4509 & -3280 & 971 & 3801 \\ -3280 & 2450 & -709 & -2706 \\ 971 & -709 & 244 & 791 \\ 3801 & -2706 & 791 & 3462 \end{bmatrix}.$$

Table 2.1: MPCs performance indices for Case 1.

Controller	N_s	p_s	N_v	$\mathrm{IAE}_\mathrm{avg}$	$\mathrm{IAU}_\mathrm{avg}$	t_avg	σ_max	PO_avg	C_OCP
MPC n/c	0	0.00	2416	43.88	5.35	5.6 ms	0.009	20.98%	0
MPC w/c	3	0.03	702	49.01	7.29	5.9 ms	0.031	2.45%	24
CC-MPC	64	0.64	135	49.85	7.39	5.7 ms	0.029	1.78%	24
SCMPC	84	0.84	168	50.61	7.55	79.0 ms	0.036	6.78%	21504
SCMPC (robust)	74	0.74	30	52.50	8.70	235.7 ms	0.054	6.01%	21504

Case 1 Results

Table 2.1 shows high probabilities of success p_s (0.84, 0.74 and 0.64) by the stochastic MPCs. However, the biggest success of the SCMPC and Robust SCMPC required longer times t_avg (79.0 ms and 235.7 ms) to obtain the control sequence than CC-MPC (5.7 ms), which works as a classic MPC with constraints. This makes sense since in each iteration SCMPC and Robust SCMPC select 896 random realisations for w and solve the OCP (2.38) for all of them ($C_\mathrm{OCP} = 21504$ constraints) using (2.37) or (2.39).

Figure 2.4 shows the $N_\mathrm{r} = 100$ trajectories made by the real states and input (thin solid lines), starting from $\hat{x}_0 = [0.5\ 0.5\ 0\ 0]^\top$ towards the origin. The MPC n/c (Figure 2.4a), having no constraints, presents the highest violations ($N_\mathrm{v} = 2416$) and overshoots ($\mathrm{PO}_\mathrm{avg} = 20.98\%$), while the mean trajectories (thick solid lines) of the constrained MPCs do not exceed the limits (black dashed lines).

Notice how stochastic approaches (Figures 2.4c–e) are within these limits or barely exceed them, showing that the probability that a state is within the allowed limits is 68%. The largest standard deviations σ_max occurred in the scenario-based MPCs (0.036 and 0.054) due to the randomness mentioned in [36] and because the worst case is not always the closest to reality (hence, the highest $\mathrm{IAE}_\mathrm{avg}$ (52.50) and $\mathrm{IAU}_\mathrm{avg}$ (8.70) of all). Also note that the conservatism of the Robust SCMPC provides it with the lowest number of violated constraints ($N_\mathrm{v} = 30$) of the MPCs. However, its probability of success ($p_\mathrm{s} = 0.74$) is below that of the SCMPC ($p_\mathrm{s} = 0.84$), which has the highest number of violated constraints ($N_\mathrm{v} = 168$). This is because the 30 constraints violations of the Robust SCMPC are concentrated in 26 unsuccessful runs, while the 168 of the SCMPC are concentrated only in 16 unsuccessful runs.

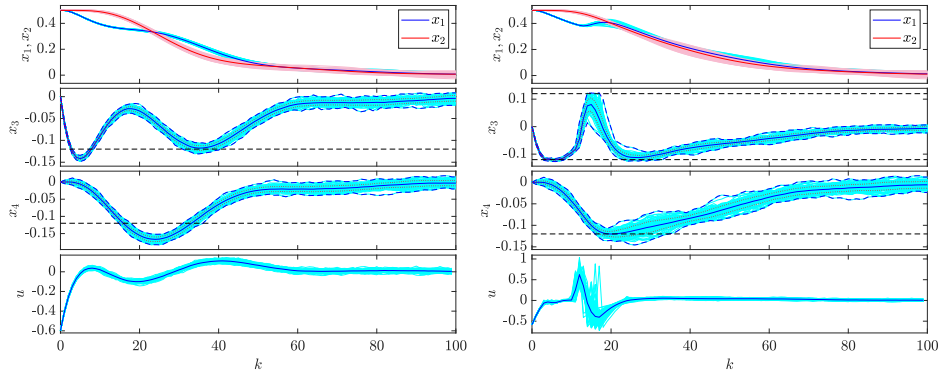

(a) MPC n/c

(b) MPC w/c

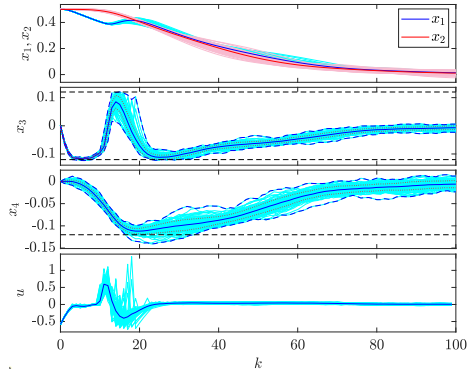

(c) CC-MPC ($p = 0.95$)

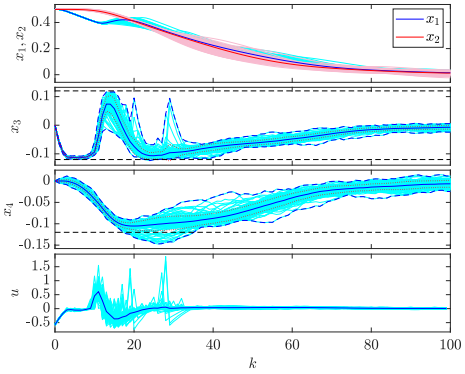

(d) SCMPC ($p = 0.95, C = 896$)

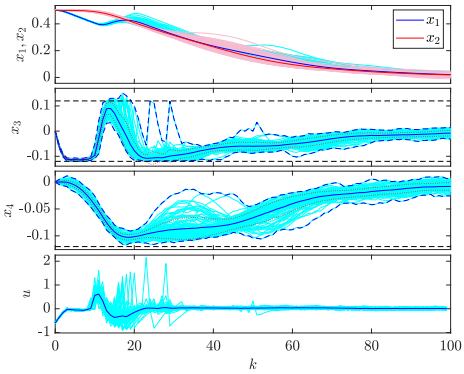

(e) Robust SCMPC ($p = 0.95, C = 896$)

Figure 2.4: Case 1: Two-mass spring system controlled with different MPCs, for 100 Monte Carlo simulations. Trajectories of the real states and input (thin solid lines), mean value (thick solid lines), mean value with standard deviation (dotted lines), minimum and maximum values (blue dashed lines) and constraints (black dashed lines) $|x_3|, |x_4| \leq 0.12$.

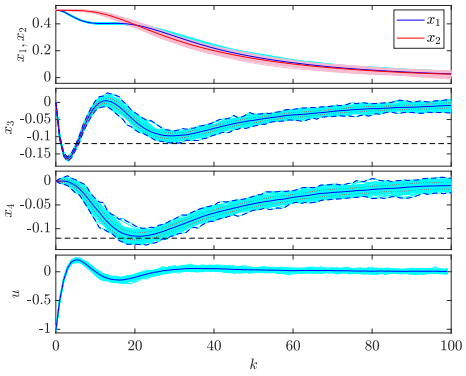

(a) MPC n/c

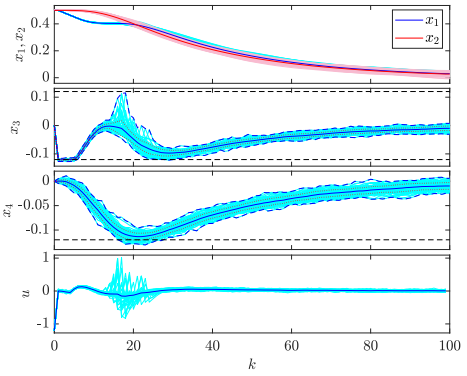

(b) MPC w/c

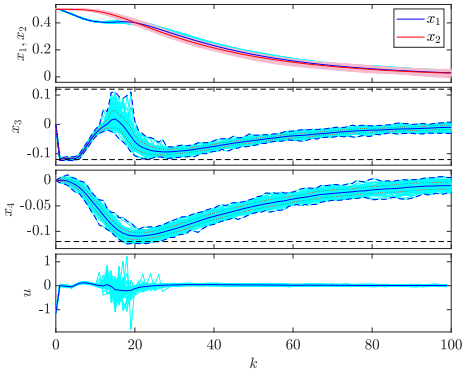

(c) CC-MPC ($p = 0.95$)

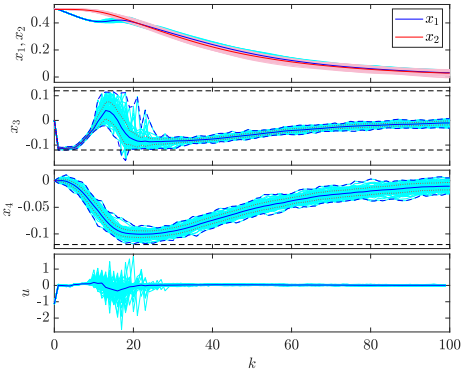

(d) SCMPC ($p = 0.95, C = 896$)

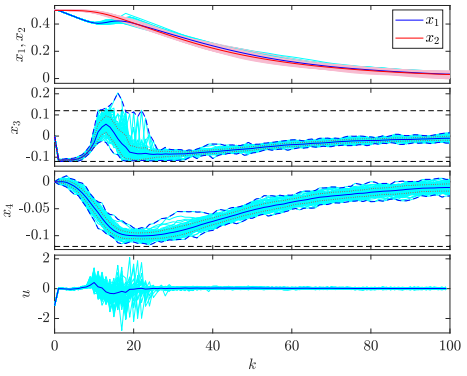

(e) Robust SCMPC ($p = 0.95, C = 896$)

Figure 2.5: Case 2: Two-mass spring system controlled with different MPCs, for 100 Monte Carlo simulations. Trajectories of the real states and input (thin solid lines), mean value (thick solid lines), mean value with standard deviation (dotted lines), minimum and maximum values (blue dashed lines) and constraints (black dashed lines) $|x_3|, |x_4| \leq 0.12$.

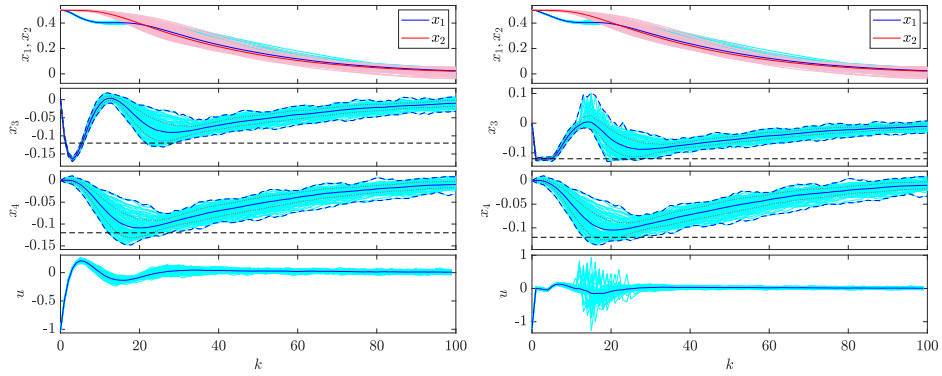

(a) MPC n/c

(b) MPC w/c

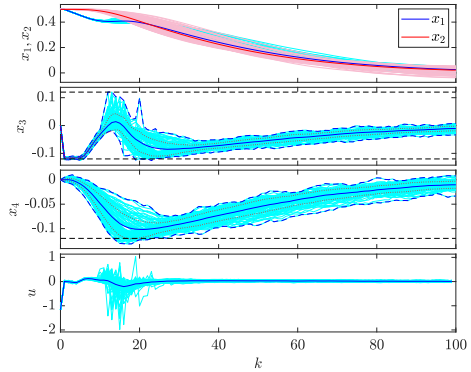

(c) CC-MPC ($p = 0.95$)

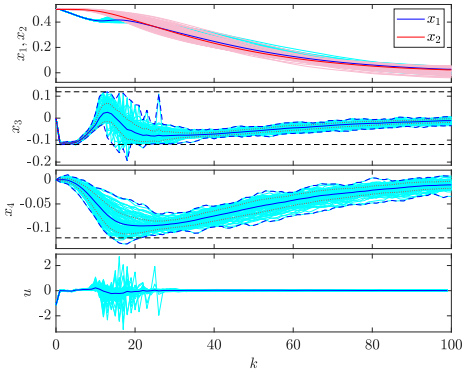

(d) SCMPC ($p = 0.95, C = 896$)

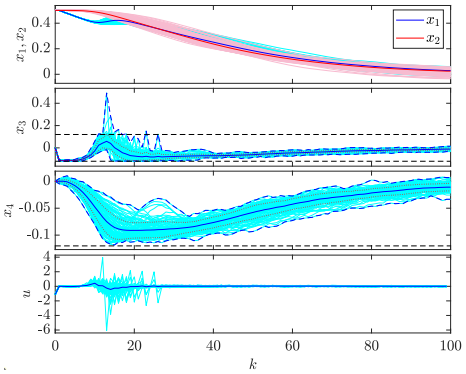

(e) Robust SCMPC ($p = 0.95, C = 896$)

Figure 2.6: Case 3: Two-mass spring system controlled with different MPCs, for 100 Monte Carlo simulations. Trajectories of the real states and input (thin solid lines), mean value (thick solid lines), mean value with standard deviation (dotted lines), minimum and maximum values (blue dashed lines) and constraints (black dashed lines) $|x_3|, |x_4| \leq 0.12$.

Table 2.2: MPCs performance indices for Case 2.

Controller	N_s	p_s	N_v	$\mathrm{IAE}_\mathrm{avg}$	$\mathrm{IAU}_\mathrm{avg}$	t_avg	σ_max	PO_avg	C_OCP
MPC n/c	0	0.00	611	50.58	6.16	6.3 ms	0.010	20.97%	0
MPC w/c	4	0.04	362	51.37	5.59	6.4 ms	0.027	1.75%	24
CC-MPC	65	0.65	77	51.98	5.87	6.3 ms	0.031	1.13%	24
SCMPC	94	0.94	7	52.91	6.96	220.3 ms	0.045	13.67%	21504
SCMPC (robust)	86	0.86	21	53.14	8.70	311.8 ms	0.055	6.29%	21504

Table 2.3: MPCs performance indices for Case 3.

Controller	N_s	p_s	N_v	$\mathrm{IAE}_\mathrm{avg}$	$\mathrm{IAU}_\mathrm{avg}$	t_avg	σ_max	PO_avg	C_OCP
MPC n/c	0	0.00	754	51.27	6.14	5.8 ms	0.028	19.38%	0
MPC w/c	1	0.01	462	52.16	5.74	6.1 ms	0.032	2.07%	24
CC-MPC	57	0.57	107	52.56	5.73	5.9 ms	0.036	1.90%	24
SCMPC	85	0.85	28	53.42	6.95	220.9 ms	0.046	11.22%	21504
SCMPC (robust)	79	0.79	27	53.97	8.67	327.5 ms	0.062	28.23%	21504

Case 2 Results

The performance indices and the closed-loop trajectories are shown in Table 2.2 and Figure 2.5, respectively. As in Case 1, stochastic MPCs had the highest p_s, observing an increase in the scenario-based schemes (0.94 and 0.86), despite the randomness of k_s. Nevertheless, these schemes are the ones who take the longest to calculate the solution t_avg (220.3 ms and 311.8 ms) due to the fact that, in addition to selecting 896 random scenarios for w, it should also be done for k_s.

As seen in Figure 2.5, the mean trajectories that include the standard deviations of the stochastic MPCs are the only ones that stay within the limits, indicating that the probability that a state is within the allowed limits is 68%. This kind of robustness on stochastic strategies implies high values of $\mathrm{IAE}_\mathrm{avg}$ and $\mathrm{IAU}_\mathrm{avg}$ indicators compared to the others.

Case 3 Results

As can be seen in Table 2.3 and Figure 2.6, it is once again corroborated that the highest p_s and average trajectories with standard deviations within the limits belongs to stochastic MPCs.

Regarding Case 2, the indicators t_{avg} are very similar, but for this case higher standard deviations σ_{max} of the three cases are observed. The high PO_{avg} (28.23%) presented by the robust SCMPC can be seen in the trajectories of the x_3 (Figure 2.6e) state; however, this strategy presents the lowest N_v (27) of all MPCs.

2.4.2 Example 2: Quadruple-Tank System

Consider the quadruple-tank system [102], [103] of Figure 2.7, in which the aim is to control the level of liquid h_i in tank $i\ \forall i \in \{1,2,3,4\}$, by means of pumps 1 and 2 whose flows are proportional to the applied voltage ($Q_{\mathbb{P}_1} = k_1 v_1$, $Q_{\mathbb{P}_2} = k_2 v_2$) and are distributed by the valves in proportions determined by $\gamma_1, \gamma_2 \in [0,1]$

Let A_i be the cross section of tank i; a_i and a_{12} are the areas of the tank outlet pipes; and g is the acceleration due to gravity. By performing a mass balance and applying Bernoulli's law, the equations that describe the behaviour of the nonlinear system are given by

$$\begin{aligned}
\frac{dh_1}{dt} &= -\frac{a_1}{A_1}\sqrt{2gh_1} - \frac{a_{12}}{A_1}\text{sgn}(h_1-h_2)\sqrt{2g|h_1-h_2|} + \frac{(1-\gamma_2)k_2}{A_1}v_2,\\
\frac{dh_2}{dt} &= -\frac{a_2}{A_2}\sqrt{2gh_2} + \frac{a_{12}}{A_2}\text{sgn}(h_1-h_2)\sqrt{2g|h_1-h_2|} + \frac{(1-\gamma_1)k_1}{A_2}v_1,\\
\frac{dh_3}{dt} &= \frac{a_1}{A_3}\sqrt{2gh_1} - \frac{a_3}{A_3}\sqrt{2gh_3} + \frac{\gamma_1 k_1}{A_3}v_1,\\
\frac{dh_4}{dt} &= \frac{a_2}{A_4}\sqrt{2gh_2} - \frac{a_4}{A_4}\sqrt{2gh_4} + \frac{\gamma_2 k_2}{A_4}v_2.
\end{aligned} \tag{2.53}$$

Let us define the state vectors $x = [x_1\ x_2\ x_3\ x_4]^\top$ and inputs $u = [u_1\ u_2]^\top$; where $x_i = h_i - h_i^0$ and $u_i = v_i - v_i^0$ represent the deviations from the operating point $P^0 = \{h_1^0, h_2^0, h_3^0, h_4^0, v_1^0, v_2^0\} = \{7.873\text{cm}, 8.187\text{cm}, 7.720\text{cm}, 8.039\text{cm}, 4.0\text{V}, 3.5\text{V}\}$. Linearising around P^0 and using Euler's approximation, for a sampling period T_s, the linear model in the discrete state space can be represented by

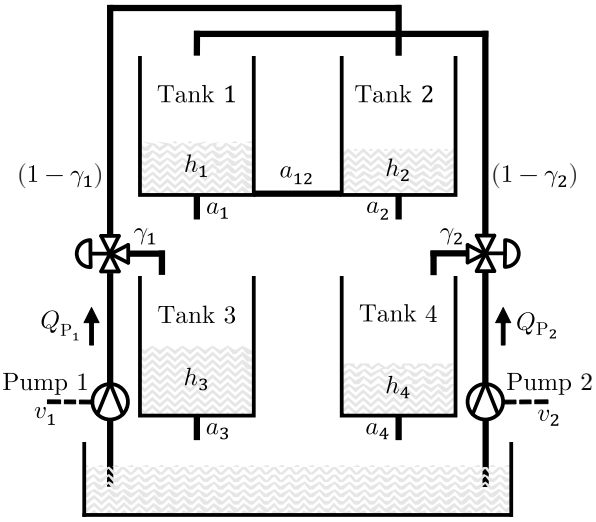

Figure 2.7: Quadruple-tank system.

$$x_{k+1} = Ax_k + Bu_k,$$

$$A = \begin{bmatrix} -\frac{\beta_1+\beta_x}{A_1}+1 & \frac{\beta_x}{A_1} & 0 & 0 \\ \frac{\beta_x}{A_2} & -\frac{\beta_2+\beta_x}{A_2}+1 & 0 & 0 \\ \frac{\beta_1}{A_3} & 0 & -\frac{\beta_3}{A_3}+1 & 0 \\ 0 & \frac{\beta_2}{A_4} & 0 & -\frac{\beta_4}{A_4}+1 \end{bmatrix},$$

$$B = \begin{bmatrix} 0 & \frac{(1-\gamma_2)k_2}{A_1}T_\mathrm{s} \\ \frac{(1-\gamma_1)k_1}{A_2}T_\mathrm{s} & 0 \\ \frac{\gamma_1 k_1}{A_3}T_\mathrm{s} & 0 \\ 0 & \frac{\gamma_2 k_2}{A_4}T_\mathrm{s} \end{bmatrix}, \qquad \beta_i = a_i\sqrt{\tfrac{g}{2h_i^0}}T_\mathrm{s}, \qquad \beta_x = a_{12}\sqrt{\tfrac{g}{2|h_1^0-h_2^0|}}T_\mathrm{s}$$

where $A_i = 144$ cm^2, $a_1, a_2, a_{12} = 0.352$ cm^2, $a_3, a_4 = 1.006$ cm^2; $k_1, k_2 = 33.333$cm^3/Vs; $\gamma_1 = 0.6$, $\gamma_2 = 0.7$; $g = 981$cm/s^2, $T_\mathrm{s} = 5$ s.

The constraints $|x_3|, |x_4| \leq 1.5$cm, $|u_1|, |u_2| \leq 1.0$V must be satisfied, and the process has additive disturbances w in its states, with normal distribution $w \sim \mathcal{N}(0, \Sigma_w)$cm with zero mean and covariance matrix $\Sigma_w = \mathrm{diag}(0.1^2, 0.1^2, 0.1^2, 0.1^2)$, which are truncated $|w_i| \leq 0.3$cm and $G = \mathrm{diag}(1, 1, 1, 1)$.

Table 2.4: Performance indices.

Controller	N_s	p_s	N_v	IAE_{avg}	IAU_{avg}	t_{avg}	σ_{max}	PO_{avg}	C_{OCP}
MPC w/c	2	0.02	263	78.63	21.51	6.7 ms	0.218	5.76%	40
SCMPC $\left(\begin{smallmatrix} p=0.6 \\ C=133 \end{smallmatrix}\right)$	87	0.87	15	78.40	21.22	12.3 ms	0.218	1.55%	5320
SCMPC $\left(\begin{smallmatrix} p=0.7 \\ C=177 \end{smallmatrix}\right)$	88	0.88	14	78.39	21.21	14.2 ms	0.218	1.60%	7080
SCMPC $\left(\begin{smallmatrix} p=0.8 \\ C=266 \end{smallmatrix}\right)$	91	0.91	10	78.38	21.18	18.1 ms	0.218	1.78%	10640
SCMPC $\left(\begin{smallmatrix} p=0.9 \\ C=531 \end{smallmatrix}\right)$	93	0.93	7	78.36	21.15	30.3 ms	0.217	1.06%	21240
SCMPC $\left(\begin{smallmatrix} p=0.95 \\ C=1062 \end{smallmatrix}\right)$	94	0.94	6	78.35	21.14	57.3 ms	0.217	0.48%	42480

To analyse the effect of the desired probabilities p of constraints satisfaction, on the number of considered scenarios C and on the different performance indicators, this example compares the performance of a SCMPC for five values of $p(0.6,\ 0.7,\ 0.8,\ 0.9,\ 0.95)$, $\beta = 10^{-9}$ with a constrained classic MPC (MPC w/c). For each scheme, $N_r = 100$ runs were carried out on the nonlinear model (2.53), each one with $N_{T_s} = 40$ sampling times of duration, starting from the initial state $x_{0|0} = \hat{x}_0 = [-5.5\ \ -6.9\ \ -0.5\ \ -0.2]^\top$ towards the origin as the desired state.

For all controllers, $N = 5$ (thus, each OCP consists of 10 decision variables), $Q = \text{diag}(10, 10, 1, 1)$, $R = \text{diag}(1, 1)$. Matrices K and P are

$$K = \begin{bmatrix} -0.745 & -0.649 & -0.153 & 0.054 \\ -0.556 & -0.662 & 0.045 & -0.245 \end{bmatrix},$$

$$P = \begin{bmatrix} 13.275 & 3.341 & -0.839 & -0.811 \\ 3.341 & 13.438 & -0.884 & -0.809 \\ -0.839 & -0.884 & 1.870 & 0.140 \\ -0.811 & -0.809 & 0.140 & 1.689 \end{bmatrix}.$$

Results

Table 2.4 shows the performance indices of the MPC w/c and the SCMPC, for the $N_r = 100$ runs, while Figure 2.8 depicts the closed loop simulations. SCMPCs showed the lowest violations, in both quantity N_v (15, 14, 10, 7 and 6) and percentage of deviation PO_{avg} (1.55%, 1.60%, 1.78%, 1.06% and 0.48%) compared to the MPC w/c ($N_v = 263$ and $\text{PO}_{avg} = 5.76\%$).

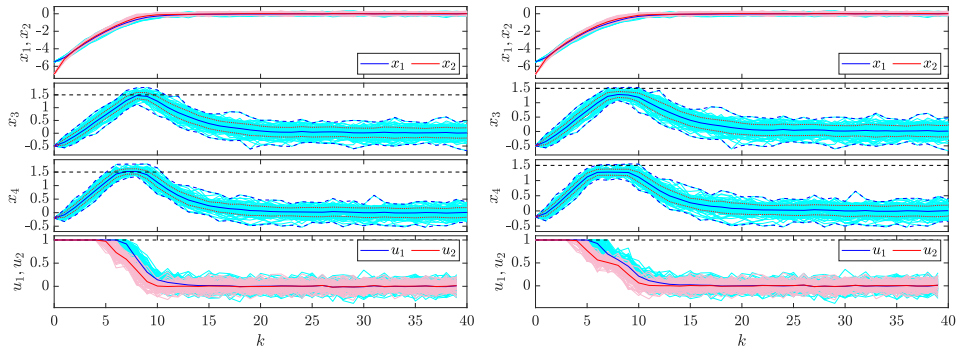

(a) MPC w/c

(b) SCMPC ($p = 0.6, C = 133$)

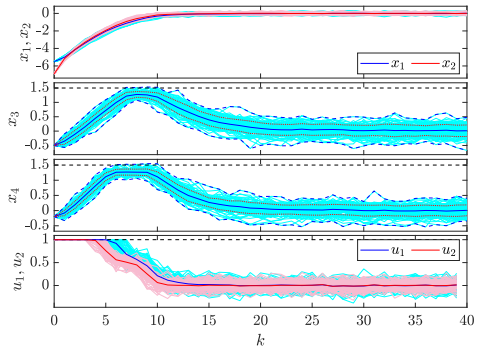

(c) SCMPC ($p = 0.7, C = 177$)

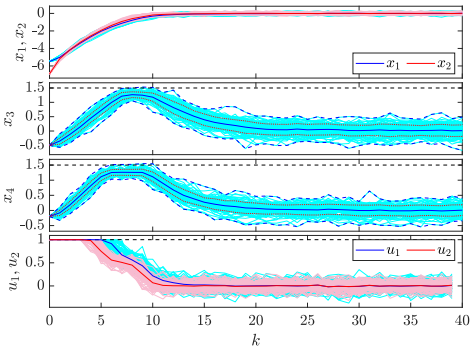

(d) SCMPC ($p = 0.8, C = 266$)

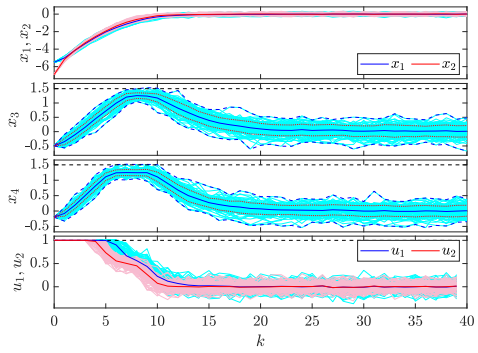

(e) SCMPC ($p = 0.9, C = 531$)

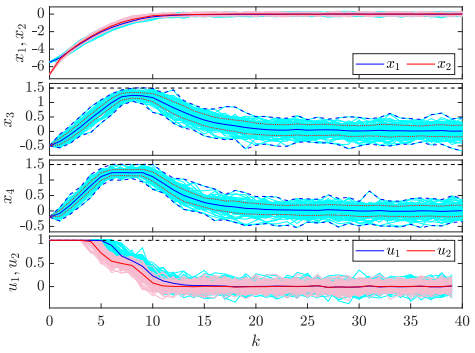

(f) SCMPC ($p = 0.95, C = 1062$)

Figure 2.8: Quadruple-tank system controlled with a constrained MPC and a SCMPC for multiple p values, for 100 Monte Carlo simulations. Trajectories of the real states and inputs (thin solid lines), mean value (thick solid lines), mean value with standard deviation (dotted lines), minimum and maximum values (blue dashed lines) and constraints (black dashed lines) $|x_3|, |x_4| \leq 1.5$, $|u_1|, |u_2| \leq 1.0$.

Furthermore, the stochastic scheme shows high values of successful runs N_s (87, 88, 91, 93 and 94) and probabilities of success p_s (0.87, 0.88, 0.91, 0.93 and 0.94), which increase in line with p. However, this improvement in p_s leads to an increase in the number of scenarios C (133, 177, 266, 531 and 1062) to be considered in the OCP (2.38), and hence an increase in the average time that the algorithm takes to find a solution at each instant k (t_{avg} (12.3 ms, 14.2 ms, 18.1 ms and 30.3 ms).

Regarding the indices IAE_{avg}, IAU_{avg} and σ_{max}, despite not observing a considerable difference between controllers, it can be concluded that the higher the p, the higher the performance values.

As can be seen in the Figure 2.8, all the $N_r = 100$ trajectories made by the states (thin solid lines) start from $N_r = 100$ towards the origin, where the mean trajectories (thick solid lines) of the SCMPCs are considerably far from the constraints (black dashed lines), opposite to that of the MPC w/c that passes very close and even violates them (that's why the highest $PO_{avg} = 5.76\%$ of them).

On the other hand, for SCMPCs, the average trajectories that include the standard deviations (dashed lines) are within the limits. It means that the probability that a state is within the allowed limits is 68%. As for the applied inputs, they start at their maximum allowed values and decrease as the states converge towards the origin

2.5 Chapter Conclusions

In this chapter, an overview of the main concepts of stochastic model predictive control was provided. Likewise, two stochastic model predictive control approaches were compared; one based on analytical methods (CC-MPC) and the other based on scenarios (SCMPC). The low computational cost of the CC-MPC is because the statistical information on uncertainties is used offline to adjust the states constraints. However, if this information changes, it cannot be considered during operation. On the other hand, this new statistical information can be incorporated into the SCMPC to generate the scenarios online, but it leads to a high computational cost.

It is shown that the CC-MPC can be summed up in a deterministic OCP (2.33) whose structure is similar to that of a classic MPC with constraints (2.10), with similar computational cost t_{avg}, but with a considerable increase in the probability of success p_s, due to offline constraint adjustment.

Scenario-based approaches SCMPC and robust SCMPC, compared to the others, gave the highest probabilities of success, at the expense of a high computational cost, since they need to solve an OCP with C random scenarios for each control period. From results shown in Table 2.4, can be concluded that an increase in the parameter p, related to the desired probability of constraints satisfaction for the state constraints, produces an increase in the probability of success p_{s}. However, this improvement results in an increase in the number of C scenarios to be considered in the OCP and therefore an increase in the average time t_{avg} that the algorithm takes to find a solution at each sampling time.

It is clear that the consideration of statistical information of the uncertainties of the process, through its inclusion in the OCP, significantly improves the probability of success p_{s}. This can be verified in Figures 2.4–2.6 and 2.8, where it is observed that only stochastic approaches reached mean trajectories with standard deviations within the limits or barely exceeding them. Thus, for a normal distribution, it means that the probability a state is within the allowed limits is 68%.

Scenario-based schemes are attractive in the sense that they have a greater probability of success and the inclusion of new statistical information online without necessarily known probability distributions. However, due to the randomness of the scenarios, their solutions may exhibit undesirable behaviour in the system as the number of scenarios to be considered in the OCP decreases. Simultaneously, the computational cost increases as the number of scenarios does. These drawbacks would prevent their implementation for the control of systems with fast dynamics such as the two-mass spring system in the example, which has T_{s} (0.1 s) close to the lowest t_{avg} (79.0 ms) of the SCMPCs of the three cases. In line with the above, improvements on issues such as reducing computational effort and the effect of improbable scenarios in scenario-based MPC schemes are of great interest.

Chapter 3

Conditional Scenario-Based Model Predictive Control (CSB-MPC)

This chapter introduces a scenario-based MPC approach called conditional scenario-based model predictive control (CSB-MPC), developed for discrete-time linear systems affected by parametric uncertainties and/or additive disturbances, which are correlated and with bounded support. At each control period, a primary set of equiprobable scenarios is generated and subsequently approximated to a new reduced set of conditional scenarios, each with their respective probabilities of occurrence. This new set is considered for solving an optimal control problem in whose cost function the predicted states and inputs are penalised according to the probabilities associated with the uncertainties on which they depend in order to give more importance to predictions that involve realisations with a higher probability of occurrence. The first section presents the highlights of the proposed CSB-MPC. The second section addresses the type of system to be considered and the formulation of the scenario-based MPC. The third section presents the concept of conditional scenario, its adaptation to MPC context and the CSB-MPC approach. In the fourth section, the proposed MPC strategy is validated by means of two numerical examples, and its performance is contrasted with that of a standard scenario-based MPC. Finally, the fifth section presents the conclusions of this chapter.

3.1 Introduction

Challenges such as improving the constraint satisfaction probabilities and the computational tractability of a scenario-based MPC (SCMPC), mentioned in introduction chapter and in the previous chapter's Conclusions, motivated the development of the new scenario-based MPC approach introduced in this chapter. In summary, the main highlights of the proposal are as follows

- Most stochastic MPC approaches consider systems with either strictly additive or parametric uncertainties; and whose realisations are independent or correlated in time. This proposal addresses discrete-time linear systems with bounded parametric and/or additive uncertainties featuring a correlation between some or the whole set of random variables.
- An algorithm that adapts the conditional scenario (CS) reduction method to the SMPC framework to approximate a primary set of equiprobable scenarios into a reduced set of CSs (that preserve the main characteristics of this primary set) with their probabilities of occurrence. The CS concept was proposed as an approximation to the two-stage stochastic mixed-integer linear programming problems, where a scenario consists of a realisation of the random vector composed of the existing set of uncertainties, which are correlated. In contrast, in the MPC context, a scenario consists of a sequence of various realisations of that vector.
- A cost function where the probabilities of occurrence of the realisations of the uncertainties are used as weights that penalise the states and inputs associated with these realisations. This mitigates the effect of unlikely scenarios on the optimal control problem by giving more relevance to states and inputs with higher probabilities of occurrence.
- The CSB-MPC has a higher probability of constraints satisfaction than a standard scenario-based MPC for the same number of scenarios and offers a similar solution time, sometimes shorter, when a smaller sized primary set is used. With the above in mind, using a CSB-MPC with a smaller number of scenarios is a viable option when a quicker solution time is required but with no performance loss.

3.2 Problem Statement

In this section, the model of the system to be considered and the formulation of a Scenario-based MPC are described.

3.2.1 System Dynamics

Consider an uncertain linear time-invariant (LTI) system whose discrete state-space dynamic is given by (3.1a) in which its input $u \in \mathbb{R}^{n_u}$ is ruled by the state feedback control law (3.1b), and subject to constraints in states (3.1c) and inputs (3.1d), for a given instant of time $i \in \mathbb{N}_0$

$$x_{i+1} = A(\delta_i)x_i + B(\delta_i)u_i + Gw(\delta_i) \tag{3.1a}$$

$$u_i = Kx_i + v_i \tag{3.1b}$$

$$x \in \mathbb{X} \tag{3.1c}$$

$$u \in \mathbb{U} \tag{3.1d}$$

where vectors $x \in \mathbb{R}^{n_x}$, $w(\delta) \in \mathbb{R}^{n_w}$ and $v_k \in \mathbb{R}^{n_u}$ represent the state, exogenous disturbances and the decision variables, respectively. $A(\delta) \in \mathbb{R}^{n_x \times n_x}$ is the state matrix, $B(\delta) \in \mathbb{R}^{n_x \times n_u}$ is the system input matrix, $G \in \mathbb{R}^{n_x \times n_w}$ is a matrix that reflects the effect of $w(\delta)$ on the system states, and $K \in \mathbb{R}^{n_u \times n_x}$ is a feedback matrix that stabilises the system. Constraints (3.1c)-(3.1d) are expressed as linear inequalities (e.g., $Hx \leq h$ for (3.1c), and $Du \leq d$ for (3.1d)).

Vector $\delta \in \mathbb{R}^{n_\delta}$ is a random vector, composed of each of the parametric and additive uncertainties present in the system, represented by the random variable ξ_n $\forall n \in \{1, 2, \ldots, n_\delta\}$. Each ξ_n is assumed bounded $\xi_n \in \mathbb{W}_n$, normally distributed $\xi_n \sim \mathcal{N}(\mu_n, \Sigma_n)$ and with zero mean $\mu_n = 0$; and there is a correlation between some or the whole set of uncertainties $\{\xi_1, \xi_2, \ldots, \xi_{n_\delta}\}$. In other words, vector δ has a multivariate normal distribution $\delta \sim \mathcal{N}_{n_\delta}(\mu, \Sigma)$ with mean vector μ, covariance matrix Σ and bounded support $\delta \in \mathbb{W}_\delta$ where

$$\delta = \begin{bmatrix} \xi_1 \\ \xi_2 \\ \vdots \\ \xi_{n_\delta} \end{bmatrix}, \qquad \mu = \begin{bmatrix} \mu_1 \\ \mu_2 \\ \vdots \\ \mu_{n_\delta} \end{bmatrix}, \qquad \Sigma = \begin{bmatrix} \Sigma_{1,1} & \cdots & \Sigma_{1,n_\delta} \\ \vdots & \ddots & \vdots \\ \Sigma_{n_\delta,1} & \cdots & \Sigma_{n_\delta,n_\delta} \end{bmatrix}$$

with $\Sigma_{n,m} = \mathrm{Cov}(\xi_n, \xi_m)$ $\forall n, m \in \{1, 2, \ldots, n_\delta\}$. Thus, $A(\delta)$, $B(\delta)$ and $w(\delta)$ are random and bounded since all or some of their elements are functions of δ, where, any sequence $\{\delta_0, \delta_1, \ldots\}$ is independent and identically distributed (i.i.d.).

Assumption 3.1. *For a given instant of time i $\forall i \in \{0, 1, \ldots\}$ some or the whole set of uncertainties $\{\xi_{1,i}, \xi_{2,i}, \ldots, \xi_{n_\delta,i}\}$ of the random vector δ_i are correlated in that instant. The vector δ has a multivariate normal distribution $\delta \sim \mathcal{N}_{n_\delta}(\mu, \Sigma)$ and bounded support $\mathbb{W}_\delta$. Any sequence $\{\delta_0, \delta_1, \ldots\}$ is independent and identically distributed (i.i.d.) and can be obtained from experimental data or by means of a random number generator.*

3.2.2 Scenario-based MPC

As outlined in the previous chapter, at each sampling time and with the availability of the current state measure, stochastic MPC strategies use a process model such as (3.1a), whose uncertainties are stochastic in nature and with known probability distributions, to solve an optimal control problem. This OCP solution generates the sequence of future controls to lead states toward the origin or a desired operating point.

According to the above, let k be the current time, $\hat{x}_k$ the state measured at that moment and N the prediction horizon. Model (3.1a) and its input (3.1b), based on dual paradigm, mentioned in the previous chapter, are used to predict the future states $x_{i+1|k}$ $\forall i \in \{0, 1, \ldots, N-1\}$ and inputs $u_{i|k}$, for N steps ahead of k; where the subscript $i|k$ indicates the predicted value of the variable for the instant i, based on the information available at time k, and $x_{0|k} = \hat{x}_k$

$$x_{i+1|k} = A(\delta_{i|k})x_{i|k} + B(\delta_{i|k})u_{i|k} + Gw(\delta_{i|k}) \tag{3.2a}$$

$$u_{i|k} = Kx_{i|k} + v_{i|k}. \tag{3.2b}$$

As discussed in section 2.3, predictions (3.2a) and (3.2b) in stochastic MPC schemes are commonly incorporated into the cost function based on the expected value, denoted by $\mathbb{E}$, in which $\|y\|_W^2 = y^\top W y$

$$J(\hat{x}_k, \boldsymbol{v}_k) = \mathbb{E}\Big[\sum_{i=0}^{N-1} \left(\|x_{i|k}\|_Q^2 + \|u_{i|k}\|_R^2 \right) + \|x_{N|k}\|_P^2 \Big]$$

and that in the scenario-based approaches, this expected cost function is approximated by the sample average (3.3), similar to (2.37), which consists of an average of the predicted trajectories of the states over a horizon N, for a finite number of C realisations of the uncertainties called scenarios

$$\hat{J}(\hat{x}_k, \boldsymbol{v}_k) = \frac{1}{C} \sum_{j=1}^{C} \Big[\sum_{i=0}^{N-1} \left(\|x_{i|k}^{[j]}\|_Q^2 + \|u_{i|k}^{[j]}\|_R^2 \right) + \|x_{N|k}^{[j]}\|_P^2 \Big] \tag{3.3}$$

where matrices $\{Q \in \mathbb{R}^{n_x \times n_x} | Q \geq 0\}$, $\{R \in \mathbb{R}^{n_u \times n_u} | R > 0\}$ and $\{P \in \mathbb{R}^{n_x \times n_x} | P > 0\}$ penalise the states, inputs, and the terminal state $x_{N|k}$, respectively.

The jth scenario, denoted by $\Delta_k^{[j]}$, represent the jth predictions of the uncertainties for N steps

$$\begin{gathered}
\{\Delta_k^{[1]}, \Delta_k^{[2]}, \ldots, \Delta_k^{[C]}\}, \\
\Delta_k^{[j]} = \{\delta_{0|k}^{[j]}, \delta_{1|k}^{[j]}, \ldots, \delta_{N-1|k}^{[j]}\}, \\
\delta_{i|k}^{[j]} = [\xi_{1,i|k}^{[j]}, \xi_{2,i|k}^{[j]}, \ldots, \xi_{n_\delta,i|k}^{[j]}]^\top, \\
\forall i \in \{0, 1, \ldots, N-1\}, \qquad \forall j \in \{1, 2, \ldots, C\}.
\end{gathered}$$

Thus, the jth predicted trajectories of states and inputs are obtained by evaluating (3.2a)-(3.2b) with $\Delta_k^{[j]}$, fulfilling $x_{0|k}^{[j]} = \hat{x}_k$ and the same decision variables $\boldsymbol{v}_k = \{v_{k|k}, v_{k+1|k}, \ldots, v_{k+N-1|k}\}$ for all C. This is

$$x_{i+1|k}^{[j]} = A(\delta_{i|k}^{[j]}) x_{i|k}^{[j]} + B(\delta_{i|k}^{[j]}) u_{i|k}^{[j]} + Gw(\delta_{i|k}^{[j]}), \qquad x_{0|k}^{[j]} = \hat{x}_k \tag{3.4a}$$

$$u_{i|k}^{[j]} = K x_{i|k}^{[j]} + v_{i|k}. \tag{3.4b}$$

For every time k, the control problem in the scenario-based MPC framework is to minimise the cost function (3.3), fulfilling the constraints on states (3.1c) and inputs (3.1d) for all $x_{i+1|k}^{[j]}$ and $u_{i|k}^{[j]}$, and in the terminal state $x_{N|k}^{[j]}$ [40], [104] if required

$$\begin{gathered}
x_{i+1|k}^{[j]} \in \mathbb{X}, \\
u_{i|k}^{[j]} \in \mathbb{U}, \\
x_{N|k}^{[j]} \in \mathbb{X}_T, \\
\forall i \in \{0, 1, \ldots, N-1\}, \qquad \forall j \in \{1, 2, \ldots, C\}.
\end{gathered}$$

The aforementioned is addressed in OCP (3.5), whose solution yields the optimal controls $\boldsymbol{v}_k^* = \{v_{0|k}^*, v_{1|k}^*, \ldots, v_{N-1|k}^*\}$

$$\min_{v_{0|k}, v_{1|k}, \ldots, v_{N-1|k}} \quad \hat{J}(\hat{x}_k, \boldsymbol{v}_k) \tag{3.5a}$$

s.t.

$$x_{i+1|k}^{[j]} = A(\delta_{i|k}^{[j]}) x_{i|k}^{[j]} + B(\delta_{i|k}^{[j]}) u_{i|k}^{[j]} + Gw(\delta_{i|k}^{[j]}) \tag{3.5b}$$

$$u_{i|k}^{[j]} = K x_{i|k}^{[j]} + v_{i|k} \tag{3.5c}$$

$$x_{i+1|k}^{[j]} \in \mathbb{X} \tag{3.5d}$$

$$u_{i|k}^{[j]} \in \mathbb{U} \tag{3.5e}$$

$$x_{N|k}^{[j]} \in \mathbb{X}_T \tag{3.5f}$$

$$x_{0|k}^{[j]} = \hat{x}_k \tag{3.5g}$$

$$\forall i \in \{0, 1, \ldots, N-1\}, \qquad \forall j \in \{1, 2, \ldots, C\} \tag{3.5h}$$

where, using the receding horizon (RH) strategy [21], only the first element of $\boldsymbol{v}_k^*$ is applied to the process in that time (i.e., $u_k = u_{0|k} = K\hat{x}_k + v_{0|k}^*$), repeating the OCP at the next sampling time.

Assumption 3.2. *Matrices Q and R are defined by the designer. For the uncertain system* (3.1a) *K and P can be obtained by solving an eigenvalues problem (EVP)*(3.1a) *from a quadratic stability analysis using Lyapunov's approach [19], [23], [90], that makes the $A(\delta_i) + B(\delta_i)K$ matrix strictly stable. The sets $\mathbb{X}$, $\mathbb{U}$ and $\mathbb{X}_T \subset \mathbb{X}$ are convex sets that contain the origin in their interiors. For any instant of time the current state $\hat{x}_k$ is assumed to be measurable, the set $\Delta_k^{[j]}$ $\forall j \in \{1, 2, \ldots, C\}$ is generated according to Assumption 3.1, and the OCP is assumed to find a feasible solution at that instant.*

About the Number of Scenarios and Samples Features

As outlined in the conclusions of the previous chapter, establishing an appropriate number of C possible realisations of uncertainties to be considered to solve the OCP (3.5) is essential. This is because optimal solutions can be obtained for a large number of realisations but at the expense of an excessive computational burden. On the other hand, if a small number of realisations is used to achieve tractability, an accurate model or approximation of the uncertainty cannot be

achieved, and due to the randomness of the scenarios, the OCP solutions, computed with unlikely scenarios, may exhibit undesirable behaviour in the closed loop. For this reason, a certain balance between the numerical tractability and quality of its solution is required.

According to subsection 2.3.2, this number can be calculated according to a defined probability level $p \in [0, 1]$ of constraint satisfaction, a very low confidence level or probability of a bad event occurring $\beta \in [0, 1]$ (e.g., $\beta = 10^{-9}$) and the number of decision variables d; where C can be obtained as the minimum value that satisfies (2.43), that is

$$\sum_{j=0}^{d-1} \binom{C}{j} (1-p)^j p^{C-j} \leq \beta \tag{3.6}$$

where, in the context of the OCP (3.5), $\mathbb{P}[x_{i+1|k} \in \mathbb{X}] \geq p$ is desired and $d = n_u N$. According to Theorem 3.1 in [51], it holds that any optimal solution $\boldsymbol{v}_k^*$ obtained by the scenario program (3.5), using C scenarios, with C defined using (3.6), has a guaranteed level $1 - \beta$ of feasibility, in a probabilistic sense, of meeting the probabilistic constraints $\mathbb{P}[x_{i+1|k} \in \mathbb{X}] \geq p$.

Despite a very low defined β, such a bad event can occur. As pointed out in [36], a drawback to this random generation of scenarios is that some may be far from the reality of the process, and consequently, the optimal controls $\boldsymbol{v}_k^*$ calculated can cause erroneous behaviour in the closed-loop system.

Sampling and discarding approaches [52], can be used to improve the cost function while $\mathbb{P}[x_{i+1|k} \in \mathbb{X}] \geq p$ holds for a sufficiently high number of C generated scenarios, D scenarios can be discarded, based on a defined removal rule, from the total of C scenarios constraints. As an example, in this context the scenario program (2.41) would be as follows

$$\begin{aligned} &\min_x c^\top x \\ &\text{s.t.} \\ &\quad f(x, \gamma^{[j]}) \leq 0, \qquad \forall j \in \mathbb{C}_C - \mathbb{D}_D \end{aligned} \tag{3.7}$$

here x is the vector of decision variables of dimension d, γ is the vector of random variables; $\mathbb{C}_C = \{1, \ldots, C\}$ is the set of indices of the C scenarios generated, $\mathbb{D}_D = \{d_1, \ldots, d_D\}$ is the set with the indices of the D scenarios to be discarded from the constraints. D can be computed as the maximum value that meets the

following inequality

$$\binom{D+d-1}{D} \sum_{j=0}^{D+d-1} \binom{C}{j} (1-p)^j p^{C-j} \leq \beta \tag{3.8}$$

or by its approximation

$$D \leq (1-p)C - d + 1 - \sqrt{2(1-p)C \ln\left(\frac{((1-p)C)^{d-1}}{\beta}\right)}$$

According to Theorem 2.1 in [52], it holds that any optimal solution $x^* = x^*\left(\left\{\gamma^{[1]}, \gamma^{[2]}, \ldots, \gamma^{[C]}\right\}\right)$ obtained by the scenario program (3.7), has a guaranteed level $1-\beta$ of feasibility of meeting the probabilistic constraints $\mathbb{P}[f(x,\gamma) \leq 0] \geq p$ in the chance-constrained optimisation problem (2.40); or referring to (3.7) $\mathbb{P}[V(x^*) \leq 1-p] \geq 1-\beta$, where $V(x^*)$ is the probability of constraint violation with x^*, i.e., $V(x^*) = \mathbb{P}[f(x^*, \gamma^{[j]}) > 0]$. The above states that any optimal solution $\boldsymbol{v}_k^*$ obtained by the scenario program (3.5), in which the constraints of D scenarios are discarded in (3.5d)-(3.5f), with C and D defined using (3.8), has a guaranteed level $1-\beta$ of feasibility of satisfying the probabilistic constraints $\mathbb{P}[x_{i+1|k} \in \mathbb{X}] \geq p$.

In [36], a sample-removal pair is proposed for MPC, and consists of calculating the pair (C, D) based in a defined risk acceptability level of constraint violation $(1-p)$ such that $\mathbb{P}[x_{i+1|k} \in \mathbb{X}] \geq p$, where C is the number of scenarios to be considered in the OCP, D is the number of scenarios that can be discarded from the constraints in the states and ρ is a parameter related to the dimension of the unconstrained subspace of the search space $\mathbb{R}^d$

$$\int_0^1 U(v)\, dv \leq 1-p, \tag{3.9}$$

$$U(v) = \min\left\{1, \binom{D+\rho-1}{D} \sum_{j=0}^{D+\rho-1} \binom{C}{j} v^j (1-v)^{C-j}\right\}.$$

Nevertheless, the use of these scenario removal schemes represents an increase in the solution time, which could result in an OCP that is expensive to solve computationally. This is because of the need for large values for C to continue fulfilling $\mathbb{P}[x_{i+1|k} \in \mathbb{X}] \geq p$ with the remaining $C-D$ scenarios; in addition to requiring an appropriate algorithm [36], [52] to identify unlikely scenarios to be removed from the constraints to reduce conservatism, which could result in an extra optimisation stage.

3.3 Model Predictive Control via Conditional Scenarios

In this section, a novel scenario-based MPC approach is presented. At each sampling time, a primary set of equiprobable scenarios is generated and is subsequently approximated to a reduced set of conditional scenarios, each with its probability of occurrence. This reduced set is used to solve an OCP whose structure is similar to that of a scenario-based MPC (3.5), but considers a new cost function in which the predicted states and inputs are penalised according to the probabilities of occurrence associated with the realisations of the uncertainties on which they depend.

3.3.1 Conditional Scenario Approach

The conditional scenario (CS) concept was presented in [105] as an approximation to the two-stage stochastic mixed-integer linear programming (SMILP) problem, where the expected value of the second stage cost is commonly stated in terms of scenarios defined as realisations of a random vector $\delta \in \mathbb{R}^{n_\delta}$, made up of n_δ random variables ξ, such that $\delta = [\xi_1, \xi_2, \ldots, \xi_{n_\delta}]^\top$. The purpose of this method is to seek a compromise between the computational tractability of the problem and an accurate representation of uncertainty by generating a number C of so-called conditional scenarios (CSs), denoted by $\{\hat{\delta}^{[j]}\}$, each with its associated probability of occurrence $\hat{p}^{[j]}$

$$\hat{\delta}^{[j]} = [\hat{\xi}_1^{[j]}, \hat{\xi}_2^{[j]}, \ldots, \hat{\xi}_{n_\delta}^{[j]}]^\top, \qquad \forall j \in \{1, 2, \ldots, C\}.$$

The above considering that each random variable ξ_n $\forall n \in \{1, 2, \ldots, n_\delta\}$ in δ has a known normal distribution $\xi_n \sim \mathcal{N}(\mu_n, \sigma_n)$ and bounds $\mathcal{I}_n$ (e.g., $\mathcal{I}_n = [\mu_n - 3\sigma_n, \mu_n + 3\sigma_n[$), and there may be a correlation between it and any or all other variables in the set $\{\xi_n\}$. Therefore, δ has a known multivariate normal distribution $\delta \sim \mathcal{N}_{n_\delta}(\mu, \Sigma)$ with mean vector μ, covariance matrix Σ and bounded support $\mathbb{W}_\delta$.

The number of C conditional scenarios depends on the number of random variables ξ that constitute δ and a defined number E of discretisation points $\forall e \in \{1, 2, \ldots, E\}$ for each bound $\mathcal{I}_n$ of ξ, that is $C = n_\delta E$. In this way, the calculation of each $\hat{\delta}^{[j]}$ and its $\hat{p}^{[j]}$ is made using the information from each ξ; and the probability density function ϕ and the cumulative distribution function Φ of a

standard normal random variable among others; such that

$$\hat{\delta}^{[(n-1)E+e]} = \mathbb{E}\left[\delta \mid \tilde{\xi}_{n,e}\right],$$
$$\hat{p}^{[(n-1)E+e]} = \mathbb{P}[\xi_n \in \mathcal{I}_{n,e}],$$
$$\forall n \in \{1, 2, \ldots, n_\delta\}, \qquad \forall e \in \{1, 2, \ldots, E\}.$$

in which each CS consists of approximating δ by the conditional expectation $\mathbb{E}\left[\delta \mid \tilde{\xi}_{n,e}\right]$, where $\tilde{\xi}_{n,e}$ is the eth representative point of discretising the random variable ξ_n and $\mathcal{I}_{n,e}$ is the eth interval of $\mathcal{I}_n$ such that $\mathcal{I}_n = \bigcup_{e=1}^{E} \mathcal{I}_{n,e}$.

The aforementioned CS approach was adapted in [82] as a scenario reduction method in which δ can have any type of distribution and not necessarily be bounded. This reduction is performed on a given large primary set $\mathbb{S}$ of S scenarios

$$\{\tilde{\delta}^{[1]}, \tilde{\delta}^{[2]}, \ldots, \tilde{\delta}^{[S]}\} \in \mathbb{S}$$

whose lth scenario and its probability are $\tilde{\delta}^{[l]}$ and $\tilde{p}^{[l]}$, respectively, in which

$$\tilde{\delta}^{[l]} = [\tilde{\xi}_1^{[l]}, \tilde{\xi}_2^{[l]}, \ldots, \tilde{\xi}_{n_\delta}^{[l]}]^\top, \qquad \forall l \in \{1, 2, \ldots, S\}.$$

Such reduction is made based on $\mathbb{S}$ and a the desired number of points E to discretise the support of each random variable $\tilde{\xi}$, and leading to a new set $\mathbb{S}_C$ of C conditional scenarios, each with its own probability of occurrence, with the jth CS and its probability are given by $\hat{\delta}^{[j]}$ and $\hat{p}^{[j]}$, respectively, and

$$\{\hat{\delta}^{[1]}, \hat{\delta}^{[2]}, \ldots, \hat{\delta}^{[C]}\} \in \mathbb{S}_C$$
$$\hat{\delta}^{[j]} = [\hat{\xi}_1^{[j]}, \hat{\xi}_2^{[j]}, \ldots, \hat{\xi}_{n_\delta}^{[j]}]^\top, \qquad \forall j \in \{1, 2, \ldots, C\}.$$

The methodology of [106], [107] for the reduction of a primary set through the CS approach is described in Algorithm 3.1, and in which the number of reduced scenarios is $C = n_\delta E$, provided that at least one scenario of $\mathbb{S}$ fulfills the condition $\tilde{\xi}_n^{[l]} \in \mathcal{I}_{n,e}$. As can be seen in step 3, this approach, rather than filtering or reducing scenarios, performs an approximation of $\mathbb{S}$ to a set of conditional expectations. Also, a simplified description of how this Algorithm works is shown in Figure 3.1.

In [107] and [82], comparisons were made of the performance of this reduction technique and two others (such as sample average approximation (SAA) [108] and scenario reduction based on probability distances (SRD) [109]) to solve portfolio optimisation and capacitated facility location problems. These three techniques yielded similar results, but with less time dedicated to the reduction by the CS (up to eight times faster).

Algorithm 3.1 Conditional Scenario Reduction Method

Input: the primary set of scenarios $\{\tilde{\delta}^{[1]}, \tilde{\delta}^{[2]}, \ldots, \tilde{\delta}^{[S]}\}$, their probability levels $\{\tilde{p}^{[1]}, \tilde{p}^{[2]}, \ldots, \tilde{p}^{[S]}\}$ and a desired integer value for E.

Output: the new set of C conditional scenarios $\{\hat{\delta}^{[1]}, \hat{\delta}^{[2]}, \ldots, \hat{\delta}^{[C]}\}$ and their respective probability levels $\{\hat{p}^{[1]}, \hat{p}^{[2]}, \ldots, \hat{p}^{[C]}\}$, where $C = n_\delta E$.

Procedure:

1. For each random variable $\tilde{\xi}_n \ \forall n \in \{1, 2, \ldots, n_\delta\}$ obtain its extreme values $\mathcal{I}_n = [a_n, b_n]$ in which

$$a_n = \min\{\tilde{\xi}_n^{[1]}, \tilde{\xi}_n^{[2]}, \ldots, \tilde{\xi}_n^{[S]}\}, \qquad b_n = \max\{\tilde{\xi}_n^{[1]}, \tilde{\xi}_n^{[2]}, \ldots, \tilde{\xi}_n^{[S]}\}$$

2. Split every $\mathcal{I}_n$ into E subintervals $\mathcal{I}_{n,e} \ \forall e \in \{1, 2, \ldots, E\}$ of equal or different lengths such that $\mathcal{I}_n = \bigcup_{e=1}^{E} \mathcal{I}_{n,e}$

$$\{\mathcal{I}_{n,1}, \mathcal{I}_{n,2}, \ldots, \mathcal{I}_{n,E}\} = \{[a_n, b_{n,1}), [b_{n,1}, b_{n,2}), \ldots, [b_{n,(E-1)}, b_n]\}$$

3. For each $\mathcal{I}_{n,e}$, construct the sets $\{\tilde{\delta}_{n,e}^{[1]}, \tilde{\delta}_{n,e}^{[2]}, \ldots, \tilde{\delta}_{n,e}^{[S_n]}\}$, $\{\tilde{p}_{n,e}^{[1]}, \tilde{p}_{n,e}^{[2]}, \ldots, \tilde{p}_{n,e}^{[S_n]}\}$ with every pair $(\tilde{\delta}^{[l]}, \tilde{p}^{[l]}) \ \forall l \in \{1, 2, \ldots, S\}$ that meet the condition $\tilde{\xi}_n^{[l]} \in \mathcal{I}_{n,e}$ and compute its respective CS $\hat{\delta}^{[n,e]}$ with probability level $\hat{p}^{[n,e]}$

$$\hat{\delta}^{[n,e]} = \mathbb{E}[\tilde{\delta} \mid \tilde{\xi}_n \in \mathcal{I}_{n,e}] = \frac{1}{S_n} \sum_{j=1}^{S_n} \tilde{\delta}_{n,e}^{[j]},$$

$$\hat{p}^{[n,e]} = \frac{1}{n_\delta} \sum_{j=1}^{S_n} \tilde{p}_{n,e}^{[j]}$$

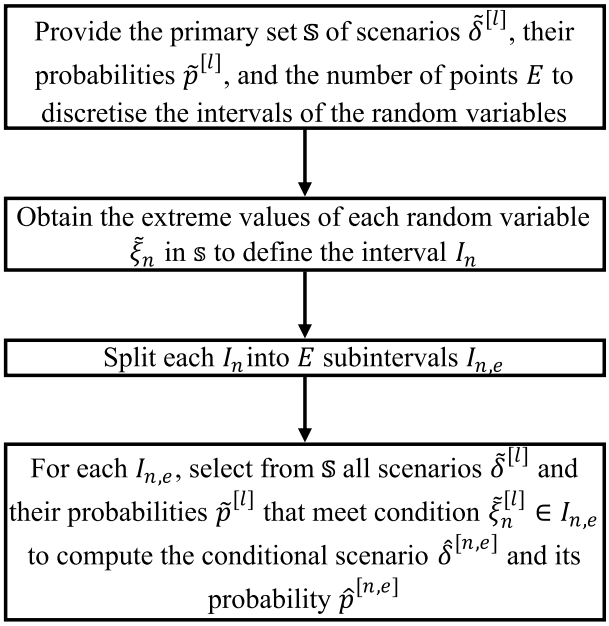

Figure 3.1: Block diagram of the operation of Algorithm 3.1.

3.3.2 Formulation of Conditional Scenarios in MPC

In the following, a procedure that adapts the CS reduction approach to the scenario-based MPC framework is proposed. As a remark, a scenario in the SMILP context consists of a realisation of the random vector δ of cardinality n_δ In the scenario-based MPC context, a scenario consists of a sequence of N realisations of δ, represented by $\Delta_k = \{\delta_{0|k}, \delta_{1|k}, \ldots, \delta_{N-1|k}\}$.

In line with the above, let $\mathbb{S}_S$ be a set, with cardinality S, of random scenarios generated at time k

$$\{\Delta_k^{[1]}, \Delta_k^{[2]}, \ldots, \Delta_k^{[S]}\} \in \mathbb{S}_S \tag{3.10}$$
$$\Delta_k^{[l]} = \{\delta_{0|k}^{[l]}, \delta_{1|k}^{[l]}, \ldots, \delta_{N-1|k}^{[l]}\}, \qquad \forall l \in \{1, 2, \ldots, S\}$$

where $\mathbb{S}_S$ is assumed to be a set of equiprobable scenarios, that is, each $\Delta_k^{[l]}$ in $\mathbb{S}_S$ has a probability of occurrence $p = 1/S$. Hence, each element of $\{\delta_{i|k}^{[1]}, \delta_{i|k}^{[2]}, \ldots, \delta_{i|k}^{[S]}\}$

has a probability $p_{i|k}^{[l]} = 1/S$

$$\begin{gathered}\{p_k^{[1]}, p_k^{[2]}, \dots, p_k^{[S]}\},\\ p_k^{[l]} = \{p_{0|k}^{[l]}, p_{1|k}^{[l]}, \dots, p_{N-1|k}^{[l]}\}, \qquad \forall l \in \{1, 2, \dots, S\},\\ p_{i|k}^{[l]} = 1/S, \qquad \forall i \in \{0, 1, \dots, N-1\}.\end{gathered}$$

With the above in mind, Algorithm 3.2 is proposed as a procedure to approximate a set of equiprobable scenarios $\mathbb{S}_S$ (3.10) to a reduced set of conditional scenarios $\mathbb{S}_C$ (3.11a) with probabilities of occurrence (3.11b) (where $\sum_{j=1}^{C} \hat{p}_{i|k}^{[j]} = 1$) , in the context of scenario-based MPC

$$\{\hat{\Delta}_k^{[1]}, \hat{\Delta}_k^{[2]}, \dots, \hat{\Delta}_k^{[C]}\} \in \mathbb{S}_C \tag{3.11a}$$

$$\{\hat{p}_k^{[1]}, \hat{p}_k^{[2]}, \dots, \hat{p}_k^{[C]}\} \tag{3.11b}$$

$$\begin{gathered}\hat{\Delta}_k^{[j]} = \{\hat{\delta}_{0|k}^{[j]}, \hat{\delta}_{1|k}^{[j]}, \dots, \hat{\delta}_{N-1|k}^{[j]}\},\\ \hat{p}_k^{[j]} = \{\hat{p}_{0|k}^{[j]}, \hat{p}_{1|k}^{[j]}, \dots, \hat{p}_{N-1|k}^{[j]}\},\\ \forall j \in \{1, 2, \dots, C\}.\end{gathered}$$

Assumption 3.3. *Defining the integers C and E such that $C = n_\delta E$. At every control period, a new primary set of equiprobable scenarios $\mathbb{S}_S$ is generated in accordance with Assumption 3.1 and is later approximated to the CSs reduced set $\mathbb{S}_C$ applying the steps of Algorithm 3.2.*

A graphic description of the operation of this Algorithm is also illustrated in Figure 3.2. Note that, to do this, the integers C and E, corresponding to the number of desired CSs and the number of subintervals, respectively, must first be defined taking into account that they must satisfy the condition $C = n_\delta E$. It is also noted that implementing this procedure is straightforward, since Algorithm 3.2 does not require an optimisation stage or knowledge about how the random variables are distributed to perform the reduction.

Algorithm 3.2 From Scenarios to Conditional Scenarios in MPC

Input: the primary set of equiprobable scenarios (3.10) and a desired integer E such that $C = n_\delta E$.

Output: the new set of CSs $\{\hat{\Delta}_k^{[1]}, \hat{\Delta}_k^{[2]}, \dots, \hat{\Delta}_k^{[C]}\}$ and their respective probabilities sequences $\{\hat{p}_k^{[1]}, \hat{p}_k^{[2]}, \dots, \hat{p}_k^{[C]}\}$.

Procedure:

1. Classify all the realisations of the uncertainties into N groups δ_i and p_i $\forall i \in \{0, 1, \dots, N-1\}$, with cardinality S so that each pair corresponds to the ith prediction step

$$\delta_i = \{\delta_{i|k}^{[1]}, \delta_{i|k}^{[2]}, \dots, \delta_{i|k}^{[S]}\}, \qquad p_i = \{p_{i|k}^{[1]}, p_{i|k}^{[2]}, \dots, p_{i|k}^{[S]}\}, \qquad p_{i|k}^{[\cdot]} = 1/S$$

2. Apply Algorithm 3.1 to each pair $(\delta_i,\ p_i)$ to obtain $\hat{\delta}_i^{[n,e]}$ and its probability $\hat{p}_i^{[n,e]}$, $\forall n \in \{1, 2, \dots, n_\delta\}$ $\forall e \in \{1, 2, \dots, E\}$
3. Construct the new reduced set $\hat{\delta}_i = \{\hat{\delta}_{i|k}^{[1]}, \hat{\delta}_{i|k}^{[2]}, \dots, \hat{\delta}_{i|k}^{[C]}\}$ and its probabilities $\hat{p}_i = \{\hat{p}_{i|k}^{[1]}, \hat{p}_{i|k}^{[2]}, \dots, \hat{p}_{i|k}^{[C]}\}$

$$\hat{\delta}_i = \{\hat{\delta}_i^{[1,1]}, \hat{\delta}_i^{[1,2]}, \dots, \hat{\delta}_i^{[1,E]}, \dots, \hat{\delta}_i^{[n\delta,1]}, \hat{\delta}_i^{[n\delta,2]}, \dots, \hat{\delta}_i^{[n\delta,E]}\}$$
$$\hat{p}_i = \{\hat{p}_i^{[1,1]}, \hat{p}_i^{[1,2]}, \dots, \hat{p}_i^{[1,E]}, \dots, \hat{p}_i^{[n\delta,1]}, \hat{p}_i^{[n\delta,2]}, \dots, \hat{p}_i^{[n\delta,E]}\}$$

4. Randomly rearrange the $\hat{\delta}_i$ and $\hat{p}_i$ sequences ensuring that any pair $(\hat{\delta}_{i|k}^{[j]}, \hat{p}_{i|k}^{[j]})$ $\forall j \in \{1, 2, \dots, C\}$ share the same positions.
5. Construct jth conditional scenario $\hat{\Delta}_k^{[j]}$ and its respective sequence of probabilities $\hat{p}_k^{[j]}$

$$\hat{\Delta}_k^{[j]} = \{\hat{\delta}_{0|k}^{[j]}, \hat{\delta}_{1|k}^{[j]}, \dots, \hat{\delta}_{N-1|k}^{[j]}\},$$
$$\hat{p}_k^{[j]} = \{\hat{p}_{0|k}^{[j]}, \hat{p}_{1|k}^{[j]}, \dots, \hat{p}_{N-1|k}^{[j]}\}$$

6. Group them such that

$$\{\hat{\Delta}_k^{[1]}, \hat{\Delta}_k^{[2]}, \dots, \hat{\Delta}_k^{[C]}\},$$
$$\{\hat{p}_k^{[1]}, \hat{p}_k^{[2]}, \dots, \hat{p}_k^{[C]}\}$$

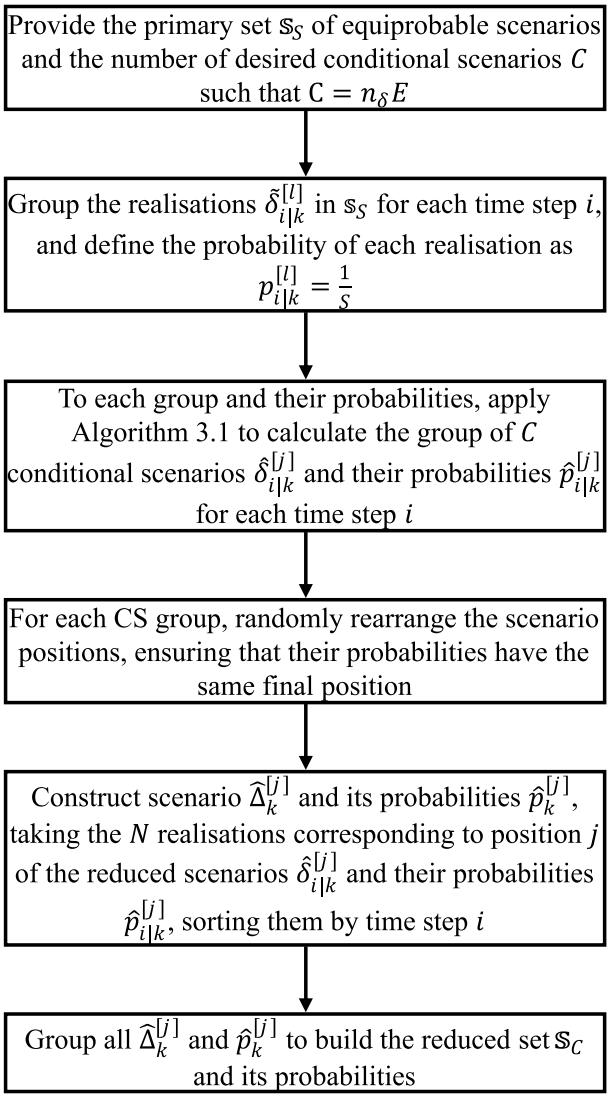

Figure 3.2: Block diagram of the operation of Algorithm 3.2.

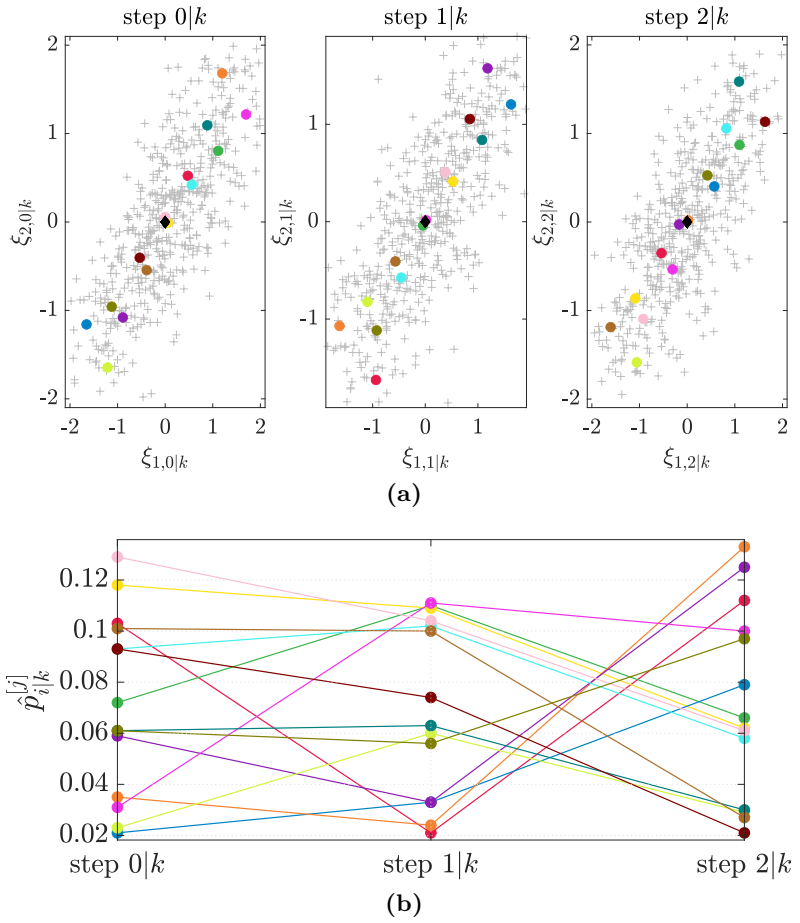

Figure 3.3: Illustrative example of Algorithm 3.2. (a) The primary set $\mathbb{S}_S$ of 500 equiprobable scenarios (plus signs) for a prediction horizon $N = 3$, the new reduced set $\mathbb{S}_C$ of 14 CSs (each with their respective single-coloured dots), and the origin (black rhombus). (b) Probabilities of occurrence of the $\hat{\delta}^{[\cdot]}_{i|k}$ of each scenario at each time-step.

To illustrate how Algorithm 3.2 works, Figure 3.3a shows a primary set $\mathbb{S}_S$ of 500 scenarios for a prediction horizon $N = 3$, considering a random vector $\delta = [\xi_1, \xi_2]^\top$ with multivariate normal distribution $\delta \sim \mathcal{N}_2(\mu, \Sigma)$, mean μ, covariance Σ and bounds given by

$$\mu = \begin{bmatrix} 0 \\ 0 \end{bmatrix}, \qquad \Sigma = \begin{bmatrix} 1.0 & 0.8 \\ 0.8 & 1.0 \end{bmatrix}, \qquad |\delta| \leq \begin{bmatrix} 2 \\ 2 \end{bmatrix}$$

by setting $E = 7$, a new set $\mathbb{S}_C$ of 14 CSs is obtained. For both $\mathbb{S}_S$ and $\mathbb{S}_C$, the elements $\delta_{i|k}^{[\cdot]}$ of $\Delta_k^{[\cdot]}$, and $\hat{\delta}_{i|k}^{[\cdot]}$ of $\hat{\Delta}_k^{[\cdot]}$ are plotted on its corresponding $i|k$-step graph. As illustrated in Figure 3.3b, every approximation $\hat{\delta}_{i|k}^{[\cdot]}$ belonging to each CS, has a probability of occurrence in accordance with the number of primary scenarios surrounding it. Considering the first CS (coloured yellow), its values are

$$\hat{\Delta}_k^{[1]} = \left\{ \begin{bmatrix} 0.0553 \\ -0.0085 \end{bmatrix}, \begin{bmatrix} 0.5295 \\ 0.4130 \end{bmatrix}, \begin{bmatrix} -1.0872 \\ -0.8625 \end{bmatrix} \right\}, \qquad \hat{p}_k^{[1]} = \{0.118, 0.109, 0.062\}.$$

3.3.3 Cost Function and Control Problem

As mentioned in the previous section, two of the most important drawbacks in scenario-based MPC are the unlikely scenarios that could cause undesired behaviour in the closed-loop system, and the computational tractability when the number of scenarios to be considered is large. For this reason, an approximation of the primary set of equiprobable scenarios to a set of conditional scenarios is suitable since it would allow addressing both the drawbacks mentioned above.

Given current instant k and according to Assumption 3.3, consider $\mathbb{S}_S$ the primary set of generated scenarios (3.10) for N steps, whose subsequent approximation through Algorithm 3.2 produces the new reduced set $\mathbb{S}_C$ given by (3.11). The value of C can be defined according to any criterion, e.g., (3.6), (3.8) or (3.9).

Evaluating (3.4a)-(3.4b) with (3.11a), produces the predictions of the states and inputs for such reduced scenarios, which are then incorporated in the cost function given by

$$\hat{J}_{CS}(\hat{x}_k, \boldsymbol{v}_k) = \frac{1}{C} \sum_{j=1}^{C} \Big[\sum_{i=0}^{N-1} \left(\hat{p}_{i-1|k}^{[j]} \|x_{i|k}^{[j]}\|_Q^2 + \hat{p}_{i|k}^{[j]} \|u_{i|k}^{[j]}\|_R^2 \right) + \hat{p}_{N-1|k}^{[j]} \|x_{N|k}^{[j]}\|_P^2 \Big]. \tag{3.12}$$

This new function, in addition to taking into account the terms $x_{i|k}^{[j]}$ and $u_{i|k}^{[j]}$, also includes the set of probabilities (3.11b) as weights. This means that, the predicted state $x_{i|k}^{[j]}$ and input $u_{i|k}^{[j]}$, which depends on the realisations $\hat{\delta}_{i-1|k}^{[j]}$ and $\hat{\delta}_{i|k}^{[j]}$, respectively, are penalised with the probability of occurrence $\hat{p}_{i-1|k}^{[j]}$ and $\hat{p}_{i|k}^{[j]}$ that are associated with such a realisation, where $\hat{p}_{-1|k}^{[j]} = 1/C$ since $x_{0|k}^{[j]} = \hat{x}_k$.

Thus, the control problem to be solved in the context of conditional scenario-based model predictive control (CSB-MPC) is as follows

$$\min_{v_{0|k}, v_{1|k}, \ldots, v_{N-1|k}} \quad \hat{J}_{CS}(\hat{x}_k, \boldsymbol{v}_k) \tag{3.13a}$$

s.t.

$$x^{[j]}_{i+1|k} = A(\hat{\delta}^{[j]}_{i|k}) x^{[j]}_{i|k} + B(\hat{\delta}^{[j]}_{i|k}) u^{[j]}_{i|k} + Gw(\hat{\delta}^{[j]}_{i|k}) \tag{3.13b}$$

$$u^{[j]}_{i|k} = K x^{[j]}_{i|k} + v_{i|k} \tag{3.13c}$$

$$x^{[j]}_{i+1|k} \in \mathbb{X} \tag{3.13d}$$

$$u^{[j]}_{i|k} \in \mathbb{U} \tag{3.13e}$$

$$x^{[j]}_{N|k} \in \mathbb{X}_T \tag{3.13f}$$

$$x^{[j]}_{0|k} = \hat{x}_k \tag{3.13g}$$

$$\forall i \in \{0, 1, \ldots, N-1\}, \qquad \forall j \in \{1, 2, \ldots, C\}. \tag{3.13h}$$

If sampling and removal schemes (3.8) or (3.9) are used, the OCP takes the form

$$\min_{v_{0|k}, v_{1|k}, \ldots, v_{N-1|k}} \quad \hat{J}_{CS}(\hat{x}_k, \boldsymbol{v}_k) \tag{3.14a}$$

s.t.

$$x^{[j]}_{i+1|k} = A(\hat{\delta}^{[j]}_{i|k}) x^{[j]}_{i|k} + B(\hat{\delta}^{[j]}_{i|k}) u^{[j]}_{i|k} + Gw(\hat{\delta}^{[j]}_{i|k}) \tag{3.14b}$$

$$u^{[j]}_{i|k} = K x^{[j]}_{i|k} + v_{i|k} \tag{3.14c}$$

$$x^{[r]}_{i+1|k} \in \mathbb{X} \tag{3.14d}$$

$$u^{[r]}_{i|k} \in \mathbb{U} \tag{3.14e}$$

$$x^{[r]}_{N|k} \in \mathbb{X}_T \tag{3.14f}$$

$$x^{[j]}_{0|k} = \hat{x}_k \tag{3.14g}$$

$$\forall i \in \{0, 1, \ldots, N-1\}, \qquad \forall j \in \{1, 2, \ldots, C\}, \qquad \forall r \in \mathbb{C}_C - \mathbb{D}_D. \tag{3.14h}$$

where, $\mathbb{C}_C = \{1, \ldots, C\}$ is the set of indices of the C conditional scenarios. The set of D scenarios, with indices $\mathbb{D}_D = \{d_1, \ldots, d_D\}$, to be discarded are those with the lowest probability of occurrence calculated as $\hat{p}^{[j]} = \sum_{i=0}^{N-1} \hat{p}^{[j]}_{i|k}$. Thus, only scenarios with r indices $r \in \mathbb{C}_C - \mathbb{D}_D$ are considered in the constraints.

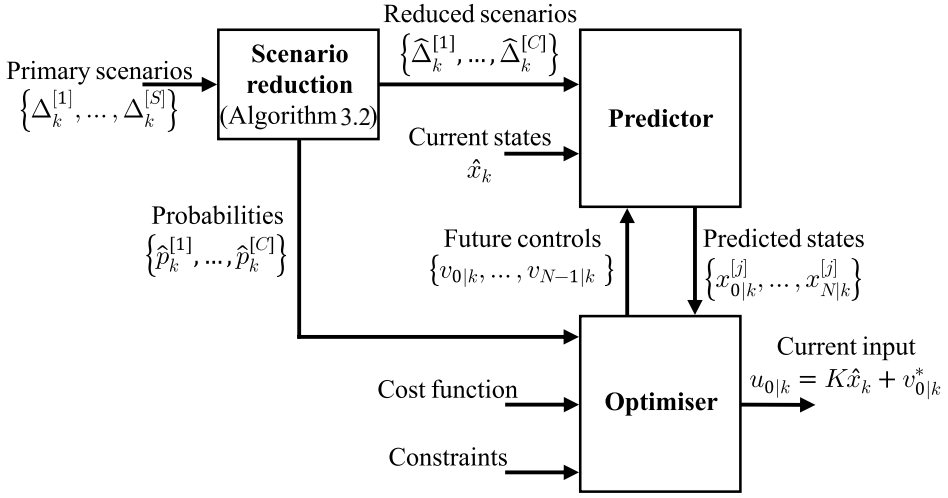

Figure 3.4: Block diagram of CSB-MPC. The Predictor block consists of Eqs. (3.4a)-(3.4b), the Cost function is (3.12). The Optimiser and Constraints are (3.13a) and (3.13b)-(3.13h), respectively, or (3.14a) and (3.14b)-(3.14h) depending on the CSB-MPC scheme.

As can be seen, the structure of (3.13) is similar to that of (3.5), but with the difference that this new structure is based on a reduced set $\mathbb{S}_C$, obtained through the reduction stage, and the new cost function (3.12).

The OCPs (3.13) and (3.14) of a CSB-MPC, and whose schematic diagram of its operation is depicted in Figure 3.4, covers the topic related to unlikely scenarios by giving more relevance to the states and inputs that involve realisations with more probability of occurrence, and less importance given to those that are related to unlikely realisations, by means of their associated probabilities.

Likewise, according to Theorem 3.1 in [51] and Theorem 2.1 in [52], it holds that any optimal solution $\boldsymbol{v}_k^*$ obtained by the scenario programs (3.13) and (3.14), using C conditional scenarios, with C defined using either (3.6) or (3.8), has a guaranteed level $1-\beta$ of feasibility, in a probabilistic sense, of meeting the probabilistic constraints $\mathbb{P}[x_{i+1|k} \in \mathbb{X}] \geq p$.

On the other hand, if solving (3.13) for C conditional scenarios presents better the probability of constraints satisfaction, compared to solving (3.5) for C random equiprobable scenarios, the topic related to computational tractability can be improved using a CSB-MPC with a number of conditional scenarios smaller than C.

Alternatively, if scheme (3.14) is used, the scenarios to be discarded are directly identified by their probability of occurrence $\hat{p}^{[j]} = \sum_{i=0}^{N-1} \hat{p}_{i|k}^{[j]}$, which becomes computationally lightweight. This contrasts significantly with the need for removal algorithms [36], [52] that, in MPC, usually require an extra stage of optimisation, which can become prohibitive depending on how greedy they are.

Feasibility and Stability

Recursive feasibility and stability in MPC is to ensure that the OCP is always feasible and that the system states, over time, converge asymptotically to a desired operating point. Based on the dual paradigm, recursive feasibility and stability are obtained through the terminal cost $\|x_N\|_P^2$, the terminal set $\mathbb{X}_T$ and additional conditions [18], [40].

If the initial state x_0 belongs to the feasible set $\mathbb{X}_f \subset \mathbb{X}$, there will exist a parametrised control law $u_i = Kx_i + v_i$ ($\forall i \in \{0, 1, \ldots, N-1\}$), whereby the states converge asymptotically to the origin, such that $x_N \in \mathbb{X}_T$. For instants from N, the system is governed by the law $u_i = Kx_i$ ($\forall i \in \{N, N+1, \ldots\}$), for which $\mathbb{X}_T$ is positively invariant, ensuring that the OCP is feasible indefinitely.

In a Scenario-based MPC in the current form of (3.5) or (3.13), recursive feasibility and stability remains a subject of research. This is because (3.1a) considers both parametric and additive uncertainties, with a δ of stochastic nature, where all elements of the sequence of uncertainties $\{\delta_0, \delta_1, \ldots\}$ are assumed to be independent and identically distributed (i.i.d.), i.e., independent in time; and whose δ characteristics can be time-varying in nature.

An unbounded δ can produce realisations with very large values of the uncertainties, making the OCP unable to find a solution that satisfies the constraints, while a bounded δ, as proposed here and as is the case in most real processes, prevents these large and unlikely realisations from appearing, besides allowing the calculation of an appropriate cost $\|x_N\|_P^2$ and a robust invariant set $\mathbb{X}_T$ to be obtained.

A practical way to ensure that the OCP (3.13) is always feasible is by introducing slack variables that soften the constraints [35], [37]. These new decision variables are incorporated and penalised in the cost function to force their values to be zero if an optimum solution can be obtained without violating the softened constraints.

On the other hand, a combination (through Algorithm 3.2 to extract the most representative scenarios of $\mathbb{S}_S$) with approaches based on offline uncertainty sam-

pling [30], [33], [34], [41] (which in general use either (3.6) or (3.8)) can be used to guarantee the recursive feasibility and stability of (3.13) but require that the characteristics of the uncertainties (mean, covariance, bounds) remain invariant, thus missing the attractiveness of the approach, which is the possibility to include new uncertainty data online, which may be the case for several processes.

For example, in [30], a first-step constraint $\mathbb{D}_R$ and a terminal set $\mathbb{X}_T$ are proposed, considering that (3.1a) has only parametric uncertainties, bounded and with i.i.d. sequences. In [41], a constraint for MPC initialisation, and a terminal robust invariant set $\mathbb{X}_T$ are proposed employing probabilistic reachable sets (PRS), considering that (3.1a) has only additive uncertainties, whose sequences are time-correlated (non-i.i.d.) and possibly unbounded. In [34], a system (3.1a) with only additive and unbounded uncertainties with i.i.d. sequences is considered. As in [41], it uses PRS to address probabilistic constraints; feasibility and stability are addressed by incorporating slack variables in the initial state constraints (called therein as flexible initial state constraint) and a robustly invariant terminal set, respectively.

For the proposed CSB-MPC scheme, in order to maintain the classical formulation of a scenario-based MPC, the feasibility of the OCP at each time-step is assumed according to Assumption 3.2.

3.4 Numerical Examples

In this section, two numerical examples are presented to illustrate and compare the behaviour of a scenario-based MPC (3.5) and a CSB-MPC (3.13) for $N_r = 1000$ Monte Carlo simulations each. In both techniques, at each control period, a primary set $\mathbb{S}_S$ of scenarios is generated where the OCP (3.5) in the scenario-based MPC (for simplicity, hereafter referred to as SCMPC) is solved by considering C scenarios taken randomly from $\mathbb{S}_S$. The CSB-MPC (3.13) is solved for C conditional scenarios obtained from the reduction of $\mathbb{S}_S$ by applying Algorithm 3.2. In each simulation, the purpose of each MPC strategy is to control the system and steer its states from the initial point $x_{0|k}^{[j]} = \hat{x}_0$ to the origin (assuming that the current state is measurable).

All N_r simulations were carried out using Matlab R2018b, installed on a standard computer and the control actions were calculated with the quadprog toolbox [110] available in the Mosek 9.2. optimisation software. Through a stability analysis of Lyapunov's [19], [23], K and P matrices were computed using YALMIP [111] to solve a problem based on linear matrix inequalities; and the robust invariant set $\mathbb{X}_T$, consisting of a polytope, was computed using the multi-parametric toolbox (MPT) [112]. Readers can reproduce the simulation results here presented or simulate an CSB-MPC with the specialised software *conditional scenario-based MPC toolbox* as developed by the authors and available at MATLAB Central [113].

The behaviour of both MPC strategies is analysed by means of performance indices, which were computed based on the N_r closed-loop state responses and inputs. These are:

- $p_\mathrm{s} = 100\,(N_\mathrm{s}/N_r)$: probability (in percentage) of success of a simulation, where N_s is the number of simulations out of all N_r where no constraints were violated.
- p_c: the minimum probability (in percentage) that all states do not violate the constraints.
- N_v: the total number of constraints that were violated in all simulations.
- PD_avg: average percentage of deviation of violated constraints in the states.
- $\mathrm{IAE}_\mathrm{avg}$: mean value of the integral absolute error of all states.
- $\mathrm{IAU}_\mathrm{avg}$: mean value of the integral of the absolute value of the applied inputs.

- t_{avg}: average time taken by the MPC algorithm to obtain a solution. For SCMPC and CSB-MPC, this time also includes the times it takes to generate the primary set $\mathbb{S}_S$, plus select C or approximate to C scenarios, depending on the case.
- C_{OCP}: number of OCP constraints.

3.4.1 Example 1: Double Integrator System

Consider the second order discrete system in the form (3.1a), given by

$$x_{i+1} = \begin{bmatrix} 1 & 0.93 \\ 0 & 1 \end{bmatrix} x_i + \begin{bmatrix} 0.28 \\ 0.82 \end{bmatrix} u_i + \begin{bmatrix} 1 & 0 \\ 0 & 1 \end{bmatrix} w(\delta_i).$$

The sampling time is $T_{\text{s}} = 0.5$ s, the system state and input constraints are $|x_2| \leq 1$ for the second state and $|u| \leq 0.8$, respectively. The two random variables, ξ_1 and ξ_2, contained in the vector of additive disturbances $w(\delta_i) = [\xi_{1,i}, \xi_{2,i}]^\top$ make up the random vector $\delta = [\xi_1, \xi_2]^\top$ ($n_\delta = 2$), which has a truncated multivariate normal distribution $\delta \sim \mathcal{N}_2(\mu, \Sigma)$ with mean vector μ, covariance matrix Σ and bounds

$$\mu = \begin{bmatrix} 0 \\ 0 \end{bmatrix}, \qquad \Sigma = \begin{bmatrix} 0.0004 & 0.0017 \\ 0.0017 & 0.01 \end{bmatrix}, \qquad |\delta| \leq \begin{bmatrix} 0.05 \\ 0.2 \end{bmatrix}.$$

Simulation Setup

The performances in this example of a SCMPC and a CSB-MPC for various C used to solve the OCP are compared for the cases of primary sets $\mathbb{S}_S$, consisting of 5000 and 1200 scenarios

$$C = \{100, 80, 60, 40, 20\}$$

all elements in this sequence meet the condition $C = n_\delta E$ (see Assumption 3.3), and through (3.6), with $\beta = 10^{-9}$, their theoretical probabilities of constraints satisfaction $\mathbb{P}[x_{i+1} \in \mathbb{X}] \geq p_{\text{t}}$ are

$$p_{\text{t}}(C) = \{57.5\%, 49.5\%, 37.5\%, 20.2\%, 0.52\%\}.$$

The duration of each of the N_r simulations in both MPCs is 20 sampling periods, starting from the initial state $x_{0|k}^{[j]} = \hat{x}_0 = [8, 0.7]^\top$. The prediction horizon is $N = 15$, yielding 15 decision variables; the cost function weights are $Q = \text{diag}(1, 1)$ and $R = 0.1$; the terminal set $\mathbb{X}_T$ consisting of a polytope of 6 linear inequalities and K and P matrices are

$$K = \begin{bmatrix} -0.7421 & -1.5891 \end{bmatrix}, \qquad P = \begin{bmatrix} 2.3026 & 0.8572 \\ 0.8572 & 1.6983 \end{bmatrix}.$$

Table 3.1: Performance Indices of the MPCs in Example 1 for a $\mathbb{S}_S$ of 5000 Scenarios.

Controller	p_s	p_c	N_v	PD_avg	$\mathrm{IAE}_\mathrm{avg}$	$\mathrm{IAU}_\mathrm{avg}$	t_avg	C_OCP
SCMPC_{100}	92.8%	98.8%	74	1.22%	69.054	4.239	22.0 ms	6400
$\mathrm{CSB\text{-}MPC}_{100}$	98.1%	99.6%	19	0.20%	69.554	4.198	43.8 ms	6400
SCMPC_{80}	91.0%	98.6%	93	1.34%	68.925	4.251	19.1 ms	5120
$\mathrm{CSB\text{-}MPC}_{80}$	97.7%	99.6%	23	0.26%	69.492	4.201	38.2 ms	5120
SCMPC_{60}	87.8%	98.0%	127	1.53%	68.728	4.268	16.3 ms	3840
$\mathrm{CSB\text{-}MPC}_{60}$	96.9%	99.3%	31	0.35%	69.399	4.207	31.7 ms	3840
SCMPC_{40}	81.4%	96.5%	201	1.88%	68.387	4.300	13.1 ms	2560
$\mathrm{CSB\text{-}MPC}_{40}$	95.1%	99.1%	49	0.52%	69.216	4.217	25.0 ms	2560
SCMPC_{20}	63.9%	94.6%	424	2.81%	67.643	4.390	10.1 ms	1280
$\mathrm{CSB\text{-}MPC}_{20}$	87.7%	98.2%	131	0.98%	68.649	4.250	18.3 ms	1280

Table 3.2: Performance Indices of the MPCs in Example 1 for a $\mathbb{S}_S$ of 1200 Scenarios.

Controller	p_s	p_c	N_v	PD_avg	$\mathrm{IAE}_\mathrm{avg}$	$\mathrm{IAU}_\mathrm{avg}$	t_avg	C_OCP
SCMPC_{100}	91.6%	98.5%	87	1.27%	69.051	4.238	18.3 ms	6400
$\mathrm{CSB\text{-}MPC}_{100}$	98.5%	99.7%	15	0.24%	70.180	4.173	26.6 ms	6400
SCMPC_{80}	89.4%	98.3%	111	1.46%	68.924	4.250	15.7 ms	5120
$\mathrm{CSB\text{-}MPC}_{80}$	97.9%	99.6%	21	0.27%	69.843	4.190	22.2 ms	5120
SCMPC_{60}	86.2%	97.9%	144	1.72%	68.721	4.270	13.1 ms	3840
$\mathrm{CSB\text{-}MPC}_{60}$	96.9%	99.5%	31	0.38%	69.509	4.207	18.1 ms	3840
SCMPC_{40}	80.3%	97.1%	217	2.13%	68.380	4.304	10.6 ms	2560
$\mathrm{CSB\text{-}MPC}_{40}$	95.0%	99.2%	50	0.57%	69.207	4.218	14.1 ms	2560
SCMPC_{20}	66.0%	94.5%	415	2.83%	67.652	4.396	8.2 ms	1280
$\mathrm{CSB\text{-}MPC}_{20}$	87.4%	98.0%	133	1.04%	68.624	4.251	10.5 ms	1280

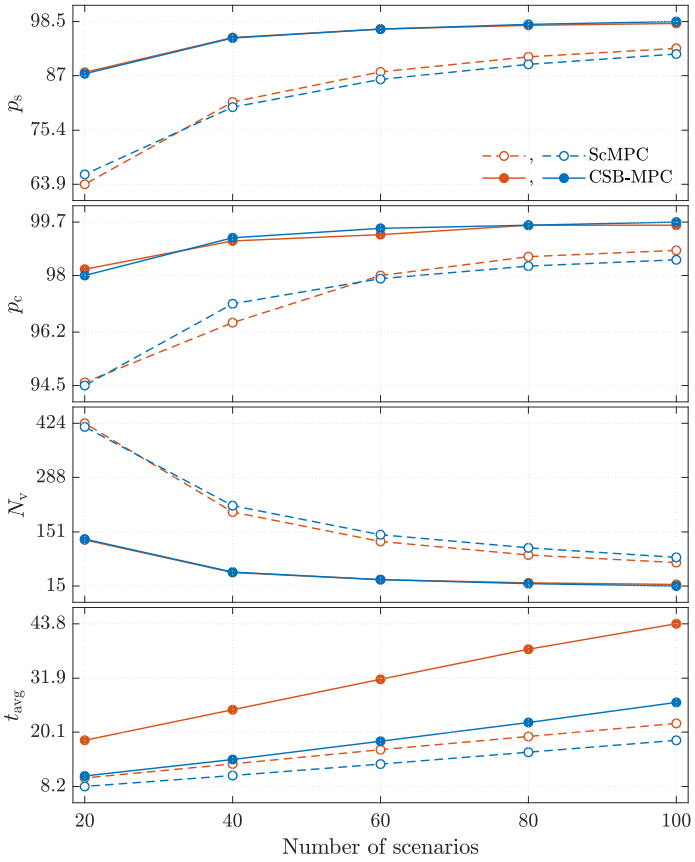

Figure 3.5: Graphs of the performance indices p_s, p_c, N_v and t_{avg} from Tables 3.1 ($\mathbb{S}_S(5000)$, orange lines) and 3.2 ($\mathbb{S}_S(1200)$, blue lines), corresponding to SCMPC (dashed lines) and CSB-MPC (solid lines), for $20, 40, 60, 80$ and 100 scenarios.

Results

Tables 3.1 and 3.2 show the performance results of each MPC for the primary sets $\mathbb{S}_S(5000)$ and $\mathbb{S}_S(1200)$, respectively. The first column corresponds to the type of controller, whose subscript indicates the number of scenarios used to solve its respective OCP. The subsequent columns indicate the performance indices, as defined at the beginning of this section and which were computed based on the N_r closed-loop responses. Furthermore, these indices are depicted in Figures 3.5-3.6, in which the orange and blue lines represent those in Tables 3.1 and 3.2, respectively.

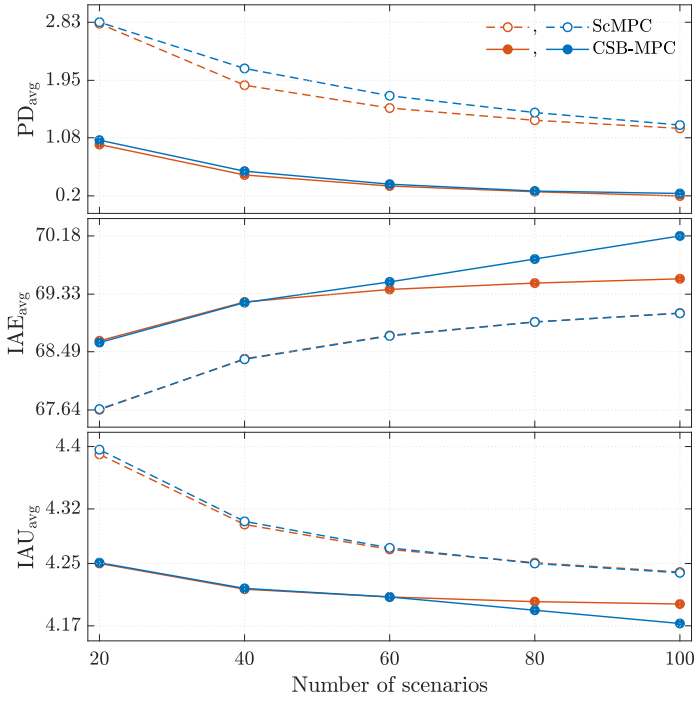

Figure 3.6: Graphs of the performance indices $\mathrm{PD}_{\mathrm{avg}}, \mathrm{IAE}_{\mathrm{avg}}$ and $\mathrm{IAU}_{\mathrm{avg}}$ from Tables 3.1 ($\mathbb{S}_S(5000)$, orange lines) and 3.2 ($\mathbb{S}_S(1200)$, blue lines), corresponding to SCMPC (dashed lines) and CSB-MPC (solid lines), for $20, 40, 60, 80$ and 100 scenarios.

Both tables reveal that for the two cases of $\mathbb{S}_S$ primary sets, CSB-MPCs obtained higher constraint satisfaction probabilities p_{s} and p_{c} than SCMPCs; where, according to Figure 3.5 a greater difference is noted as the number of scenarios decreases. Likewise, it is verified that the empirical probabilities p_{s} of the CSB-MPCs satisfy the theoretical probabilities p_{t}, presenting values significantly above the estimated ones. Moreover, this improvement in the probability of constraint satisfaction by CSB-MPCs produces lower numbers of violated constraints N_{v} and lower percentages of deviations from constraints $\mathrm{PD}_{\mathrm{avg}}$ than SCMPCs, being almost one-third of those reported by SCMPCs (e.g., SCMPC_{20} and $\mathrm{CSB\text{-}MPC}_{20}$ in Table 3.1).

In addition, Figure 3.7 shows the closed-loop state trajectories and applied inputs for $C = 20$ in Table 3.2, contrasted with those of a standard MPC with constraints (in which $p_{\mathrm{s}} = 0.1\%$ and $p_{\mathrm{c}} = 46.5\%$) that is based on the nominal model of the system. As can be seen in the detailed view, the state trajectories of the SCMPC

($N_{\mathrm{v}} = 415$, $\mathrm{PD}_{\mathrm{avg}} = 2.83\%$) transgress the limits, more times than those of the CSB-MPC ($N_{\mathrm{v}} = 133$, $\mathrm{PD}_{\mathrm{avg}} = 1.04\%$), which has better probabilities p_{s} and p_{c}.

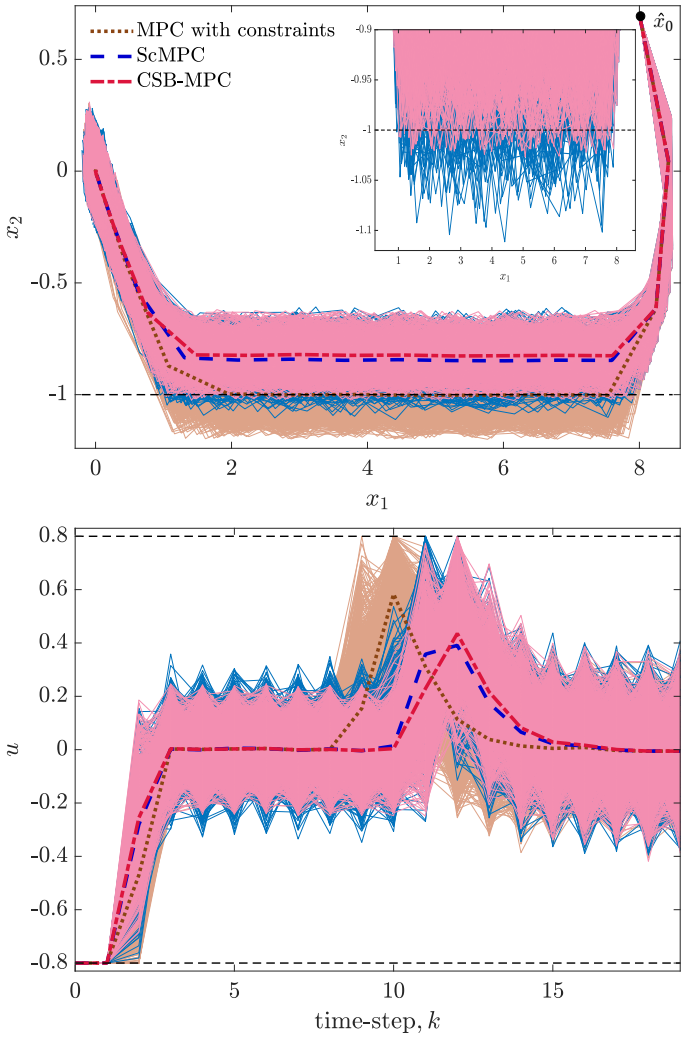

Figure 3.7: 1000 system closed-loop responses and applied inputs to a standard MPC with constraints (light brown solid lines), SCMPC_{20} (light blue solid lines) and $\mathrm{CSB\text{-}MPC}_{20}$ (light red solid lines) controllers, for a $\mathbb{S}_S$ of 1200 Scenarios. The brown dotted line, blue dashed line, and red dash-dotted line represent the mean trajectories of standard MPC, SCMPC and CSB-MPC, respectively; and the system constraints, $|x_2| \leq 1.0$, $|u| \leq 0.8$, represented by black dashed lines.

Note that for both primary sets $\mathbb{S}_S = 5000$ and $\mathbb{S}_S = 1200$ (see Figures 3.5-3.6), the CSB-MPC do not show considerable variations in indicators p_s, p_c, N_v and PD_avg, as is the case for indicator t_avg, which decreases with $\mathbb{S}_S(1200)$, approaching those of the SCMPC. This decrease in t_avg is because the time used in the additional scenario-reduction stage of the CSB-MPC, is less as the primary set to approximate is smaller. With this in mind and with an appropriately sized $\mathbb{S}_S$, a CSB-MPC against a SCMPC with the same number of scenarios is a good option due to its higher probabilistic feasibility of constraints satisfaction, with similar solution times t_avg. Furthermore, in case of needing a decrease in the solution time t_avg, a CSB-MPC with a smaller number of scenarios than a SCMPC could be used.

For example, considering the MPCs in Table 3.2, if similar performance indices to those of the SCMPC_{100} ($t_\text{avg} = 18.3$ ms) are required, but with a lower solution time, the CSB-MPC_{60} ($t_\text{avg} = 18.1$ ms) or CSB-MPC_{40} ($t_\text{avg} = 14.1$ ms) could be used. Note that the others SCMPC reported in Table 3.2 do not offer similar or superior characteristics to those required, as do the mentioned CSB-MPCs, which even offer higher probabilities, lower violated constraints N_v and lower PD_avg.

Regarding indicators IAE_avg and IAU_avg, both controllers presented similar values with slight variations and close to 69 and 4.2, respectively, which compared to those of a MPC with a perfect forecast ($\text{IAE}_\text{pf} = 60.969$ and $\text{IAU}_\text{pf} = 4.304$), they are close to IAU_pf but, because of uncertainties, considerably above IAE_pf. In some moments, in all the MPC simulations, the states exceeded their allowed limits. This was not the case for the applied inputs, which reached their allowed values without violating them.

3.4.2 Example 2: Quadruple-Tank Process

This example consists of the quadruple-tank process presented in the subsection 2.4.2, whose schematic diagram is depicted in Figure 3.8 and whose control objective is to maintain the liquid level in the tank T_i $\forall i \in \{1, 2, 3, 4\}$ at a desired setpoint h_i by means of the flow rates Q_1 and Q_2 delivered by pumps 1 and 2, respectively. These flows are proportional to the applied voltage $Q_1 = k_1 v_1$, $Q_2 = k_2 v_2$ and are subsequently split by the valves in proportions determined by the parameters $\gamma_1, \gamma_2 \in [0, 1]$.
By linearising the nonlinear equations of the system (2.53), around the operating point

$$\begin{aligned} P^o =& \{h_1^o, h_2^o, h_3^o, h_4^o, v_1^o, v_2^o\} \\ =& \{7.873 \text{ cm}, 8.187 \text{ cm}, 7.720 \text{ cm}, 8.039 \text{ cm}, 4.0 \text{ V}, 3.5 \text{ V}\} \end{aligned}$$

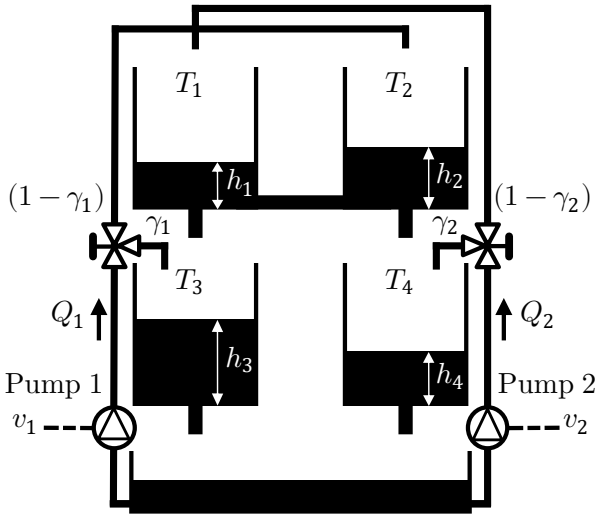

Figure 3.8: Quadruple tank process schematic diagram.

with $A_i = 144$ cm^2; $a_1, a_2, a_{12} = 0.352$ cm^2; $a_3 = 1.006 + \xi_1$ cm^2, $a_4 = 1.006 + \xi_2$ cm^2; $k_1, k_2 = 33.333$ cm^3/(V.s); $\gamma_1 = 0.6$, $\gamma_2 = 0.7$, $g = 981$ cm/s^2; and discretising for a sampling time $T_\mathrm{s} = 5$ s the resulting equations using Euler's approximation, and taking into account additive disturbances caused by other hydraulic connections, we obtain the discrete time model of the form (3.1a)

$$x_{i+1} = A(\delta_i)x_i + Bu_i + Gw(\delta_i)$$

with

$$A(\delta_i) = \begin{bmatrix} 0.421 & 0.483 & 0 & 0 \\ 0.483 & 0.422 & 0 & 0 \\ 0.097 & 0 & 0.722 - 0.277\xi_{1,i} & 0 \\ 0 & 0.095 & 0 & 0.727 - 0.271\xi_{2,i} \end{bmatrix},$$

$$B = \begin{bmatrix} 0 & 0.347 \\ 0.463 & 0 \\ 0.694 & 0 \\ 0 & 0.810 \end{bmatrix}, \qquad G = \begin{bmatrix} 1 & 0 & 0 & 0 \\ 0 & 1 & 0 & 0 \\ 0 & 0 & 1 & 0 \\ 0 & 0 & 0 & 1 \end{bmatrix}$$

where the state $x = [x_1, x_2, x_3, x_4]^\top$ and input $u = [u_1, u_2]^\top$ vectors represent the deviations of the liquid levels in centimetres and voltages from the selected operating point, respectively.

The constraints on the system states, corresponding to the deviations in the liquid levels in tanks 3 and 4, are $[-1.2, -1.2]^\top \leq [x_3, x_4]^\top \leq [1.2, 1.2]^\top$ cm. Similarly, the constraints on the inputs are $[-1.0, -1.0]^\top \leq [u_1, u_2]^\top \leq [1.0, 1.0]^\top$ V, which corresponds to the variations in the voltages applied to the pumps 1 and 2.

All uncertainties ($n_\delta = 6$) are stacked in the random vector $\delta = [\xi_1, \xi_2, \ldots, \xi_6]^\top$, which has a truncated multivariate normal distribution $\delta \sim \mathcal{N}_6(\mu, \Sigma)$, with mean vector μ, covariance matrix Σ and bounds with values

$$\mu = \begin{bmatrix} 0 \\ 0 \\ 0 \\ 0 \\ 0 \\ 0 \end{bmatrix}, \; \Sigma = 10^{-3} \times \begin{bmatrix} 0.0250 & 0.0225 & 0 & 0 & 0 & 0 \\ 0.0225 & 0.0250 & 0 & 0 & 0 & 0 \\ 0 & 0 & 6.40 & 0 & 0 & 5.12 \\ 0 & 0 & 0 & 6.40 & 5.12 & 0 \\ 0 & 0 & 0 & 5.12 & 6.40 & 0 \\ 0 & 0 & 5.12 & 0 & 0 & 6.40 \end{bmatrix}, \; |\delta| \leq \begin{bmatrix} 0.01 \\ 0.01 \\ 0.17 \\ 0.17 \\ 0.17 \\ 0.17 \end{bmatrix}.$$

Simulation Setup

In this example, the performances of a SCMPC and a CSB-MPC for a primary set $\mathbb{S}_S$ consisting of 10000 and a smaller set of 1300 scenarios are compared. The numbers of scenarios selected are

$$C = \{330, 240, 150, 90, 60, 42\}$$

which fulfil the condition $C = n_\delta E$ (see Assumption 3.3), and through (3.6), with $\beta = 10^{-9}$, their theoretical probabilities of constraints satisfaction $\mathbb{P}[x_{i+1} \in \mathbb{X}] \geq p_\mathrm{t}$ are

$$p_\mathrm{t}(C) = \{81.3\%, 74.9\%, 62.0\%, 42.5\%, 24.2\%, 9.0\%\}.$$

The duration of each simulation is 40 sampling periods for both MPCs and the nonlinear system initial state is $x_{0|k}^{[j]} = \hat{x}_0 = [-6.7, -6.5, -1, -1]^\top$. The MPCs parameters are prediction horizon $N = 12$ (thus, each OCP consists of 24 decision variables), cost function weights matrices $Q = \mathrm{diag}(3, 3, 1, 1)$ and $R = I_2$. The robust invariant set $\mathbb{X}_T$ consisting of a polytope of 54 hyperplanes, and K and P matrices are

$$K = \begin{bmatrix} -0.4824 & -0.2867 \\ -0.4075 & -0.3645 \\ -0.2635 & 0.0402 \\ 0.0484 & -0.3402 \end{bmatrix}^\top, \quad P = \begin{bmatrix} 5.0037 & 2.0305 & -0.5713 & -0.4862 \\ 2.0305 & 5.0796 & -0.6271 & -0.4581 \\ -0.5713 & -0.6271 & 1.7320 & 0.1207 \\ -0.4862 & -0.4581 & 0.1207 & 1.5524 \end{bmatrix}.$$

Table 3.3: Performance Indices of the MPCs in Example 2 for a $\mathbb{S}_S$ of 10000 Scenarios.

Controller	p_s	p_c	N_v	PD_{avg}	IAE_{avg}	IAU_{avg}	t_{avg}	C_{OCP}
$SCMPC_{330}$	92.0%	96.6%	88	1.40%	76.702	18.772	678 ms	48180
CSB-MPC_{330}	92.7%	96.9%	79	1.32%	76.699	18.760	780 ms	48180
$SCMPC_{240}$	90.9%	96.2%	99	1.45%	76.703	18.777	463 ms	35040
CSB-MPC_{240}	92.5%	96.9%	82	1.37%	76.699	18.761	554 ms	35040
$SCMPC_{150}$	89.5%	95.6%	115	1.55%	76.707	18.789	314 ms	21900
CSB-MPC_{150}	91.2%	96.7%	95	1.40%	76.700	18.764	393 ms	21900
$SCMPC_{90}$	86.7%	94.8%	144	1.78%	76.712	18.804	205 ms	13140
CSB-MPC_{90}	89.0%	95.9%	118	1.51%	76.704	18.771	267 ms	13140
$SCMPC_{60}$	83.9%	94.0%	175	1.94%	76.718	18.823	154 ms	8760
CSB-MPC_{60}	85.9%	94.8%	152	1.68%	76.708	18.779	203 ms	8760
$SCMPC_{42}$	80.1%	92.8%	220	2.03%	76.728	18.848	78 ms	6132
CSB-MPC_{42}	80.8%	93.0%	213	1.84%	76.713	18.789	124 ms	6132

Results

Tables 3.3 and 3.4 show the performance results of each MPC for cases $\mathbb{S}_S(10000)$ and $\mathbb{S}_S(1300)$, respectively; where, as in Example 1, the first column corresponds to the type of controller and the subsequent columns indicate the performance indices as defined at the beginning of this section (which were computed based on the N_r closed-loop responses of the nonlinear system). Furthermore, these indices are depicted in Figures 3.9-3.10, in which the orange and blue lines represent those in Tables 3.3 and 3.4, respectively.

As in Example 1, it is verified that the CSB-MPCs obtained higher empirical probabilities of constraint satisfaction p_s and p_c than SCMPCs; and their p_s are significantly above the theoretical probabilities of constraint satisfaction p_t, signifying higher feasibility of an OCP solution, in a probabilistic sense. Moreover, the CSB-MPCs reported better N_v and PD_{avg} indices than the SCMPCs, except for the case $C = 240$ in Table 3.4, where the CSB-MPC obtained a slightly higher PD_{avg}, but with fewer constraints violated.

Table 3.4: Performance Indices of the MPCs in Example 2 for a $\mathbb{S}_S$ of 1300 Scenarios.

Controller	p_s	p_c	N_v	PD_{avg}	IAE_{avg}	IAU_{avg}	t_{avg}	C_{OCP}
$SCMPC_{330}$	91.8%	96.5%	89	1.46%	76.703	18.770	577 ms	48180
CSB-MPC_{330}	95.1%	98.1%	52	1.36%	76.682	18.725	572 ms	48180
$SCMPC_{240}$	90.3%	95.8%	104	1.35%	76.702	18.775	415 ms	35040
CSB-MPC_{240}	92.4%	96.9%	83	1.40%	76.698	18.759	407 ms	35040
$SCMPC_{150}$	89.6%	95.7%	113	1.62%	76.707	18.784	238 ms	21900
CSB-MPC_{150}	90.7%	96.4%	100	1.40%	76.702	18.768	247 ms	21900
$SCMPC_{90}$	87.0%	94.7%	141	1.83%	76.713	18.800	141 ms	13140
CSB-MPC_{90}	88.5%	95.8%	123	1.53%	76.705	18.775	149 ms	13140
$SCMPC_{60}$	84.1%	93.8%	175	2.01%	76.723	18.820	95 ms	8760
CSB-MPC_{60}	85.7%	94.8%	155	1.73%	76.709	18.782	100 ms	8760
$SCMPC_{42}$	79.8%	92.0%	225	2.10%	76.730	18.844	67 ms	6132
CSB-MPC_{42}	80.3%	92.7%	217	1.86%	76.714	18.792	71 ms	6132

The closed-loop trajectories of the nonlinear system and the applied inputs for $SCMPC_{330}$, CSB-MPC_{330}, and CSB-MPC_{42} in Table 3.4 are shown in Figures 3.11a, 3.11b and 3.11c, respectively. In Figures 3.11a and 3.11b, very similar behaviours are observed by both controllers; however, the best performances are presented by the CSB-MPC_{330} (see Figures 3.9-3.10). Comparing the performances of CSB-MPC_{330} con CSB-MPC_{42}, it is noted that a decrease in the number of scenarios use to solve the OCP leads to an increase in the number of trajectories that violate the limits. Nevertheless, the mean trajectories with standard deviations (dotted lines) are kept within the limits (black dashed lines), indicating that the probability that a state is within the allowed limits is at least 68 %.

As in Example 1, it is observed for a CSB-MPC that the solution time t_{avg} decreases significantly as the primary set becomes small, but does not significantly alter the probabilities p_s and p_c. This can be seen for the $\mathbb{S}_S(1300)$ case in Figure 3.9, where the t_{avg} times of the CSB-MPC are very close to those of a SCMPC, in some cases lower; e.g., CSB-MPC_{240} and CSB-MPC_{330} in Table 3.4. These CSB-MPCs mentioned, in addition to having shorter solution times t_{avg} than their corresponding SCMPC, have better p_s, p_c and N_v. In this way, with suitable size of $\mathbb{S}_S$, if an improvement of the time t_{avg} is required, a CSB-MPC is a viable alternative compared to a SCMPC. For example, if similar or superior

performance indices to those of the SCMPC$_{330}$ ($t_{\text{avg}} = 577$ ms) in Table 3.4 are required, but with a lower solution time, the CSB-MPC$_{240}$ ($t_{\text{avg}} = 407$ ms) with a 170 ms quicker solution time could be used.

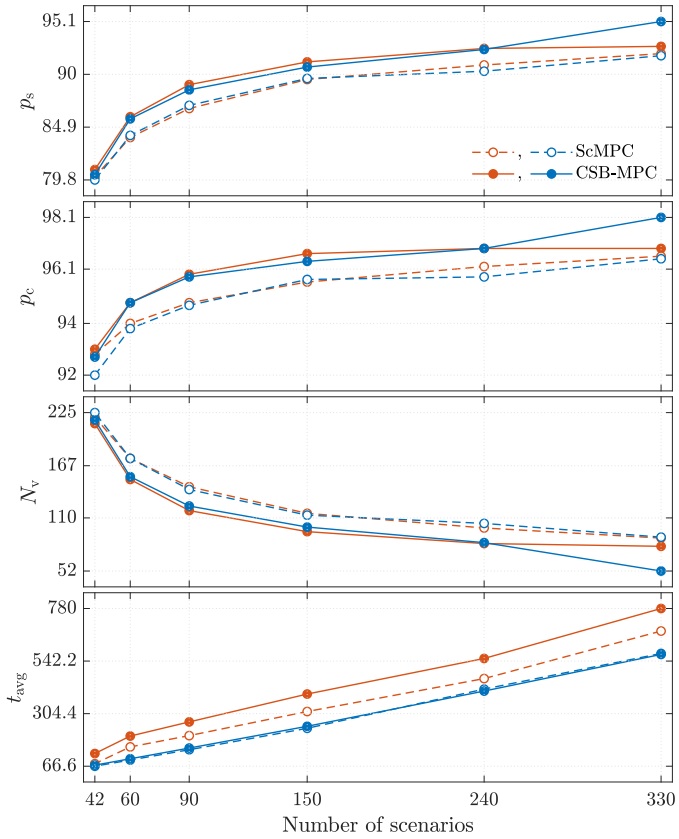

Figure 3.9: Graphs of the performance indices p_s, p_c, N_v and t_{avg} from Tables 3.3 ($\mathbb{S}_S(10000)$, orange lines) and 3.4 ($\mathbb{S}_S(1300)$, blue lines), corresponding to SCMPC (dashed lines) and CSB-MPC (solid lines), for $42, 60, 90, 150, 240$ and 330 scenarios.

The lowest IAE$_{\text{avg}}$ and IAU$_{\text{avg}}$ indicators where obtained by the CSB-MPCs, although very similar to those of SCMPC at values close to IAE$_{\text{avg}} = 76.7$ and IAU$_{\text{avg}} = 18.8$, which compared to those of a MPC with a perfect forecast, they are close to IAE$_{\text{pf}} = 74.908$ and IAU$_{\text{pf}} = 19.440$. In the same way as in Example 1, the closed-loop trajectories exceeded their allowed limits at some moments in all the simulations in both controllers. The inputs applied initially reached their allowed maximums without transgressing them.

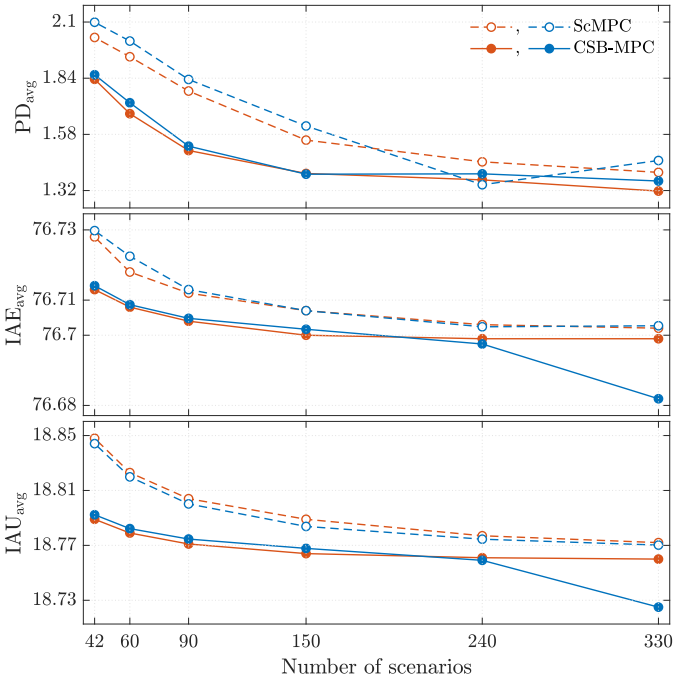

Figure 3.10: Graphs of the performance indices $\mathrm{PD}_{\mathrm{avg}}, \mathrm{IAE}_{\mathrm{avg}}$ and $\mathrm{IAU}_{\mathrm{avg}}$ from Tables 3.3 ($\mathbb{S}_S(10000)$, orange lines) and 3.4 ($\mathbb{S}_S(1300)$, blue lines), corresponding to SCMPC (dashed lines) and CSB-MPC (solid lines), for $42, 60, 90, 150, 240$ and 330 scenarios.

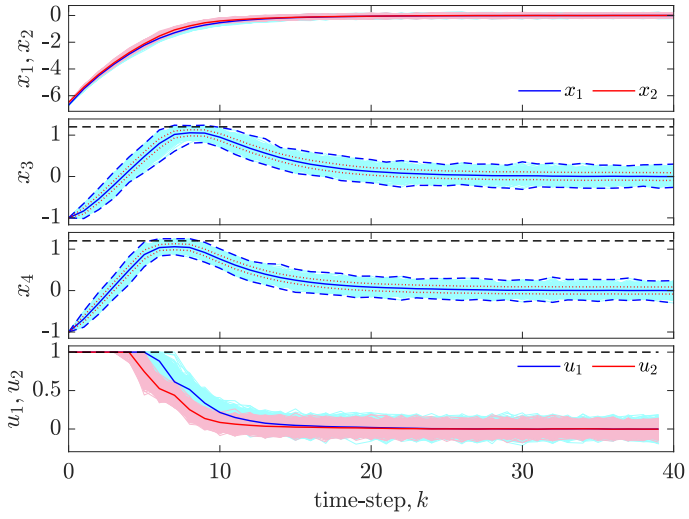

(a)

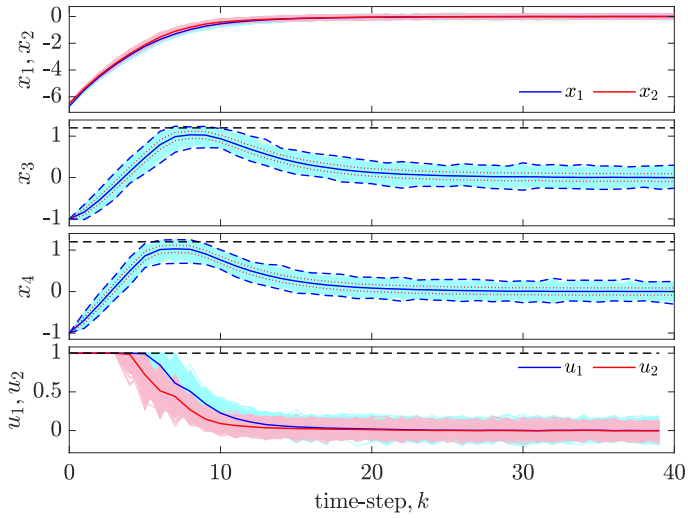

(b)

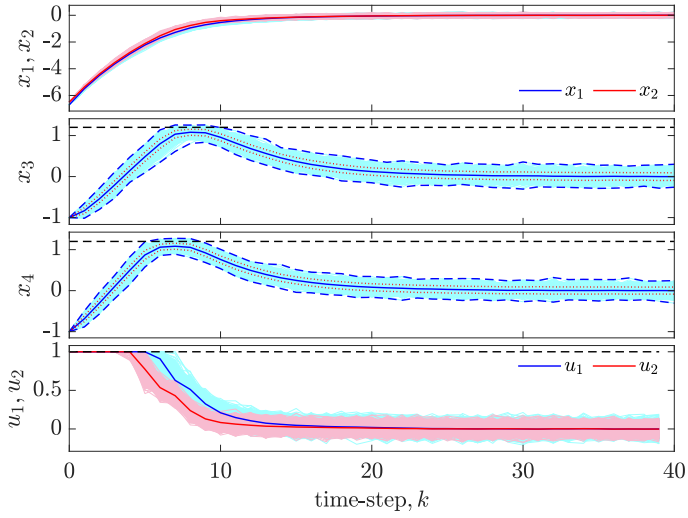

(c)

Figure 3.11: Nonlinear system responses to a SCMPC$_{330}$, CSB-MPC$_{330}$ and CSB-MPC$_{42}$ controllers, for a $\mathbb{S}_S$ of 1300 Scenarios. The 1000 closed-loop trajectories and applied inputs (thin solid lines), mean trajectory (thick solid lines), mean trajectory with standard deviation (dotted lines), minimum and maximum values (blue dashed lines) and constraints (black dashed lines) $|x_3|, |x_4| \leq 1.2$, $|u_1|, |u_2| \leq 1.0$. (a) SCMPC$_{330}$. (b) CSB-MPC$_{330}$. (c) CSB-MPC$_{42}$.

3.5 Chapter Conclusions

A new scenario-based model predictive control approach was introduced in this chapter. This MPC scheme, called conditional scenario-based model predictive control (CSB-MPC), is designed for discrete-time linear systems affected by correlated and bound parametric uncertainties and/or additive disturbances. In this approach, a primary set of equiprobable and randomly generated scenarios is approximated to a set of conditional scenarios with their respective probabilities of occurrence. These are incorporated in the cost function of an optimal control problem where the predicted states and inputs are penalised according to the probabilities associated with the uncertainties on which they depend.

The performances of the CSB-MPC and those of a scenario-based MPC were compared using two numerical examples, whose results showed greater empirical probabilities of constraints satisfaction, above the theoretical one, by the former, increasing the feasibility of an OCP solution, in a probabilistic sense. Also, the CSB-MPC showed a decrease in the number of times constraints are violated, with less distance outside the constraints, even when have a smaller number of scenarios than the scenario-based MPCs.

Finally, for a smaller primary set, the CSB-MPC offers similar solution times, in some cases shorter than those of a standard scenario-based MPC. Consequently, if a trade-off between the level of constraints satisfaction and the computational tractability is required, using a CSB-MPC with a smaller number of scenarios than a scenario-based MPC is a viable option.

Chapter 4

CSB-MPC for Energy Management in Microgrids with Correlated Forecasts

This chapter presents a conditional scenario-based model predictive control (CSB-MPC) for energy management in a microgrid with correlated power generation and demand forecasts. The microgrid includes renewable energy sources such as photovoltaic generators and wind turbines, as well as a battery-based energy storage system. At each sampling time, a large set of scenarios of possible evolutions of power generation and demand forecasts are generated and further approximated to a reduced set of conditional scenarios, with their probabilities of occurrence. Then, the set of reduced scenarios and their probabilities are used to solve a feasible scenario-based mixed-integer linear program (MILP) with finite horizon, where the cost of the energy consumed from the main grid and the discarded generated power are minimised. The first section presents the highlights of the proposed CSB-MPC as an energy management system (EMS) in a microgrid. The second section describes the structure of the microgrid under consideration, its mathematical model, and how uncertainties influence RES power generation and demand forecasts. The third section discusses the CSB-MPC adaptation to the context of energy management in a microgrid, and the optimal control problem to be solved, as well as its numerical and probabilistic feasibility. In the fourth section, a case study is proposed and its results are discussed. Finally, the fifth section presents the conclusions of this chapter.

4.1 Introduction

Photovoltaic and wind power generation forecasts, and possibly demand forecast, are strongly influenced by meteorological conditions that can be highly fluctuating, which can also affect the type or distribution of uncertainties. Therefore, a energy management based on a scenario-based MPC is desirable, given its possibility to include updated statistical information in real-time, to make better decisions consistent with the actual situation of the system. Additionally, there are cases, due to working hours, off-hours, activity in a household, etc., where there is a high correlation between powers [83]–[87], either between the output powers of RES generators, PV-wind, PV-demand, wind-demand, or between various loads on the demand side.

The challenges mentioned above motivate the adaptation of the conditional scenario-based model predictive control (CSB-MPC), introduced in the previous chapter, to manage energy in a microgrid with correlated forecasts. The CSB-MPC strategy, developed for uncertain linear systems with correlated uncertainties, where such uncertainties characteristics are exploited in the solution of a OCP that assigns greater importance to predictions with a higher probability of occurrence. In summary, the main highlights of the proposal are as follows

- A mathematical model of a standard microgrid that includes uncertainties in power generation and demand forecasts, with the possibility of being correlated. This model can improve EMS performance in a microgrid with these characteristics.
- A CSB-MPC adapted to the framework of energy management in a MG with correlated forecasts. These correlation features are exploited in the solution of a OCP with guaranteed numerical and probabilistic feasibilities, that assigns greater importance to predictions with a higher probability of occurrence.
- To validate improvements in the probability of constraint satisfaction of the CSB-MPC, a case study of the simulation of the behaviour of a microgrid whose energy management is performed by a CSB-MPC. Additionally, as a baseline, the performance of the microgrid with the proposed CSB-MPC is compared with that of a deterministic MPC, that of a stochastic MPC of the deterministic group and that of a scenario-based MPC, whose feasibilities of the OCPs, in a probabilistic sense, and other performance indices are provided.

Nomenclature

Parameters

$E^{\min}, E^{\max}$	Minimum/maximum energy storage of the ESS (kWh)
$P_{\mathrm{c}}^{\max}, P_{\mathrm{d}}^{\max}$	Maximum ESS charging and discharging powers (kW)
$P_{\mathrm{g}}^{\max}$	Maximum main grid power (kW)
$\eta_{\mathrm{c}}, \eta_{\mathrm{d}}$	ESS charging and discharging efficiencies
n_q, n_r	Numbers of PV generators and wind turbines, respectively
T_{s}	Sampling time (h)
N	Prediction horizon (number of sampling instants)
S, C	Number of scenarios of the primary $\mathbb{S}_S$ and reduced $\mathbb{S}_C$ sets, respectively
$\alpha_1, \cdots, \alpha_5$	Objective function weights
N_ξ, D_ξ	Number of random variables ξ, and number of divisions to discretise the support of each ξ

State and other variables

$\boldsymbol{x}_k$	State vector
$P_{\mathrm{pvg},q}, \bar{P}_{\mathrm{pvg},q}$	Generated and forecasted powers of the qth PV generator (kW)
$P_{\mathrm{wg},r}, \bar{P}_{\mathrm{wg},r}$	Generated and forecasted powers of the rth wind turbine (kW)
$P_{\mathrm{pv}}, P_{\mathrm{w}}$	PV power (kW) and wind power consumed (kW)
P_{g}	Power consumed from the main grid (kW)
P_{l}	Power consumed by load (kW)
E	ESS state of charge (kWh)
C_{g}	Electricity price (€/kWh)
$\hat{P}_{\mathrm{pvg},q}, \hat{P}_{\mathrm{wg},r}$	Current powers available from RES generators (kW)
$\hat{P}_{\mathrm{l}}, \hat{E}$	Current demand (kW) and SOC (kWh)
$\Psi_k^{[m]}, p_k^{[m]}$	mth equiprobable scenario and probabilities of its elements
$\tilde{\Psi}_k^{[j]}, \tilde{p}_k^{[j]}$	jth conditional scenario and probabilities of its elements
ξ, γ	Random variable (kW) and random vector
$\mu, \Sigma, \mathbb{W}$	Mean, covariance and support of random vector γ

Decision variables

$L_{\mathrm{pv}}, L_{\mathrm{w}}$	Discarded available PV and wind power levels
$P_{\mathrm{c}}, P_{\mathrm{d}}$	ESS charging and discharging powers (kW)
$\delta_{\mathrm{c}}, \delta_{\mathrm{d}}$	ESS charging and discharging modes (binary)
ρ_e, ρ_g	Slack variables of ESS energy (kWh) and main grid power (kW)
$\boldsymbol{d}_k$	Vector of decision variables

Indices

k, i	Current time instant and time step ahead of k, respectively
m, j	Equiprobable scenario and conditional scenario indices
q, r	PV generator and wind turbine indices, respectively

4.2 Microgrid Modelling

The schematic diagram of the microgrid (MG) considered here and its components are illustrated in Figure 4.1, where the arrows indicate the flow of power between its components, which includes power penetration produced by renewable energy sources (RES) such as solar and wind; and an energy storage system (ESS) based on a battery energy storage system (BESS). Furthermore, the proposed MG model considers that that only energy can be imported from the main grid, without the possibility of reselling stored or produced energy that is not consumed. However, in the case of also assuming the sale of energy, its inclusion in the MG model and OCP is straightforward.

In accordance with this, being T_s the sampling period and i the discrete-time index, the mathematical models of the microgrid components are described below.

4.2.1 Renewable Energy Sources (RES)

The photovoltaic (PV) power $P_\mathrm{pv}(i)$ consumed by the MG in the instant of time i is given in (4.1a), where $P_{\mathrm{pvg},q}(i)$ is the PV power generated by the qth $\forall q \in \{1, 2, \dots n_q\}$ PV generator at that instant, which is a function of the efficiency of the PV generator, its array area and the solar irradiance [114]

$$P_\mathrm{pv}(i) = (1 - L_\mathrm{pv}(i)) \sum_{q=1}^{n_q} P_{\mathrm{pvg},q}(i) \tag{4.1a}$$

$$0 \leq L_\mathrm{pv}(i) \leq 1 \tag{4.1b}$$

$L_\mathrm{pv}(i)$ is a decision variable that determines the level of the total PV power generated that is not consumed, and is bounded by the constraint (4.1b).

On the other hand, the wind power consumed $P_\mathrm{w}(i)$ is given in (4.2a), where $P_{\mathrm{wg},r}(i)$ is the generated power by the rth $\forall r \in \{1, 2, \dots n_r\}$ wind turbine (WT), wich depends on the wind speed, the air density, the area swept by blades and the rotor power coefficient [115]

$$P_\mathrm{w}(i) = (1 - L_\mathrm{w}(i)) \sum_{r=1}^{n_r} P_{\mathrm{wg},r}(i) \tag{4.2a}$$

$$0 \leq L_\mathrm{w}(i) \leq 1 \tag{4.2b}$$

Constraint (4.2b) is a constraint on the decision variable $L_\mathrm{w}(i)$, which determines the level of the total wind power generated that is not consumed.

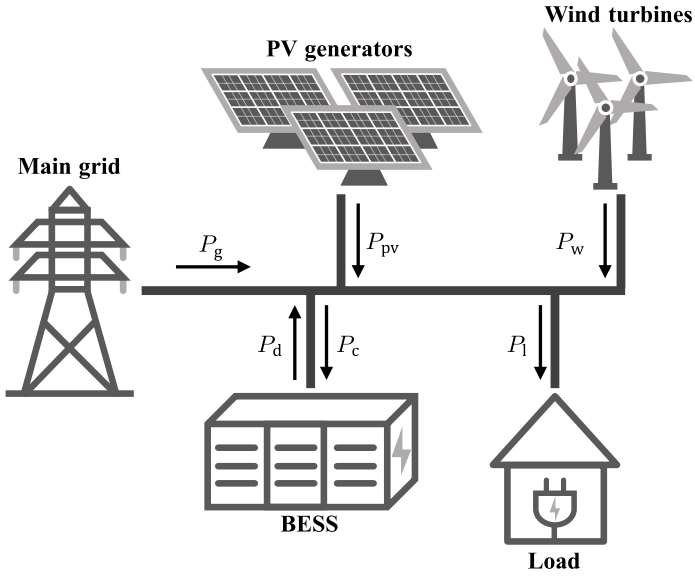

Figure 4.1: Microgrid schematic diagram. The arrows indicate the power flow between its components.

4.2.2 Energy Storage System (ESS)

The energy storage is performed by a battery energy storage system (BESS) [61], [116]. The prediction of the state of charge (SOC) $E(i+1)$ for instant $i+1$ is given by the dynamic model (4.3a), which is a function of the previous SOC $E(i)$, and the charging power $P_{\mathrm{c}}(i)$ and discharging power $P_{\mathrm{d}}(i)$ decision variables

$$E(i+1) = E(i) + \eta_{\mathrm{c}} T_{\mathrm{s}} P_{\mathrm{c}}(i) - \frac{1}{\eta_{\mathrm{d}}} T_{\mathrm{s}} P_{\mathrm{d}}(i) \tag{4.3a}$$

$$E^{\min} \leq E(i+1) \leq E^{\max} \tag{4.3b}$$

$$0 \leq P_{\mathrm{c}}(i) \leq P_{\mathrm{c}}^{\max} \delta_{\mathrm{c}}(i) \tag{4.3c}$$

$$0 \leq P_{\mathrm{d}}(i) \leq P_{\mathrm{d}}^{\max} \delta_{\mathrm{d}}(i) \tag{4.3d}$$

$$\delta_{\mathrm{c}}(i), \delta_{\mathrm{d}}(i) \in \{0, 1\} \tag{4.3e}$$

$$\delta_{\mathrm{c}}(i) + \delta_{\mathrm{d}}(i) \leq 1 \tag{4.3f}$$

where η_{c} and η_{d} are the charging and discharging efficiencies of the storage system, respectively.

The set of constraints on the BESS SOC (4.3a) are stated in (4.3b)-(4.3d). In this, (4.3b) are the constraints on the energy storage capacity; (4.3c) and (4.3d) are the

constraints on the charging and discharging powers, respectively, conditioned by the binary decision variables $\delta_{\mathrm{c}}(i)$ (charging mode) and $\delta_{\mathrm{d}}(i)$ (discharging mode) to avoid simultaneous charging and discharging of the battery through constraints (4.3e)-(4.3f).

4.2.3 Power Balance

The balance between the delivered power $P_{\mathrm{del}}(i)$ and the consumed power $P_{\mathrm{con}}(i)$ in the MG, for all i, must satisfy

$$P_{\mathrm{del}}(i) = P_{\mathrm{con}}(i)$$
$$P_{\mathrm{g}}(i) + P_{\mathrm{pv}}(i) + P_{\mathrm{w}}(i) + P_{\mathrm{d}}(i) = P_{\mathrm{l}}(i) + P_{\mathrm{c}}(i)$$

where $P_{\mathrm{g}}(i)$ is the power imported from the main grid and $P_{\mathrm{l}}(i)$ is the power demanded by the load.

By rearranging the previous power balance equation, the power delivered by the main grid is expressed as (4.4a), and its constraints as (4.4b)

$$P_{\mathrm{g}}(i) = P_{\mathrm{l}}(i) - P_{\mathrm{pv}}(i) - P_{\mathrm{w}}(i) + P_{\mathrm{c}}(i) - P_{\mathrm{d}}(i) \tag{4.4a}$$
$$0 \leq P_{\mathrm{g}}(i) \leq P_{\mathrm{g}}^{\max}. \tag{4.4b}$$

4.2.4 System Uncertainties

Considering that both the power generated by each RES generator and the power demand have uncertainties, each $P_{\mathrm{pvg},q}(i)$, $P_{\mathrm{wg},r}(i)$ and $P_{\mathrm{l}}(i)$ in (4.1a), (4.2a) and (4.4a), respectively, can be split and expressed as the sum of two components. One known component representing the forecasted power ($\bar{P}_{\mathrm{pvg},q}(i)$, $\bar{P}_{\mathrm{wg},r}(i)$, $\bar{P}_{\mathrm{l}}(i)$) and one stochastic component representing the forecast error ($\xi_{\mathrm{pvg},q}(i)$, $\xi_{\mathrm{wg},r}(i)$, $\xi_{\mathrm{l}}(i)$), this is

$$P_{\mathrm{pvg},q}(i) = \bar{P}_{\mathrm{pvg},q}(i) + \xi_{\mathrm{pvg},q}(i) \tag{4.5a}$$
$$P_{\mathrm{wg},r}(i) = \bar{P}_{\mathrm{wg},r}(i) + \xi_{\mathrm{wg},r}(i) \tag{4.5b}$$
$$P_{\mathrm{l}}(i) = \bar{P}_{\mathrm{l}}(i) + \xi_{\mathrm{l}}(i). \tag{4.5c}$$

Furthermore, each random variable is normally distributed and with zero mean. Some or all the set of random variables $\xi_{\mathrm{pvg},q}$, $\xi_{\mathrm{wg},r}$ and ξ_{l} are correlated (e.g. there is a correlation between powers [83]–[85], [87], either between generators in

the RES, or between demand and generated power) and make up the random vector $\gamma \in \mathbb{R}^{n_q+n_r+1}$, that is

$$\gamma(i) = [\xi_{\text{pvg},1}(i), \ldots, \xi_{\text{pvg},n_q}(i), \xi_{\text{wg},1}(i), \ldots, \xi_{\text{wg},n_r}(i), \xi_{\text{l}}(i)]^\top$$

This vector has a multivariate normal distribution $\gamma(i) \sim \mathcal{N}_{n_q+n_r+1}(\mu(i), \Sigma(i))$ with zero mean vector $\mu(i) = [0, \ldots, 0]^\top$, a known covariance matrix $\Sigma(i)$, and unbounded or with bounded support (if exist) $\mathbb{W}_\gamma(i)$. Any sequence $\{\gamma(0), \gamma(1), \ldots\}$ is independent and identically distributed (i.i.d.). Additionally, uncertainties in the BESS (4.3a), such as parametric (e.g., in η_c and/or η_d) and/or in the current SOC $E(i)$, can also be considered by including them in γ.

4.3 CSB-MPC Energy Management System

This section discusses how the conditional scenario-based MPC (CSB-MPC) strategy is adapted to propose a control strategy for energy management in a MG with forecast uncertainties. At each instant of time k, the MPC predicts the evolutions of the states and inputs of the process, across a prediction horizon N. This using a model of the process and assuming that the current measures of its states and inputs at that instant are available. These predictions are used to solve an optimal control problem (OCP) subject to constraints on the predicted states and inputs, whose solution is the sequence of future inputs that steer the process towards a target operating point while satisfying the constraints. According to the receding horizon principle (RH) [21], only the first element of the optimal input sequence is applied, executing the OCP in the next time instant $k + 1$ again.

The CSB-MPC is a strategy that belongs to the scenario-based group [35], [36] of stochastic MPC (SMPC) [54], [117], where the uncertainties present in the system are considered to have a stochastic nature and whose characteristics, such as mean, covariance and bounds (if they exist), are known. With this knowledge, a primary set $\mathbb{S}_S$ of S equiprobable scenarios is generated and further approximated to a reduced set $\mathbb{S}_C$ of C conditional scenarios (CS), with their respective probabilities of occurrence. This reduced set and its probability of occurrence are incorporated into the prediction model to solve an OCP with constraints that must be fulfilled for all C scenarios, and in whose quadratic objective function the predicted states and inputs are penalised according to their probabilities of occurrence.

In the framework of a MG energy management system (EMS) [66], [68], the OCP consists of an objective function that minimises the cost of energy consumed, based on energy tariffs, from the main grid. Typically, this function incorporates the predictions of the SOC, predictions of the power delivered by the main grid,

and the forecast of the power demand and power generated by the RES. The decision variables are the power used of the total power generated by the RES and the charging/discharging powers of the ESS. When uncertainties exist, for example, in generation and demand forecasts, an OCP that takes them into account is most appropriate.

4.3.1 Scenario Generation and Reduction

In the following, the notation $x^{[m]}(i|k)$ is interpreted as the predicted value of the variable x of scenario m, for the time step i ahead of the current time instant k. Since uncertainties are present in the powers generated by RES and demand, as noted in (4.5), a set of scenarios $\{\Psi_k^{[1]}, \Psi_k^{[2]}, \ldots, \Psi_k^{[S]}\} \in \mathbb{S}_S$ in the EMS proposed here consists of S possible evolutions of $P_{\text{pvg},q}$, $P_{\text{wg},w}$ and P_{l}, for N time steps ahead of k, in which the mth scenario $\Psi_k^{[m]}$ $\forall m \in \{1, 2, \ldots, S\}$ has the structure

$$\begin{aligned}\Psi_k^{[m]} &= \left\{\psi^{[m]}(1|k), \psi^{[m]}(2|k), \ldots, \psi^{[m]}(N|k)\right\} \\ &= \left\{ \begin{bmatrix} P^{[m]}_{\text{pvg},1}(1|k) \\ \vdots \\ P^{[m]}_{\text{pvg},n_q}(1|k) \\ P^{[m]}_{\text{wg},1}(1|k) \\ \vdots \\ P^{[m]}_{\text{wg},n_r}(1|k) \\ P^{[m]}_{\text{l}}(1|k) \end{bmatrix}, \begin{bmatrix} P^{[m]}_{\text{pvg},1}(2|k) \\ \vdots \\ P^{[m]}_{\text{pvg},n_q}(2|k) \\ P^{[m]}_{\text{wg},1}(2|k) \\ \vdots \\ P^{[m]}_{\text{wg},n_r}(2|k) \\ P^{[m]}_{\text{l}}(2|k) \end{bmatrix}, \ldots, \begin{bmatrix} P^{[m]}_{\text{pvg},1}(N|k) \\ \vdots \\ P^{[m]}_{\text{pvg},n_q}(N|k) \\ P^{[m]}_{\text{wg},1}(N|k) \\ \vdots \\ P^{[m]}_{\text{wg},n_r}(N|k) \\ P^{[m]}_{\text{l}}(N|k) \end{bmatrix} \right\}.\end{aligned} \tag{4.6}$$

Assumption 4.1. *Given the current time instant k, updated forecasts of power generation $\bar{P}_{pvg,q}(i|k)$, $\bar{P}_{wg,r}(i|k)$ and demand $\bar{P}_l(i|k)$ for a window $\forall i \in \{1, \ldots, N\}$ of N steps ahead of k, together with the characteristics $\mu(i|k)$, $\Sigma(i|k)$, $\mathbb{W}_\gamma(i|k)$ of the random vector γ are available.*

In line with Assumption 4.1, each $\Psi_k^{[m]}$ is calculated using (4.5), which consists of the sum of a known part $\bar{\Psi}_k^{[m]} = \{\bar{\psi}^{[m]}(1|k), \bar{\psi}^{[m]}(2|k), \ldots, \bar{\psi}^{[m]}(N|k)\}$ with a stochastic part $\Gamma_k^{[m]} = \{\gamma^{[m]}(1|k), \gamma^{[m]}(2|k), \ldots, \gamma^{[m]}(N|k)\}$

$$\begin{aligned}\Psi_k^{[m]} &= \bar{\Psi}_k^{[m]} + \Gamma_k^{[m]}, \\ \psi^{[m]}(i|k) &= \bar{\psi}^{[m]}(i|k) + \gamma^{[m]}(i|k).\end{aligned}$$

The known part of $\Psi_k^{[m]}$ are the forecasts $\bar{P}_{\text{pvg},q}(i|k)$, $\bar{P}_{\text{wg},r}(i|k)$ and $\bar{P}_{\text{l}}(i|k)$, which will be the same for all scenarios $\bar{P}^{[m]}_{\text{pvg},q}(i|k) = \bar{P}_{\text{pvg},q}(i|k)$, $\bar{P}^{[m]}_{\text{wg},r}(i|k) = \bar{P}_{\text{wg},r}(i|k)$ and $\bar{P}^{[m]}_{\text{l}}(i|k) = \bar{P}_{\text{l}}(i|k)$

$$\begin{aligned}\bar{\Psi}_k^{[m]} &= \left\{\bar{\psi}^{[m]}(1|k), \bar{\psi}^{[m]}(2|k), \ldots, \bar{\psi}^{[m]}(N|k)\right\} \\ &= \left\{ \begin{bmatrix} \bar{P}_{\text{pvg},1}(1|k) \\ \vdots \\ \bar{P}_{\text{pvg},n_q}(1|k) \\ \bar{P}_{\text{wg},1}(1|k) \\ \vdots \\ \bar{P}_{\text{wg},n_r}(1|k) \\ \bar{P}_{\text{l}}(1|k) \end{bmatrix}, \begin{bmatrix} \bar{P}_{\text{pvg},1}(2|k) \\ \vdots \\ \bar{P}_{\text{pvg},n_q}(2|k) \\ \bar{P}_{\text{wg},1}(2|k) \\ \vdots \\ \bar{P}_{\text{wg},n_r}(2|k) \\ \bar{P}_{\text{l}}(2|k) \end{bmatrix}, \ldots, \begin{bmatrix} \bar{P}_{\text{pvg},1}(N|k) \\ \vdots \\ \bar{P}_{\text{pvg},n_q}(N|k) \\ \bar{P}_{\text{wg},1}(N|k) \\ \vdots \\ \bar{P}_{\text{wg},n_r}(N|k) \\ \bar{P}_{\text{l}}(N|k) \end{bmatrix} \right\}.\end{aligned}$$

In addition, since the data $\mu(i|k)$, $\Sigma(i|k)$ and $\mathbb{W}_\gamma(i|k)$ of the forecast errors vector γ are known, S realisations $\{\Gamma_k^{[1]}, \Gamma_k^{[2]}, \ldots, \Gamma_k^{[S]}\}$ of γ, for N steps each, are performed (e.g. by means of a random number generator), thus constituting the stochastic part

$$\begin{aligned}\Gamma_k^{[m]} &= \left\{\gamma^{[m]}(1|k), \gamma^{[m]}(2|k), \ldots, \gamma^{[m]}(N|k)\right\} \\ &= \left\{ \begin{bmatrix} \xi^{[m]}_{\text{pvg},1}(1|k) \\ \vdots \\ \xi^{[m]}_{\text{pvg},n_q}(1|k) \\ \xi^{[m]}_{\text{wg},1}(1|k) \\ \vdots \\ \xi^{[m]}_{\text{wg},n_r}(1|k) \\ \xi^{[m]}_{\text{l}}(1|k) \end{bmatrix}, \begin{bmatrix} \xi^{[m]}_{\text{pvg},1}(2|k) \\ \vdots \\ \xi^{[m]}_{\text{pvg},n_q}(2|k) \\ \xi^{[m]}_{\text{wg},1}(2|k) \\ \vdots \\ \xi^{[m]}_{\text{wg},n_r}(2|k) \\ \xi^{[m]}_{\text{l}}(2|k) \end{bmatrix}, \ldots, \begin{bmatrix} \xi^{[m]}_{\text{pvg},1}(N|k) \\ \vdots \\ \xi^{[m]}_{\text{pvg},n_q}(N|k) \\ \xi^{[m]}_{\text{wg},1}(N|k) \\ \vdots \\ \xi^{[m]}_{\text{wg},n_r}(N|k) \\ \xi^{[m]}_{\text{l}}(N|k) \end{bmatrix} \right\}.\end{aligned}$$

As discussed in the conclusions of the chapter 2 and in subsection 3.2.2, the main limiting factor of randomised schemes resides in the size of the set $\mathbb{S}_S$ used to solve the OCP, which defines the optimal solution and its computational tractability. The latter because a huge $\mathbb{S}_S$ better represents the characteristics of the uncertainties present in the system, but may result in a numerically intractable OCP. In contrast, a very small $\mathbb{S}_S$ decreases the computational burden, but may have improbable scenarios far from the reality of the system. One way to decrease the computational burden when $\mathbb{S}_S$ is large lies in solving the OCP for a reduced set

$\mathbb{S}_C$, which is obtained using scenario reduction techniques; where the technique selected will determine how closely the reduced set represents the statistical moments of the random vector γ, and the time used for the reduction.

The CSB-MPC, developed for discrete-time linear systems with both additive and/or parametric uncertainties, which are correlated, exploits the conditional scenario (CS) concept [105] and its reduction method [82] in the two-stage stochastic mixed-integer linear programming (SMILP) context and extends it to the MPC framework. In CSB-MPC, $\mathbb{S}_S$ is referred to as the primary set of equiprobable scenarios, that is, each element $\psi^{[m]}(i|k)$ in $\Psi_k^{[m]}$, has a probability of occurrence $p^{[m]}(i|k) = 1/S$. The number of conditional scenarios C, desired for $\mathbb{S}_C$, must be defined such that $C = N_\xi D_\xi$ is satisfied, where $N_\xi = n_q + n_r + 1$ is the number of random variables ξ present in the system and D_ξ is the number of divisions to discretise the support of each ξ.

Via Algorithm 3.2, with the primary set $\mathbb{S}_S$ and C as inputs, $\mathbb{S}_S$ is approximated to a reduced set $\mathbb{S}_C$ of C conditional scenarios (4.7a), with their probabilities of occurrence (4.7b)

$$\left\{\tilde{\Psi}_k^{[1]}, \ldots, \tilde{\Psi}_k^{[C]}\right\} \in \mathbb{S}_C, \qquad \tilde{\Psi}_k^{[j]} = \left\{\tilde{\psi}^{[j]}(1|k), \tilde{\psi}^{[j]}(2|k) \ldots, \tilde{\psi}^{[j]}(N|k)\right\} \tag{4.7a}$$

$$\left\{\tilde{p}_k^{[1]}, \tilde{p}_k^{[2]}, \ldots, \tilde{p}_k^{[C]}\right\}, \qquad \tilde{p}_k^{[j]} = \left\{\tilde{p}^{[j]}(1|k), \tilde{p}^{[j]}(2|k), \ldots, \tilde{p}^{[j]}(N|k)\right\} \tag{4.7b}$$

$$\forall j \in \{1, \ldots, C\}$$

where each CS $\tilde{\Psi}_k^{[j]}$ has the same equiprobable scenario structure (4.6), hence

$$\tilde{\psi}^{[j]}(i|k) = \begin{bmatrix} \tilde{P}^{[j]}_{\text{pvg},1}(i|k) \\ \vdots \\ \tilde{P}^{[j]}_{\text{pvg},n_q}(i|k) \\ \tilde{P}^{[j]}_{\text{wg},1}(i|k) \\ \vdots \\ \tilde{P}^{[j]}_{\text{wg},n_r}(i|k) \\ \tilde{P}^{[j]}_{\text{l}}(i|k) \end{bmatrix}, \qquad \forall i \in \{1, \ldots, N\}$$

and keeping in mind that, in contrast to other techniques, the reduction is carried out without requiring an optimisation stage.

4.3.2 Prediction Model and Constraints

Before defining the prediction model, the following assumption must be addressed

Assumption 4.2. *For any current instant k, the real values of the PV production, wind production, demand and ESS SOC for that instant are assumed to be known and are denoted by $\hat{P}_{pvg,q}(k)$, $\hat{P}_{wg,r}(k)$, $\hat{P}_l(k)$ and $\hat{E}(k)$, respectively.*

Using the MG model presented in the previous section and replacing $\mathbb{S}_C$ (4.7a) in (4.1a), (4.2a) and (4.4a), the prediction model (4.8) can be derived $\forall i \in \{0, \dots, N\}$, where, with real information available, predictions for instant $i = 0$ will be the same for all scenarios, i.e. $\tilde{P}^{[j]}_{\mathrm{pvg},q}(0|k) = \hat{P}_{\mathrm{pvg},q}(k)$, $\tilde{P}^{[j]}_{\mathrm{wg},r}(0|k) = \hat{P}_{\mathrm{wg},r}(k)$, $E(0|k) = \hat{E}(k)$ and $\tilde{P}^{[j]}_{\mathrm{l}}(0|k) = \hat{P}_{\mathrm{l}}(k)$, this in line with Assumption 4.2

$$\tilde{P}^{[j]}_{\mathrm{pv}}(i|k) = (1 - L_{\mathrm{pv}}(i|k)) \sum_{q=1}^{n_q} \tilde{P}^{[j]}_{\mathrm{pvg},q}(i|k) \tag{4.8a}$$

$$\tilde{P}^{[j]}_{\mathrm{w}}(i|k) = (1 - L_{\mathrm{w}}(i|k)) \sum_{r=1}^{n_r} \tilde{P}^{[j]}_{\mathrm{wg},r}(i|k) \tag{4.8b}$$

$$E(i+1|k) = E(i|k) + \eta_{\mathrm{c}} T_{\mathrm{s}} P_{\mathrm{c}}(i|k) - \frac{1}{\eta_{\mathrm{d}}} T_{\mathrm{s}} P_{\mathrm{d}}(i|k) \tag{4.8c}$$

$$\tilde{P}^{[j]}_{\mathrm{g}}(i|k) = \tilde{P}^{[j]}_{\mathrm{l}}(i|k) - \tilde{P}^{[j]}_{\mathrm{pv}}(i|k) - \tilde{P}^{[j]}_{\mathrm{w}}(i|k) + P_{\mathrm{c}}(i|k) - P_{\mathrm{d}}(i|k). \tag{4.8d}$$

A model of the BESS less close to the real one may result in a real SOC outside the defined operating limits [118]. Usually, the $E^{\min}$ and $E^{\max}$ limits of the SOC are set at a percentage within those supplied by the manufacturer (e.g. between 15-20%) to extend the life of the BESS [61], [118].

Likewise, $P^{\max}_{\mathrm{g}}$ is set as the value of the contracted power, or a smaller value when a reduction in consumption from the main grid is required at peak hours through load curtailment [68]. Hence an unusual peak in demand may cause the power delivered by the RES and ESS to be insufficient, making it necessary to use a power above $P^{\max}_{\mathrm{g}}$ to maintain the power balance.

In accordance with the aforementioned, to ensure the feasibility of the OCP at any instant, the hard constraints on SOC (4.3b) and delivered power (4.4b) are reformulated as new soft constraints, by incorporating the slack variables ρ_e and ρ_g. Therefore, all predictions in (4.8) must satisfy the operational constraints

(4.1b), (4.2b), (4.3b)-(4.3f) and (4.4b), which are listed below

$$0 \leq L_{\mathrm{pv}}(i|k) \leq 1 \tag{4.9a}$$
$$0 \leq L_{\mathrm{w}}(i|k) \leq 1 \tag{4.9b}$$
$$E^{\min} - \rho_e(i|k) \leq E(i+1|k) \leq E^{\max} + \rho_e(i|k) \tag{4.9c}$$
$$0 \leq P_{\mathrm{c}}(i|k) \leq P_{\mathrm{c}}^{\max}\delta_{\mathrm{c}}(i|k) \tag{4.9d}$$
$$0 \leq P_{\mathrm{d}}(i|k) \leq P_{\mathrm{d}}^{\max}\delta_{\mathrm{d}}(i|k) \tag{4.9e}$$
$$\delta_{\mathrm{c}}(i), \delta_{\mathrm{d}}(i) \in \{0,1\} \tag{4.9f}$$
$$\delta_{\mathrm{c}}(i|k) + \delta_{\mathrm{d}}(i|k) \leq 1 \tag{4.9g}$$
$$0 \leq \tilde{P}_{\mathrm{g}}^{[j]}(i|k) \leq P_{\mathrm{g}}^{\max} + \rho_g(i|k) \tag{4.9h}$$
$$0 \leq \rho_e(i|k) \tag{4.9i}$$
$$0 \leq \rho_g(i|k) \tag{4.9j}$$

where the new decision variables ρ_e and ρ_g are restricted to be zero or positive through (4.9i) and (4.9j), and are penalised in the objective function to force their values to be zero if an optimum solution can be obtained without violating the softened constraints.

The state vector of the jth scenario for instant i $\forall i \in \{0,\dots,N\}$ is denoted by $x^{[j]}(i|k)$, and the states of all instants are grouped in $\boldsymbol{x}_k^{[j]}$, this is

$$\begin{aligned} x^{[j]}(i|k) = [&\tilde{P}^{[j]}_{\mathrm{pvg},1}(i|k),\dots \tilde{P}^{[j]}_{\mathrm{pvg},n_q}(i|k), \tilde{P}^{[j]}_{\mathrm{pv}}(i|k),\\ &\tilde{P}^{[j]}_{\mathrm{wg},1}(i|k),\dots \tilde{P}^{[j]}_{\mathrm{wg},n_r}(i|k), \tilde{P}^{[j]}_{\mathrm{w}}(i|k),\\ &E(i|k), \tilde{P}^{[j]}_{\mathrm{l}}(i|k), \tilde{P}^{[j]}_{\mathrm{g}}(i|k)]^\top,\\ \boldsymbol{x}_k^{[j]} = &\{x^{[j]}(0|k),\dots,x^{[j]}(N|k)\}. \end{aligned}$$

Similarly, the vector $d(i|k)$ groups the decision variables of the instant i, and $\boldsymbol{d}_k$ groups the full set of decision variables of the OCP, which are the same for all C scenarios

$$\begin{aligned} d(i|k) &= [L_{\mathrm{pv}}(i|k), L_{\mathrm{w}}(i|k), P_{\mathrm{c}}(i|k), P_{\mathrm{d}}(i|k), \delta_{\mathrm{c}}(i|k), \delta_{\mathrm{d}}(i|k), \rho_e(i|k), \rho_g(i|k)]^\top,\\ \boldsymbol{d}_k &= \{d(0|k),\dots,d(N|k)\}. \end{aligned}$$

4.3.3 Objective Function and Optimisation Problem

Originally, as stated in section 3.3, the OCP in CSB-MPC consists of a quadratic programming problem (QP) with constraints, in whose quadratic objective function the predicted states and inputs for each scenario are penalised by their associated probabilities of occurrence to give higher weight to the most likely realisations.

The objective function considered in this context, is a linear function of $\boldsymbol{d}_k$, which consists of an average of all C scenarios, in terms of the cost of energy consumed from the main grid and the power generated by RES that is discarded, and is given by

$$\begin{aligned} J(\boldsymbol{d}_k) = \frac{1}{C}\sum_{j=1}^{C}\sum_{i=0}^{N}\Bigg[\tilde{p}^{[j]}(i|k)\Bigg(&\alpha_1 C_{\mathrm{g}}(i|k)\tilde{P}_{\mathrm{g}}^{[j]}(i|k) \\ &+ \alpha_2 L_{pv}(i|k)\sum_{q=1}^{n_q}\tilde{P}_{\mathrm{pvg},q}^{[j]}(i|k) \\ &+ \alpha_3 L_{w}(i|k)\sum_{r=1}^{n_r}\tilde{P}_{\mathrm{wg},r}^{[j]}(i|k) \\ &+ \alpha_4\rho_g(i|k) + \alpha_5\rho_e(i|k)\Bigg)\Bigg] \end{aligned} \tag{4.10}$$

where $\{\alpha_1, \ldots, \alpha_5\}$ are user-defined weights.

The first term within the parenthesis penalises the cost of energy consumed from the main grid through α_1 and electricity prices C_{g}, whose values or forecasts are considered to be known $\{C_{\mathrm{g}}(0|k), \ldots, C_{\mathrm{g}}(N|k)\}$.

In the second and third terms, α_2 and α_3 penalise the power that is discarded from the power generated by the PV generators and wind turbines to reduce the use of the ESS.

The last two terms, corresponding to the slack variables ρ_g and ρ_e, are penalised with the weights α_4 and α_5, which are often set to high values compared to the remaining weights, to make their values close to zero.

For each j, the above five terms are penalised via their respective probabilities $\tilde{p}_k^{[j]}$ given in (4.7b), where, based on Assumption 4.2, where accurate current information is available, $\tilde{p}^{[j]}(0|k) = 1/C$ is defined.

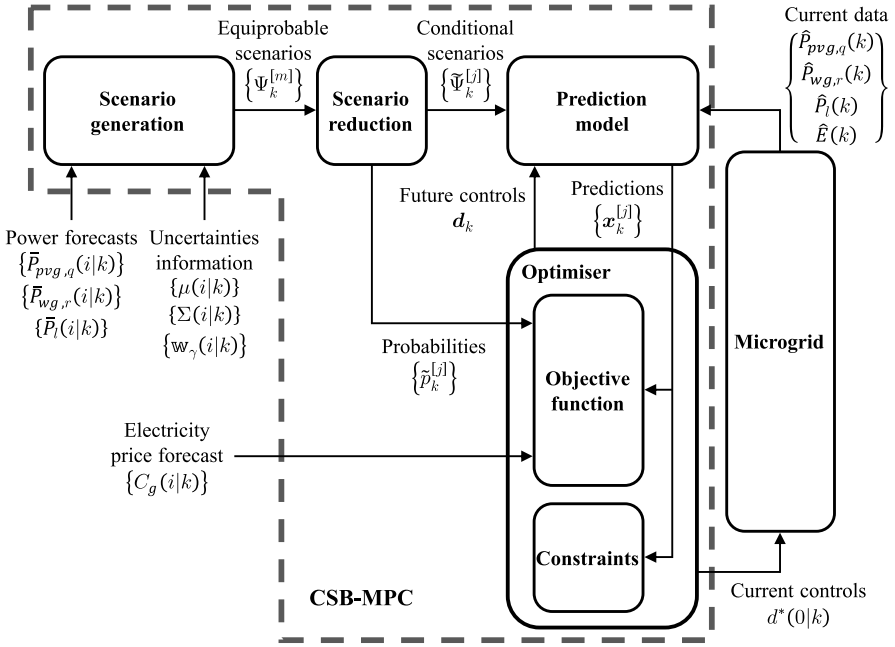

Figure 4.2: Schematic diagram of the microgrid with a CSB-MPC acting as EMS.

Since the vector of decision variables $\boldsymbol{d}_k$ includes the discrete variables δ_c and δ_d, strictly of binary type $\delta_\mathrm{c}, \delta_\mathrm{d} \in \{0,1\}$, the OCP in the energy management of the MG under consideration is to minimise $J(\boldsymbol{d}_k)$ by solving the following scenario-based mixed-integer linear program (MILP) with finite horizon

$$\min_{\boldsymbol{d}_k} \; J(\boldsymbol{d}_k) \tag{4.11}$$

s.t.

$$\begin{aligned}
&(4.8\mathrm{a}) - (4.8\mathrm{d}),\\
&(4.9\mathrm{a}) - (4.9\mathrm{j}),\\
&\tilde{P}^{[j]}_{\mathrm{pvg},q}(0|k) = \hat{P}_{\mathrm{pvg},q}(k),\\
&\tilde{P}^{[j]}_{\mathrm{wg},r}(0|k) = \hat{P}_{\mathrm{wg},r}(k),\\
&\tilde{P}^{[j]}_{\mathrm{l}}(0|k) = \hat{P}_{\mathrm{l}}(k),\\
&E(0|k) = \hat{E}(k),\\
&\tilde{p}^{[j]}(0|k) = 1/C,\\
&\forall i \in \{0,1,\ldots,N\}, \qquad \forall j \in \{1,2,\ldots,C\}
\end{aligned}$$

Algorithm 4.1 Operation of the Microgrid CSB-MPC

1. Define the number S of scenarios in the primary set $\mathbb{S}_S$ and the desired number C of CS in the reduced set $\mathbb{S}_C$, where $C = N_\xi D_\xi$.
2. At the current instant k, obtain the current MG data $\hat{P}_{\mathtt{pvg},q}(k), \hat{P}_{\mathtt{wg},r}(k), \hat{P}_{\mathtt{l}}(k), \hat{E}(k)$; the updated forecasts of powers $\bar{P}_{\mathtt{pvg},q}(i|k), \bar{P}_{\mathtt{wg},r}(i|k), \bar{P}_{\mathtt{l}}(i|k)$, and the characteristics $\mu(i|k), \Sigma(i|k), \mathbb{W}_\gamma(i|k)$ of their uncertainties, for N steps $\forall i \in \{1, \ldots, N\}$ ahead of k. Also, the updated electricity prices forecasts $C_{\mathtt{g}}(i|k)$.
3. Use $\bar{P}_{\mathtt{pvg},q}(i|k)$, $\bar{P}_{\mathtt{wg},r}(i|k)$, $\bar{P}_{\mathtt{l}}(i|k)$ to obtain the known part $\bar{\Psi}_k^{[m]}$ of $\Psi_k^{[m]}$ in (4.6), and generate S realisations of γ for N steps each to obtain its stochastic part $\Gamma_k^{[m]}$.
4. Construct mth scenario $\Psi_k^{[m]} = \bar{\Psi}_k^{[m]} + \Gamma_k^{[m]}$ according to the structure in (4.6), and group the scenarios $\{\Psi_k^{[1]}, \ldots, \Psi_k^{[S]}\}$ to build the primary set $\mathbb{S}_S$.
5. Use Algorithm 3.2 to obtain the reduced set $\mathbb{S}_C$ (4.7a) and its probabilities (4.7b).
6. Replace $\mathbb{S}_C$ in (4.8), (4.9) and (4.10) and obtain the optimal solution vector $\boldsymbol{d}_k^*$ by solving the MILP (4.11).
7. Apply the first value $d^*(0|k)$ of vector $\boldsymbol{d}_k^*$ to the MG. Set $k = k + 1$, wait until $T_{\mathtt{s}}$ has elapsed and then return to Step 2.

where, using the receding horizon strategy, OCP (4.11) is solved at each instant k, and only the values of $d^*(0|k)$ for the instant $i = 0$ of the obtained optimal vector $\boldsymbol{d}_k^*$ are applied to the MG, i.e.

$$\left\{L_{\mathrm{pv}}^*(0|k), L_{\mathrm{w}}^*(0|k), P_{\mathrm{c}}^*(0|k), P_{\mathrm{d}}^*(0|k), \delta_{\mathrm{c}}^*(0|k), \delta_{\mathrm{d}}^*(0|k), \rho_e^*(0|k), \rho_g^*(0|k)\right\}.$$

The implementation and solution of MILP (4.11) can be carried out using commercial software such as Mosek, Gurobi or Cplex among others. Figure 4.2 illustrates the schematic diagram of the proposed CSB-MPC for the MG. In addition, the steps in the operation of the CSB-MPC as a EMS are summarised in Algorithm 4.1, and a simplified description of such an Algorithm in Figure 4.3.

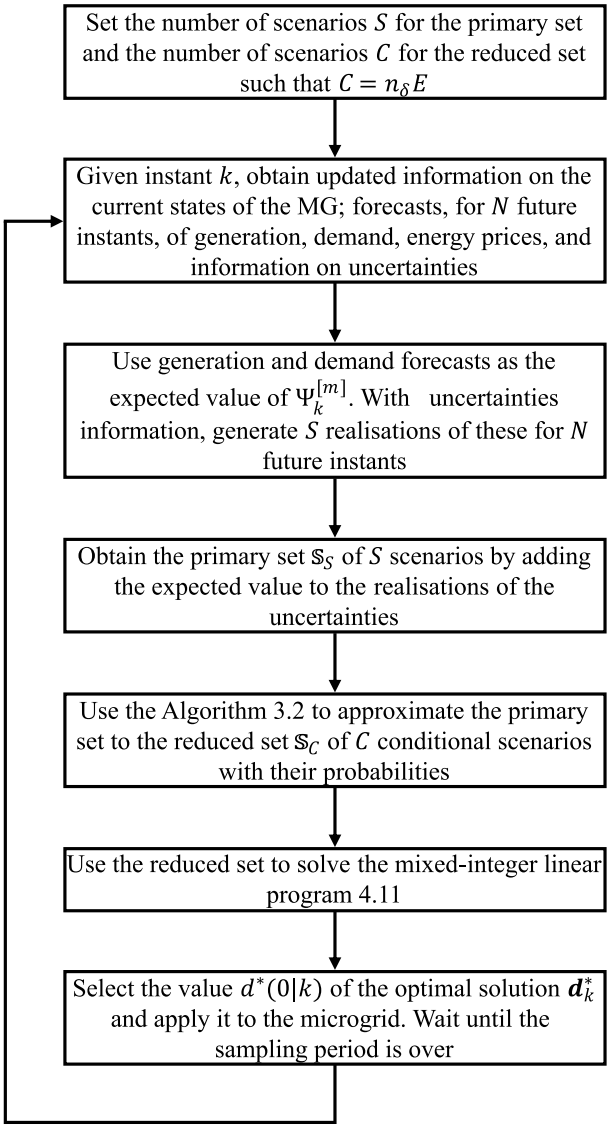

Figure 4.3: Block diagram of the operation of Algorithm 4.1.

The number of C scenarios defining the size of $\mathbb{S}_C$ can be determined by (3.6), or either by (3.8) or (3.9) if constraints of D scenarios are considered to be discarded. The equation (3.8) is used for the EMS proposed, where, p is the desired minimum

level $p \in [0,1]$ of probabilistic feasibility of constraints satisfaction $\mathbb{P}[\boldsymbol{x}_k^{[j]} \in \mathbb{X}] \geq p$ by the C scenarios in (4.11), $\beta \in [0,1]$ is the low confidence level, and d is the number of decision variables, the dimension of $\boldsymbol{d}_k$

$$\sum_{j=0}^{d-1} \binom{C}{j} (1-p)^j p^{C-j} \leq \beta \tag{4.12}$$

where, according to Theorem 3.1 in [51], it holds that any optimal solution $\boldsymbol{d}_k^*$ obtained by the scenario-based MILP (4.11), using C scenarios, with C defined using (4.12), has a guaranteed level $(1-\beta)$ of feasibility, in a probabilistic sense, of meeting the probabilistic constraints $\mathbb{P}[\boldsymbol{x}_k^{[j]} \in \mathbb{X}] \geq p$. The results obtained in the numerical examples in the previous chapter reveal that a CSB-MPC has a higher empirical probability of constraint satisfaction than the theoretical p. Such empirical probabilities also exceed those of a equiprobable scenario-based MPC (SCMPC) with the same (even higher) number of scenarios.

4.4 Case Study

In this section, the performance of the proposed CSB-MPC is tested by simulations on a microgrid as illustrated in Figure 4.1, for different operating conditions. All simulations were performed on a standard computer using Matlab R2021a and the OCP solutions were computed with the intlinprog toolbox [110] of the Mosek 10.0.38 optimisation software.

The irradiance and wind speed data used for the RES generation forecasts were collected from the U.S. Climate Reference Network (USCRN) [119]. Those used for demand forecasts were selected from UK Power Networks [120]. In particular, the energy prices data used for electricity price predictions were taken from Red Eléctrica de España [121], corresponding to the Spanish market scenario, where electricity prices are highly volatile and among the highest in Europe. The above data were adjusted for a sampling period of 0.5 h and corresponds to the 24 hours of a full day and the first 6 hours of the next day in July, and are depicted in Figure 4.4.

The generation side consist of one PV generator ($n_g = 1$) and two wind turbines ($n_r = 2$), whose power forecasts $\bar{P}_{\text{pvg},1}$, $\bar{P}_{\text{wg},1}$ and $\bar{P}_{\text{wg},2}$ are shown in Figure 4.4. The BESS parameters related to the SOC are $E^{\min} = 0.5$ kWh for its minimum level and $E^{\max} = 4.5$ kWh for its maximum level. The maximum charging and discharging powers, and the charging and discharging efficiencies are $P_{\text{c}}^{\max} = P_{\text{d}}^{\max} = 3$ kW and $\eta_{\text{c}} = \eta_{\text{d}} = 0.85$, respectively. The demand forecasts $\bar{P}_{\text{l}}$ and

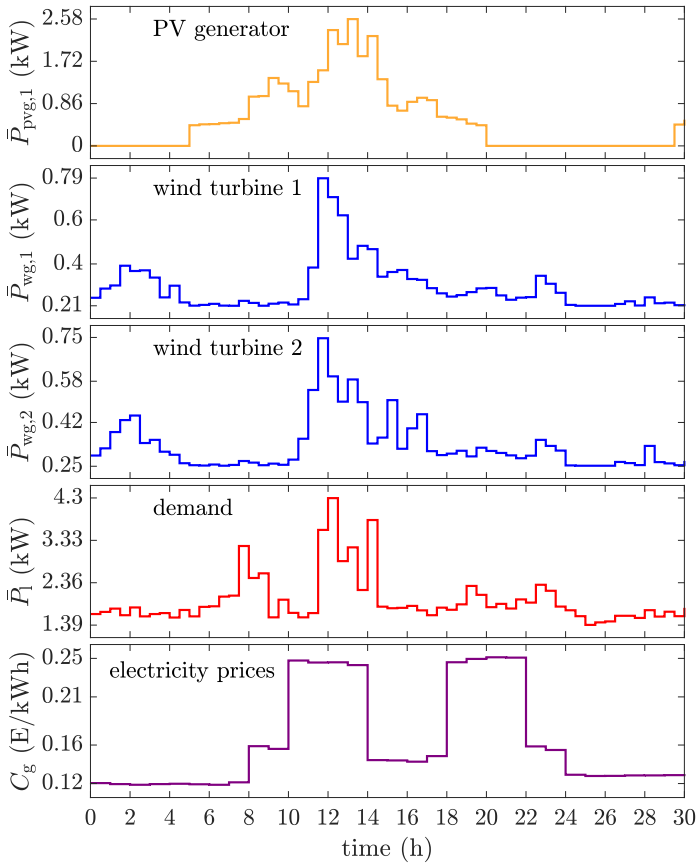

Figure 4.4: Forecasts of power generation, demand and electricity prices.

electricity prices C_{g} are also plotted in Figure 4.4, and the maximum power consumption from the main grid is $P_{\mathrm{g}}^{\max} = 5$ kW.

Correlation is assumed between the PV generation and demand forecasts, and between the forecasts of the two wind turbines. The uncertainties ($N_\xi = 4$) information is stacked in the random vector $\gamma(i|k)$, which has a multivariate normal distribution $\gamma(i|k) \sim \mathcal{N}_4(\mu(i|k), \Sigma(i|k))$, where the mean vector $\mu(i|k)$,

covariance matrix $\Sigma(i|k)$ and bounds $|\gamma(i|k)| \leq \gamma^{\max}$ are given by

$$\mu(i|k) = \begin{bmatrix} 0 \\ 0 \\ 0 \\ 0 \end{bmatrix}, \ \Sigma(i|k) = \begin{bmatrix} 0.040 & 0 & 0 & 0.028 \\ 0 & 0.0100 & 0.0108 & 0 \\ 0 & 0.0108 & 0.0144 & 0 \\ 0.028 & 0 & 0 & 0.040 \end{bmatrix}, \ |\gamma(i|k)| \leq \begin{bmatrix} 0.42 \\ 0.21 \\ 0.25 \\ 0.42 \end{bmatrix}.$$

The function of the CSB-MPC controller is to manage the energy in the MG by calculating the control signals with updated information every $T_{\mathrm{s}} = 0.5$ h for 24 hours ($k \in \{0, 1, \ldots, 48\}$). Its parameters were set to $N = 12$ steps for the prediction horizon, equivalent to 6 hours; $[\alpha_1, \alpha_2, \alpha_3, \alpha_4]^\top = [10, 1, 1, 10000]^\top$ for the objective function weights, where, only the constraint (4.9i) on the power supplied by the main grid is considered a soft constraint. α_5 is not included as (4.3a) is assumed to be an accurate model of the real BESS. Therefore, the OCP consists of 91 decision variables. The primary set $\mathbb{S}_S$ is constituted by $S = 10000$ equiprobable scenarios, which is reduced to a set $\mathbb{S}_C$ of C conditional scenarios, used to solve (4.11).

4.4.1 Simulation Case 1: Microgrid Behaviour

In Figure 4.5 is plotted the behaviour of the MG under the control of a CSB-MPC of $C = 600$ CS, for which the initial state of the SOC of the BESS was set to its minimum value, that is $\hat{E}(0) = 0.5$ kWh. The top chart shows the power flow, where the power flowing out of the MG, such as the demand and the BESS charging power, are plotted with negative values. The yellow and blue solid lines correspond to the PV and wind power consumed, respectively; the green one to the charging power (negative values) and discharging power (positive values) of the BESS, the red one to the power demanded, and the purple one to the power delivered by the main grid. The bottom chart in Figure 4.5 shows the evolution of the SOC.

In the beginning, the demand is covered only by the main grid and wind turbines because the BESS does not have enough stored energy, and the PV generation is null due to the early hours of the day. From 8 h to 14 h, the highest PV and wind power generation, and some of the highest electricity prices occur (see Figure 4.4), so the power delivered by the main grid is reduced, and the remaining power from the RES is used to charge the BESS. Between 14 h and 18 h, given that electricity prices are lower, the use of main grid power increases to cover part of the demand, in addition to recharging the BESS, anticipating the period from 18 h to 22 h when electricity prices are again very high and photovoltaic production decreases. Hence, the BESS energy is consumed during this period,

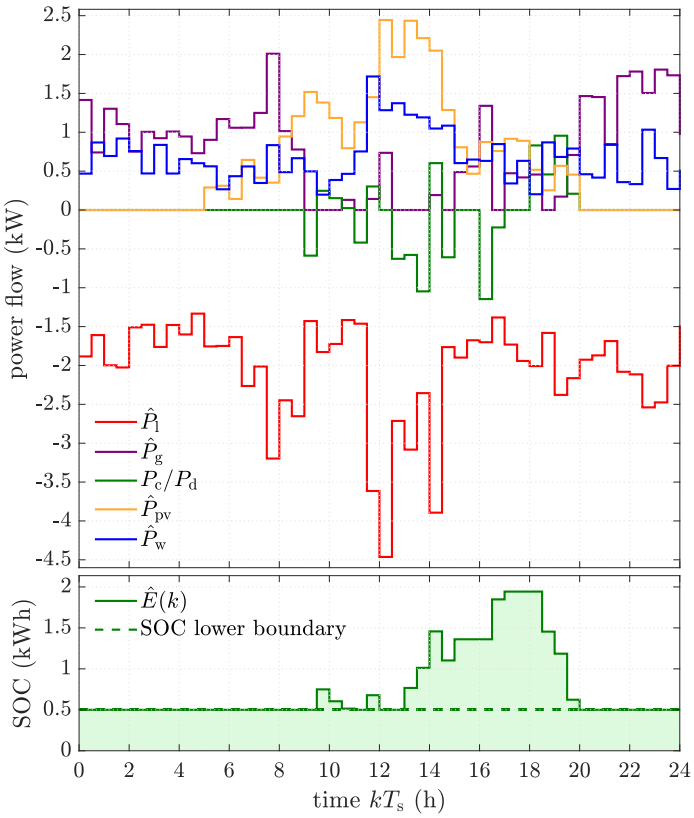

Figure 4.5: Behaviour of the power flow (top chart) and BESS state of charge (bottom chart) of the microgrid under a CSB-MPC of 600 CS.

reducing it to its minimum value where, from 20 h onwards, the demand is covered again between grid power and available wind power.

Furthermore, Figure 4.6 shows the real values measured at instant k of the demand $\hat{P}_l(k)$, power generated by the PV generator $\hat{P}_{pvg,1}(k)$, and the two wind turbines (WT) $\hat{P}_{wg,1}(k)$ and $\hat{P}_{wg,2}(k)$, represented by dark-coloured lines. As can be noticed, such values are within the region formed by the 600 CS (light-coloured lines), predicted in the previous instant (i.e., $k-1$) for the instant corresponding to k (i.e., $\tilde{P}^{[j]}_{pvg,1}(1|k-1)$, $\tilde{P}^{[j]}_{wg,1}(1|k-1)$, $\tilde{P}^{[j]}_{wg,2}(1|k-1)$, $\tilde{P}^{[j]}_{l}(1|k-1)$), which were used to solve the OCP (4.11) in such instant $k-1$.

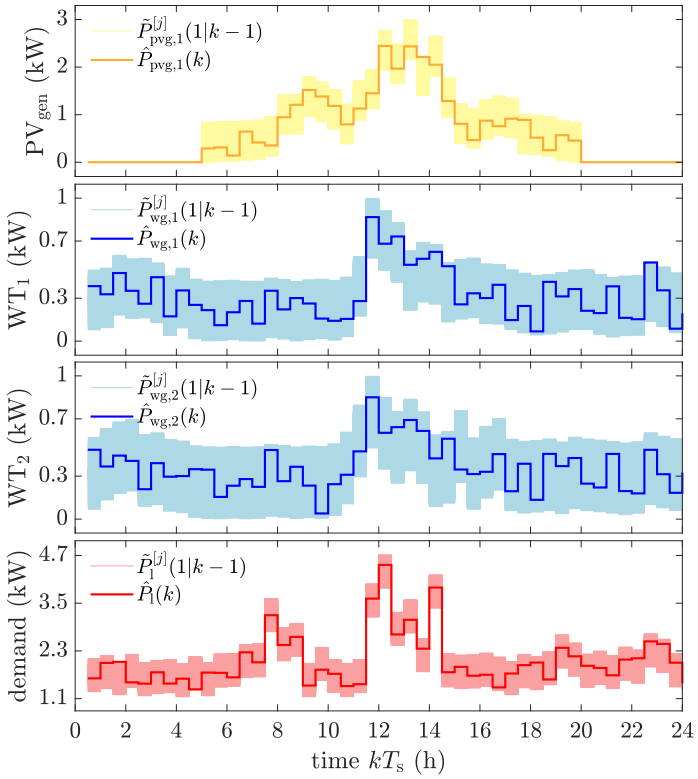

Figure 4.6: Real values of generated power and demand (dark-coloured lines) versus their respective forecasted CS (light-coloured lines).

During the entire day of operation of the CSB-MPC, the total energy delivered by the main grid was 19.14 kWh with a total cost of €3.01. If the MG does not include the BESS, these values are 20.42 kWh and €3.35. Similarly, if the MG does not include the RES, these values increase to 52.54 kWh and €8.54. In all the cases mentioned above, the purchased energy and its cost are still lower, compared to the case in which the MG does not incorporate BESS and RES (50.39 kWh and €8.90), even being €0.36 more costly than in the case where only BESS is considered and which starts at its minimum SOC.

This indicates, that an EMS that includes at least the ESS has an advantage in terms of monetary savings.

4.4.2 Simulation Case 2: Effectiveness of CSB-MPC as an EMS

The effectiveness of the proposed CSB-MPC for EMS, in terms of probabilistic feasibility, is validated using reduced sets $\mathbb{S}_C$ of various sizes

$$C = \{700, 600, 500, 400, 300, 200, 100\}$$

and whose theoretical probabilities $p(C)$, using (4.12) with $\beta = 10^{-9}$ are

$$p(C) = \{78.2\%, 74.8\%, 70.2\%, 63.4\%, 52.7\%, 34.0\%, 1.0\%\}.$$

For each $\mathbb{S}_C$ case, 1000 Monte Carlo (MC) simulations were performed, all starting with an initial BESS SOC $\hat{E}(0) = 1.5$ kWh; and the maximum capacity of the main grid was tightened to $P_{\mathrm{g}}^{\max} = 1.5$ kW. Based on the results of each case, the following controller performance indices were calculated

- E_{PR}: average cost of energy consumed from the main grid in a simulation.
- N_{BESS}: average number of instants, out of 49 instants in a simulation, in which the BESS was either charging or discharging.
- p_{s}: probability (in percentage) that the whole trajectory traced by $\hat{P}_{\mathrm{g}}(k)$ in a simulation satisfies the constraint $\hat{P}_{\mathrm{g}}(k) \leq P_{\mathrm{g}}^{\max}$. Where $p_{\mathrm{s}} = 100\,(N_{\mathrm{s}}/1000)$, and N_{s} is the number of trajectories of the 1000 MC that fulfilled the constraints.
- N_{v}: number of violations of constraint $\hat{P}_{\mathrm{g}}(k) \leq P_{\mathrm{g}}^{\max}$ in the 1000 MC simulations.
- PD: average percentage of deviation of $\hat{P}_{\mathrm{g}}(k)$ outside the constraints on the maximum capacity of the main grid $P_{\mathrm{g}}^{\max}$.
- t_{OCP}: average time spent at each instant k to generate the primary set $\mathbb{S}_S$, plus perform the reduction to the set $\mathbb{S}_C$, plus solve the MILP (4.11).

The results of the simulations for all cases are reported in Table 4.1, including the number of OCP constraints C_{OCP}. As a baseline, this Table also includes the results of various MPC strategies adjusted to the OCP (4.11) structure. These are a deterministic MPC, which does not consider uncertainties; and those of stochastic MPC strategies belonging to the deterministic group [44], [71] (chance-constrained MPC, referred to as CC-MPC hereafter), set with a minimum probability $p = 0.8$ of satisfying the probabilistic constraints $\mathbb{P}[P_{\mathrm{g}}(i|k) \leq P_{\mathrm{g}}^{\max}] \geq p$; and a scenario-based MPC [36], [57] (referred to as ScMPC hereafter) which randomly selects C scenarios from $\mathbb{S}_S$.

Table 4.1: Performance Indices of the MPCs of Simulation Case 2.

Controller	E_{PR} (€)	N_{BESS}	p_{s} (%)	N_{v}	PD (%)	t_{OCP} (s)	C_{OCP}
nominal MPC	2.74	36	3.1	2840	19.7	0.02	247
CC-MPC	2.77	31	49.0	670	9.6	0.02	247
ScMPC_{700}	3.27	43	63.6	392	10.5	2.97	18421
$\mathrm{CSB\text{-}MPC}_{700}$	2.90	37	79.7	238	7.0	3.10	18421
ScMPC_{600}	3.25	43	64.4	380	10.4	2.53	15821
$\mathrm{CSB\text{-}MPC}_{600}$	2.88	37	80.2	231	6.9	2.65	15821
ScMPC_{500}	3.22	42	62.9	395	9.5	2.10	13221
$\mathrm{CSB\text{-}MPC}_{500}$	2.87	37	79.3	232	6.4	2.18	13221
ScMPC_{400}	3.20	41	66.6	365	9.4	1.69	10621
$\mathrm{CSB\text{-}MPC}_{400}$	2.86	37	79.7	234	6.7	1.74	10621
ScMPC_{300}	3.17	41	67.5	357	9.0	1.31	8021
$\mathrm{CSB\text{-}MPC}_{300}$	2.85	37	78.6	241	6.4	1.35	8021
ScMPC_{200}	3.11	39	67.9	372	9.4	0.94	5421
$\mathrm{CSB\text{-}MPC}_{200}$	2.84	37	77.5	255	6.4	0.95	5421
ScMPC_{100}	3.02	38	59.0	516	10.6	0.58	2821
$\mathrm{CSB\text{-}MPC}_{100}$	2.82	37	75.1	289	6.5	0.58	2821

Also, the plots of the indicators in Table 4.1, corresponding to those of controllers ScMPC and CSB-MPC, are shown in Figures 4.7 and 4.8.

The nominal MPC had the lowest E_{PR} indicator, however, as expected, it has the lowest probability p_{s} (3.1%) and the highest number of violated constraints N_{v} (2840). Concerning the CC-MPC, as the OCP takes into account the uncertainties present in the forecasts, such indicators are improved $N_{\mathrm{v}} = 670$ and $p_{\mathrm{s}} = 49\%$, but this empirical probability is far below the desired theoretical one $p = 80\%$, and also all the empirical probabilities of the ScMPCs and CSB-MPCs. Since the inclusion of the uncertainties is performed offline by constraints tightening, the times t_{OCP} of this algorithm are similar to those of the nominal MPC (0.02 s), also, given the same number of constraints $C_{\mathrm{OCP}} = 247$.

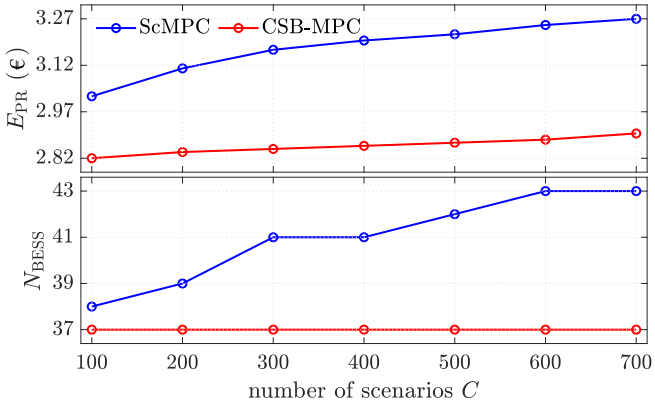

Figure 4.7: Plots of the performance indices E_{PR} and N_{BESS} of the ScMPC (blue lines) and CSB-MPC (red lines) in Table 4.1.

On the other hand, in all cases, CSB-MPCs presented lower costs for energy drawn from the main grid E_{PR} and lower number of times BESS is used N_{BESS}, than those reported by ScMPCs (see Figure 4.7). These lower indices of the CSB-MPC are beneficial in monetary terms, as it has lower operational costs, and in less degradation of the BESS as it is used less times.

Furthermore, the empirical probabilities p_{s} of the CSB-MPCs are above their corresponding theoretical probabilities $p(C)$ (solid black line in Figure 4.8), and in addition, are higher than those of the ScMPCs, which, in some cases are lower than the theoretical ones; indicating that with a CSB-MPC the probability of constraint satisfaction is improved.

It was also found that increasing the number of possible scenarios C (thus increasing the number of OCP constraints C_{OCP}) in the CSB-MPCs, results in an increase in both the probability p_{s} and the time t_{OCP} required to solve the OCP at each iteration, with the reported values of the latter indicator being very close to those of the ScMPCs, those of CSB-MPC being slightly higher, given the additional time required by its scenario reduction stage. However, for this case where the sampling period is 0.5 hours, the computation times of the MPCs analysed are not a limitation as the most significant time of all cases was the one reported by the CSB-MPC$_{700}$, which was 3.10 s.

The lowest indicators, such as the number of constraints violated N_{v} and its percentage of deviation PD, were also reported by the CSB-MPCs, which makes sense given their higher probabilities p_{s}, which are obtained due to the greater weight given in the OCP to the most likely uncertainties realisations.

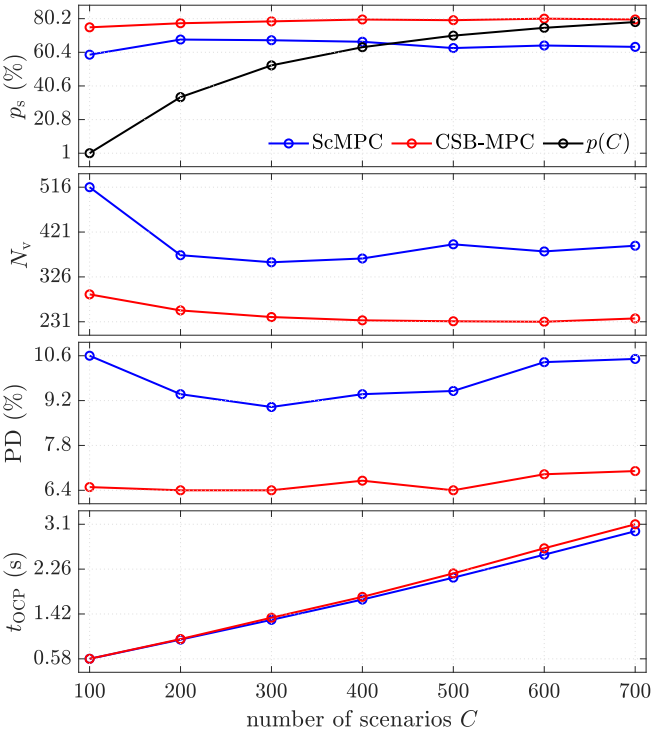

Figure 4.8: Plots of the performance indices $p_s, N_v,$ PD and t_{OCP} of the ScMPC (blue lines) and CSB-MPC (red lines) in Table 4.1, and their theoretical probabilities (black line) $p(C)$.

The plots of the evolutions of the power consumed from the main grid for the nominal MPC, CC-MPC, ScMPC$_{200}$ and CSB-MPC$_{200}$ controllers are shown in Figure 4.9. It is observed that the CSB-MPC$_{200}$ stays longer within its bounds, and the values of its trajectories within the high price intervals are lower than those of the other controllers.

Additionally, Figure 4.10 shows the behaviour (a single simulation) of the microgrid with a CSB-MPC$_{100}$ (yellow lines), a CSB-MPC$_{400}$ (orange lines) and a CSB-MPC$_{700}$ (blue lines), where it is observed that the demand profiles $\hat{P}_l(k)$ overlap, given the same conditions for all MPCs. It is also observed, in all cases, that the total power generated by the RES $\hat{P}_{pv}(k) + \hat{P}_w(k)$ is entirely consumed, thus being the same profiles for all MPCs. However, the power consumption profiles from the main grid $\hat{P}_g(k)$ are different (having CSB-MPC$_{700}$ the smallest maximum value outside the limits of the three MPCs), and therefore, causing

different charging/discharging powers $P_{\mathrm{c}}(k)/P_{\mathrm{d}}(k)$ ($P_{\mathrm{c}}(k)$ plotted with negative values) of the BESS, as well as the SOC $\hat{E}(k)$ evolutions.

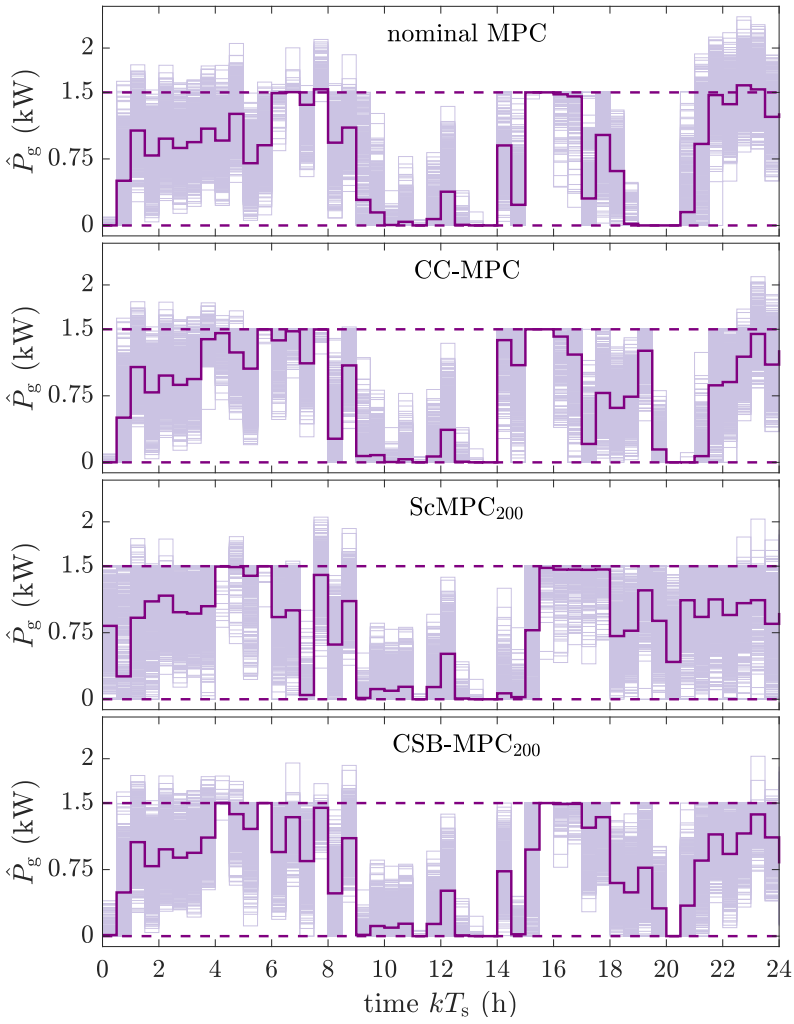

Figure 4.9: Plots of 1000 evolutions (light purple solid lines) of the power consumed from the main grid using nominal MPC, CC-MPC, ScMPC$_{200}$ and CSB-MPC$_{200}$ controllers. The dark purple continuous and dashed lines are the mean trajectory and power constraints, respectively.

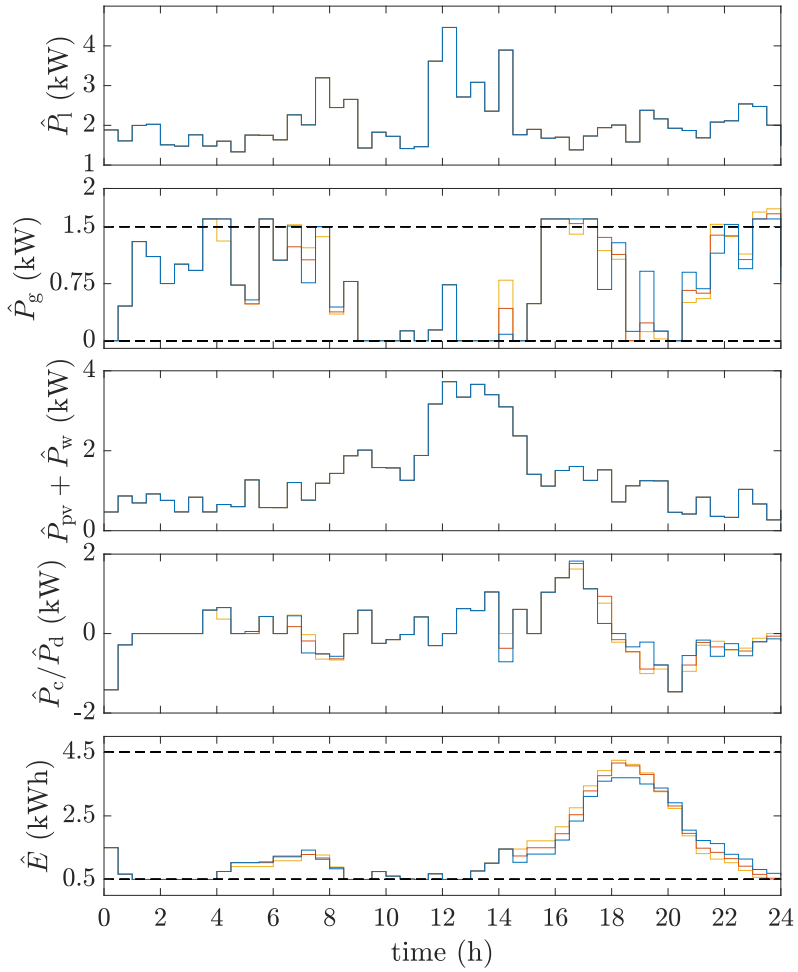

Figure 4.10: Single simulation of the MG behaviour with a CSB-MPC$_{100}$ (yellow lines), a CSB-MPC$_{400}$ (orange lines) and a CSB-MPC$_{700}$ (blue lines). Constraints, black dashed lines.

4.5 Chapter Conclusions

This chapter presented the applicability of the CSB-MPC, presented in the previous chapter, for energy management in a microgrid with renewable energy penetration and energy storage system, with correlation in generation and demand forecasts. First, at each sampling time, a large set of equiprobable scenarios of possible evolutions of PV generation, wind, and demand over a prediction horizon is generated and subsequently approximated to a reduced set of conditional scenarios, with their respective probabilities. These reduced scenarios are incorporated into the microgrid prediction model to solve a feasible scenario-based mixed-integer linear program (MILP) with finite horizon, where the objective function penalises the predictions according to their probability of occurrence.

In summary, the results suggest that using a CSB-MPC as an EMS in a microgrid is an appropriate solution if better operational performance is sought, both in conserving its components and in monetary terms. Firstly, it makes less use of the ESS, which could contribute to extending its lifetime. On the other hand, given their lower reported costs, and higher probability of constraint satisfaction which reduces the number of times constraints are violated and their deviation.

Chapter 5

Conclusions and Future Research Directions

This chapter ends this dissertation with a summary of the main conclusions and a statement of some future research directions.

5.1 Conclusions

This thesis presents a new stochastic model predictive control technique, which belongs to the group of scenario-based strategies, and its applicability in the framework of energy management in a microgrid. This led to three main contributions: a comparative study of two stochastic MPCs belonging to the deterministic and scenario-based groups; a scenario-based MPC approach for linear systems with correlated uncertainties; and a procedure for the implementation of this MPC approach as an energy management system in a microgrid with correlated forecasts.

In the following, the research questions stated in chapter 1 are answered through a sweep of the main conclusions of each chapter.

A Comparative Study of Stochastic Model Predictive Controllers

The OCP in stochastic MPC minimises a cost function based on the expected value while respecting probabilistic constraints. Such constraints are a relaxation of the original hard constraints in the sense that they must be satisfied at least with a desired probability. Most stochastic MPC approaches are clustered into deterministic and scenario-based groups, depending on how they address information related to system uncertainties.

In chapter 2, a detailed description of the theoretical background of one strategy of each group is presented, where, they are compared with an emphasis on how the OCP is set out in each strategy, i.e., consideration of uncertainties, prediction model, cost function and constraints. In addition, the worst-case OCP formulation of the second group MPC is analysed.

The MPC of the deterministic group splits the system model as the sum of two parts, a known part which is the nominal model, and a stochastic part which contains the system uncertainties. Then, offline, this stochastic part and the probability distributions of the uncertainties are used to transform the probabilistic constraints into deterministic ones by tightening the original hard constraints, which consists of solving chance-constrained optimization problems or analytically if density functions exist for the uncertainties. Hence, the original OCP becomes a deterministic one; that is, the prediction model is now the nominal model, the expected value cost function is substituted by one that considers the predictions of the nominal trajectories of the states and inputs, and the constraints are the new tightened constraints that consider the propagation of uncertainties along

the prediction horizon and that must be satisfied for the predicted nominal states and inputs.

The MPC of the scenario-based group, at each sampling period, uses the probabilities distributions and a random number generator to generate a set of scenarios, where a scenario consists of possible evolutions of uncertainties over the prediction horizon, which are incorporated into the system model with uncertainties, thus producing deterministic predictions of possible evolutions of its states and inputs. Here, the original OCP is converted into a scenario-based optimisation programme in which the cost function based on the expected value is replaced by its sample average, which includes all the predicted trajectories of the states and inputs produced by the scenarios. The worst-case OCP minimises the cost function for the scenario exhibiting the worst performance. The probabilistic constraints are replaced by the original hard constraints, which must be fulfilled for all the predicted states and inputs of each scenario.

The satisfaction of the probabilistic constraints in the scenario-based group formulation is conditioned by the number of scenarios used, so, using random convex programs concepts, the minimum number of scenarios needed to satisfy such constraints can be calculated. For this, the binomial cumulative probability function is used, which requires the desired probability, the number of OCP decision variables and a pessimistic probability level at which such probabilistic constraints are not satisfied at that desired level. Consequently, the number of scenarios needed can be calculated offline, as it does not require knowledge of system information in real-time, such as its current states and inputs.

A significant advantage of the MPC of the deterministic group is that the offline constraints tightening provide it a similarity in OCP structure and computational burden to those of a standard MPC. However, variations in the characteristics of the uncertainties can cause serious problems in the behaviour of the closed-loop system, given that new information on these could not be taken into account during the MPC operation.

Regarding the MPC of the scenario-based group, its significant advantages are, on the one hand, the ability to include changes that may occur in the characteristics of the uncertainties since the scenarios are generated online and, on the other hand, the possibility to use historical values of the uncertainties to select scenarios from them if their probability distributions are unknown or it is not possible to represent them with known types of distributions. However, compared to the deterministic group MPC that only uses nominal trajectories, its OCP presents a higher computational cost because of the time it takes to generate or build the scenarios, plus the fact that the constraints must be fulfilled for all states and

inputs of each scenario, which grows as the number of scenarios increases, thus, in some cases may become intractable.

Using a small number of scenarios to improve computational tractability may not accurately represent the original characteristics of the uncertainties, and the *randomness* in the scenario selection may cause OCP solutions to be obtained using unlikely scenarios, which could lead to possible undesired behaviour in the closed-loop system.

It is clear that considering information about the uncertainties of the process in the OCP significantly improves its probability of success, which means fewer constraints are violated. This can be verified from the results of the simulation examples which consist of a two-mass spring SISO system with parametric and additive uncertainties and a nonlinear quadruple-tank system with additive uncertainties, where controllers comparison is made by using performance indices such as the number of successful runs, number of times the constraints are violated, the mean value of the integral absolute error and the computational cost. There it is observed that only stochastic approaches achieved mean trajectories with standard deviations within or slightly exceeding the limits, which, for a normal distribution, the probability of a state being within the allowed limits is 68%.

Results also validated the similarity in computational effort between a deterministic group MPC and a standard MPC, and the considerable increase in the probability of success (the empirical probability of constraint satisfaction in one run) by the stochastic one when performing constraints tightening.

Also, both the scenario-based MPC and its worst-case approach yielded the highest probabilities of success of all controllers, because this approach computes the number of scenarios based on the joint probability of satisfying the constraints with all the uncertainty realisations, while in MPC of the deterministic group, the constraints tightening is done using single probabilistic constraints. Likewise, it is found that an increase in the number of scenarios increases the probability of success, but as expected, it results in a growth in the time the MPC needs to solve the OCP for all scenarios.

The work conducted to compare the two stochastic MPC algorithms was published as research paper [117]. Also, the files created to carry out the simulations of the two stochastic MPCs are available at MATLAB Central as a toolbox [100] to allow the results presented in chapter 2 to be reproduced or, to tune and simulate a MPC of the deterministic group or a MPC of the scenario-based group for controlling multivariable systems with additive disturbances which present Gaussian probability distributions.

Conditional Scenario-Based Model Predictive Control (CSB-MPC)

A new stochastic MPC approach called conditional scenario-based model predictive control (CSB-MPC) is introduced in chapter 3, which is designed for discrete-time linear systems affected by correlated and bound parametric uncertainties and/or additive disturbances.

Most scenario-based MPC approaches consider systems with either strictly additive or parametric uncertainties; and whose realisations are independent or correlated in time. The CSB-MPC addresses systems with bounded parametric and/or additive uncertainties featuring a correlation between some or the whole set of random variables.

Two OCP structures are proposed for the CSB-MPC with guaranteed probabilistic feasibilities, that is, the optimal solutions obtained will satisfy the original probabilistic constraints within a defined probability level.

In the CSB-MPC, at each sampling period, a large primary set of equiprobable scenarios is generated and subsequently converted into a reduced set of conditional scenarios, each with its probabilities of occurrence, which maintains, as best as possible, the characteristics of this primary set. The reduction is performed via a developed algorithm that adapts the conditional scenario (CS) reduction method to the MPC framework, that rather than filtering or reducing scenarios, this reduction method takes advantage of the correlation features between the uncertainties to approximate the primary set by means of the conditional expectations. The application of this procedure is straightforward and fast, as it does not require an optimisation stage or knowledge of how the random variables are distributed to perform the reduction.

The reduced set of CSs and their probabilities are incorporated into the quadratic cost function of an OCP in which the predicted states and inputs are penalised according to the probabilities associated with the uncertainties on which they depend; and is subject to constraints on the states and inputs built up with this reduced set, and in the terminal state through a robust invariant set.

The CSB-MPC, firstly, improves the computational effort as the OCP is based on a reduced set; secondly, addresses the negative effect that *randomness* can have on a reduced set of scenarios, as the new set represents the characteristics of the primary set as well as possible; and finally, the OCP cost function gives more relevance to the states and inputs that involve realisations with more probability of occurrence and less importance given to those that are related to unlikely realisations, by means of their associated probabilities.

In one of the proposed OCPs, which is based on sampling and discarding approaches, the scenarios to be discarded are directly identified by their probability of occurrence, which becomes computationally lightweight. This contrasts significantly with the need for removal algorithms that, in MPC, usually require an extra stage of optimisation, which can become prohibitive depending on how greedy they are.

The performances of the CSB-MPC and those of a scenario-based MPC are compared using two numerical examples consisting of a double integrator system, and a nonlinear quadruple-tank system with parametric and additive uncertainties. The results showed greater empirical probabilities of constraints satisfaction, above the theoretical ones, and less distance outside the constraints by the CSB-MPC, even when the CSB-MPCs have a smaller number of scenarios than the scenario-based MPCs. The above indicates an increase in the feasibility of an OCP solution, in a probabilistic sense.

Using a smaller primary set does not significantly affect the constraint satisfaction probabilities of the CSB-MPC, but it may offer similar solution times, in some cases shorter than those of a standard scenario-based MPC. Consequently, if a trade-off between the level of constraints satisfaction and the computational tractability is required, using a CSB-MPC with a smaller number of scenarios than a scenario-based MPC is a viable option.

The CSB-MPC strategy was written in the format of a scientific paper and was published in [122]. In addition, an open-access toolbox of the CSB-MPC was developed in Matlab and is available at MATLAB Central [113].

CSB-MPC for Energy Management in Microgrids with Correlated Forecasts

chapter 4 presents the applicability of a CSB-MPC for energy management in a microgrid with renewable energy sources (RES) penetration and energy storage system (ESS), with correlation in generation and demand forecasts.

The CSB-MPC as an energy management system (EMS), at each sampling time, generate a large set of equiprobable scenarios of possible evolutions of photovoltaic (PV) generation, wind, and demand over a prediction horizon; and then approximates it to a reduced set of conditional scenarios, with their respective probabilities. These reduced scenarios are incorporated into the microgrid (MG) prediction model to solve a feasible, numerically and probabilistically, scenario-based mixed-integer linear program (MILP) with finite horizon, where the objective function penalises the predictions of the cost of energy consumed from the

main grid and the forecasts of the power generated by RES that is discarded, according to their probability of occurrence.

One significant advantage of the CSB-MPC as an EMS in a microgrid is its ability to include online new information about uncertainties, which leads to making better decisions consistent with the actual situation of the system. The above given that, photovoltaic and wind power generation forecasts, and possibly demand forecast, are strongly influenced by meteorological conditions that can be highly fluctuating, which can also affect the type or distribution of uncertainties.

Another significant advantage of the CSB-MPC as an EMS is that it also exploits the characteristics of uncertainties, such as the correlation between them, to obtain the reduced set. Correlation between uncertainties may be common in the context of a microgrid. There are cases, due to working hours, off-hours, activity in a household, etc., where there is a high correlation between powers, either between the output powers of RES generators, PV-wind, PV-demand, wind-demand, or between various loads on the demand side.

A case study is used to simulate and analyse the behaviour of a microgrid with a CSB-MPC. The performance of the proposed CSB-MPC is compared with those of a standard MPC, a stochastic MPC of the deterministic group and a standard scenario-base MPC, where the CSB-MPC showed the highest probabilities of constraint satisfaction of all controllers.

The results further indicate that using a CSB-MPC as an EMS in a microgrid is a suitable solution if better operational performance is sought, both in conserving its components and in monetary terms. Firstly, it makes less use of the ESS, which could contribute to extending its lifetime. On the other hand, given their lower reported costs, and higher probability of constraint satisfaction which reduces the number of times constraints are violated and their deviation. For example, considering constraints on grid power, most electricity companies apply policies in which power consumption above the contracted value is penalised with much higher tariffs, so with a CSB-MPC, there would be fewer negative impacts in financial terms.

The proposal for applying a CSB-MPC as an EMS in a microgrid was written in the format of a scientific paper and was published in [123].

5.2 Future Research Directions

As mentioned in chapter 3, establishing the theoretical properties of recursive feasibility and stability of the scenario-based MPC approaches, including the CSB-MPC introduced in this thesis, remains part of the current challenges posed by these strategies, even more so when the uncertainties are not bounded, which does not enable obtaining a terminal cost and a terminal set, necessary pieces for the efficient functioning of a MPC.

Scenario-based schemes such as CSB-MPC are attractive in the sense that they have a higher probability of satisfying constraints, plus their ability to include new information on uncertainties in real time. However, such advantages have the issue related to the computational effort needed in the OCP to guarantee such a probability with the required number of scenarios, thus preventing its application for the control of some systems with fast dynamics. One way to alleviate such computational effort to enable its application would be to complement the scenario-based MPC with a technique that, before solving the OCP, quickly detects and removes redundant constraints from current constraints. The time existing algorithms take to detect redundant constraints is generally longer than the time the OCP takes to obtain a solution with the full set of constraints.

Research to analyse in more detail the impact that the prediction horizon, the cost function weights, and the sizes of the primary and reduced sets have on the effectiveness of the CSB-MPC, in order to establish a principle for selecting these parameters in a more straightforward way.

Accurate characterisation of uncertainties influences the efficiency of the MPC and thereby the performance of the process. Nevertheless, depending on their current state, some systems have alterations in uncertainties, which could lead to poor MPC performance if these alterations are not considered. The challenge of modelling uncertainties as accurately as possible is a current topic of study in the area of active uncertainty learning. Thus, a scenario-based MPC, which can include online updated uncertainty information, integrated with a technique that constantly learns the uncertainty, would strengthen its performance.

Bibliography

[1] J. Richalet, A. Rault, J. Testud, and J. Papon, "Model predictive heuristic control: Applications to industrial processes", *Automatica*, vol. 14, no. 5, pp. 413–428, Sep. 1978, ISSN: 0005-1098. DOI: 10.1016/0005-1098(78)90001-8 (cit. on p. 2).

[2] M. G. Forbes, R. S. Patwardhan, H. Hamadah, and R. B. Gopaluni, "Model predictive control in industry: Challenges and opportunities", *IFAC PapersOnLine*, vol. 48, no. 8, pp. 531 –538, 2015, ISSN: 2405-8963. DOI: 10.1016/j.ifacol.2015.09.022 (cit. on p. 2).

[3] I. Jurado, P. Millán, D. Quevedo, and F. Rubio, "Stochastic MPC with applications to process control", *International Journal of Control*, vol. 88, no. 4, pp. 792–800, Dec. 2014. DOI: 10.1080/00207179.2014.975845 (cit. on pp. 2, 21).

[4] J. Richalet, S. Abu El Ata-Doss, C. Arber, H. Kuntze, A. Jacubasch, and W. Schill, "Predictive functional control - application to fast and accurate robots", *IFAC Proceedings Volumes*, vol. 20, no. 5, Part 4, pp. 251–258, Jul. 1987, ISSN: 1474-6670. DOI: 10.1016/S1474-6670(17)55325-2 (cit. on p. 2).

[5] Y. Tan, G. Cai, B. Li, K. L. Teo, and S. Wang, "Stochastic model predictive control for the set point tracking of unmanned surface vehicles", *IEEE*

Access, vol. 8, pp. 579–588, Dec. 2020. DOI: 10.1109/access.2019.2962061 (cit. on pp. 2, 21).

[6] I. Ravanshadi, E. A. Boroujeni, and M. Pourgholi, "Centralized and distributed model predictive control for consensus of non-linear multi-agent systems with time-varying obstacle avoidance", *ISA Transactions*, pp. 1–13, Jun. 2022. DOI: 10.1109/tcst.2017.2657606 (cit. on p. 2).

[7] M. W. Mueller and R. D'Andrea, "A model predictive controller for quadrocopter state interception", in *2013 European Control Conference (ECC)*, 2013, pp. 1383–1389. DOI: 10.23919/ECC.2013.6669415 (cit. on p. 2).

[8] H. G. Tanner and J. L. Piovesan, "Randomized receding horizon navigation", *IEEE Transactions on Automatic Control*, vol. 55, no. 11, pp. 2640–2644, Nov. 2010. DOI: 10.1109/tac.2010.2063291 (cit. on p. 2).

[9] M. Y. Lamoudi, M. Alamir, and P. Béguery, "Model predictive control for energy management in buildings part 2: Distributed model predictive control", *IFAC Proceedings Volumes*, vol. 45, no. 17, pp. 226–231, 2012, 4th IFAC Conference on Nonlinear Model Predictive Control, ISSN: 1474-6670. DOI: 10.3182/20120823-5-nl-3013.00036 (cit. on p. 2).

[10] T. Salsbury, P. Mhaskar, and S. J. Qin, "Predictive control methods to improve energy efficiency and reduce demand in buildings", *Computers & Chemical Engineering*, vol. 51, pp. 77–85, Apr. 2013, ISSN: 0098-1354. DOI: 10.1016/j.compchemeng.2012.08.003 (cit. on p. 2).

[11] W. R. Sultana, S. K. Sahoo, S. Sukchai, S. Yamuna, and D. Venkatesh, "A review on state of art development of model predictive control for renewable energy applications", *Renewable & Sustainable Energy Reviews*, vol. 76, pp. 391–406, Sep. 2017, ISSN: 1364-0321. DOI: 10.1016/j.rser.2017.03.058 (cit. on p. 2).

[12] E. Luchini, A. Schirrer, and M. Kozek, "A hierarchical mpc for multi-objective mixed-integer optimisation applied to redundant refrigeration circuits", *IFAC-PapersOnLine*, vol. 50, no. 1, pp. 9058–9064, Oct. 2017. DOI: 10.1016/j.ifacol.2017.08.1629 (cit. on p. 2).

[13] A. Parisio, D. Varagnolo, M. Molinari, G. Pattarello, L. Fabietti, and K. H. Johansson, "Implementation of a scenario-based MPC for HVAC systems:

An experimental case study", *IFAC Proceedings Volumes*, vol. 47, no. 3, pp. 599–605, Aug. 2014. DOI: 10.3182/20140824-6-za-1003.02629 (cit. on pp. 2, 6, 21).

[14] P. Velarde, A. J. Gallego, C. Bordons, and E. F. Camacho, "Scenario-based model predictive control for energy scheduling in a parabolic trough concentrating solar plant with thermal storage", *Renewable Energy*, vol. 206, pp. 1228–1238, Apr. 2023. DOI: 10.1016/j.renene.2023.02.114 (cit. on pp. 2, 6).

[15] J. Rodriguez, M. P. Kazmierkowski, J. R. Espinoza, *et al.*, "State of the art of finite control set model predictive control in power electronics", *IEEE Transactions on Industrial Informatics*, vol. 9, no. 2, pp. 1003–1016, May 2013, ISSN: 1003–1016. DOI: 10.1109/tii.2012.2221469 (cit. on p. 2).

[16] H. A. Nasir, M. Cantoni, Y. Li, and E. Weyer, "Stochastic model predictive control based reference planning for automated open-water channels", *IEEE Transactions on Control Systems Technology*, vol. 29, no. 2, pp. 607–619, Mar. 2021. DOI: 10.1109/tcst.2019.2952788 (cit. on pp. 2, 6).

[17] J. M. Grosso, P. Velarde, C. Ocampo-Martinez, J. M. Maestre, and V. Puig, "Stochastic model predictive control approaches applied to drinking water networks", *Optimal Control Applications and Methods*, vol. 38, no. 4, pp. 541–558, Aug. 2016. DOI: 10.1002/oca.2269 (cit. on pp. 2, 6, 10).

[18] D. Mayne, J. Rawlings, C. Rao, and P. Scokaert, "Constrained Model Predictive Control: Stability and Optimality", *Automatica*, vol. 36, no. 6, pp. 789–814, Jun. 2000. DOI: 10.1016/S0005-1098(99)00214-9 (cit. on pp. 2, 10, 18, 19, 68).

[19] J. Maciejowski, *Predictive Control: With Constraints*, 1st ed. London, U.K.: Prentice Hall, 2002, ISBN: 9780201398236 (cit. on pp. 2, 18, 33, 34, 37, 54, 70).

[20] B. Kouvaritakis and M. Cannon, *Model Predictive Control. Classical, Robust and Stochastic*, 1st ed. Springer International Publishing, 2016, ISBN: 978-3-319-24851-6. DOI: 10.1007/978-3-319-24853-0 (cit. on pp. 2, 3, 19).

[21] J. Rawlings, *Model Predictive Control: theory, computation, and design*, 2nd ed. Madison, Wisconsin, U.S.: Nob Hill Publishing, 2017, ISBN: 978-0975937730 (cit. on pp. 2, 7, 54, 91).

[22] D. Q. Mayne, "Model Predictive Control: Recent Developments and Future Promise", *Automatica*, vol. 50, no. 12, pp. 2967–2986, Dec. 2014. DOI: 10.1016/j.automatica.2014.10.128 (cit. on pp. 2, 18).

[23] M. V. Kothare, V. Balakrishnan, and M. Morari, "Robust constrained model predictive control using linear matrix inequalities", *Automatica*, vol. 32, no. 10, pp. 1361–1379, Oct. 1996. DOI: 10.1016/0005-1098(96)00063-5 (cit. on pp. 2, 36, 54, 70).

[24] B. Kouvaritakis and M. Cannon, "Developments in robust and stochastic predictive control in the presence of uncertainty", *ASCE-ASME Journal of Risk and Uncertainty in Engineering Systems*, vol. 1, no. 2, pp. 1–9, Apr. 2015. DOI: 10.1115/1.4029744 (cit. on pp. 2, 3, 5).

[25] A. Bemporad and M. Morari, "Robust Model Predictive Control: A Survey", in *Robustness in Identification and Control*, London, U.K.: Springer London, Sep. 1999, pp. 207–226, ISBN: 978-1-84628-538-7. DOI: 10.1007/BFb0109870 (cit. on p. 2).

[26] A. Mesbah, "Stochastic Model Predictive Control: An Overview and Perspectives for Future Research", *IEEE Control Systems Magazine*, vol. 36, no. 6, pp. 30–44, Nov. 2016. DOI: 10.1109/MCS.2016.2602087 (cit. on pp. 3, 4, 20, 21, 30).

[27] D. Mayne, "Robust and Stochastic MPC: Are We Going in the Right Direction?", *IFAC-PapersOnLine*, vol. 48, no. 23, pp. 1–8, Sep. 2015. DOI: 10.1016/j.ifacol.2015.11.255 (cit. on pp. 3, 4, 20, 21, 30).

[28] B. Kouvaritakis and M. Cannon, "Stochastic model predictive control", in *Encyclopedia of Systems and Control*, 1st ed. London, U.K.: Springer London, Jul. 2015, pp. 1350–1357, ISBN: 978-1-4471-5058-9. DOI: 10.1007/978-1-4471-5058-9_7 (cit. on pp. 3, 4, 20, 37).

[29] M. Farina, L. Giulioni, and R. Scattolini, "Stochastic Linear Model Predictive Control with Chance Constraints - A Review", *Journal of Process*

Control, vol. 44, pp. 53–67, Aug. 2016. DOI: 10.1016/j.jprocont.2016.03.005 (cit. on pp. 3–6, 20, 21, 25, 28, 29, 31).

[30] M. Lorenzen, F. Dabbene, R. Tempo, and F. Allgöwer, "Stochastic MPC with offline uncertainty sampling", *Automatica*, vol. 81, pp. 176–183, Jul. 2017. DOI: 10.1016/j.automatica.2017.03.031 (cit. on pp. 4, 69).

[31] H. Wang, J. Wang, H. Xu, and S. Zhao, "Distributed stochastic model predictive control for systems with stochastic multiplicative uncertainty and chance constraints", *ISA Transactions*, vol. 121, pp. 11–20, Feb. 2022. DOI: 10.1016/j.isatra.2021.03.038 (cit. on p. 4).

[32] L. M. Chaouach, M. Fiacchini, and T. Alamo, "Stochastic model predictive control for linear systems affected by correlated disturbances", *IFAC-PapersOnLine*, vol. 55, no. 25, pp. 133–138, Oct. 2022. DOI: 10.1016/j.ifacol.2022.09.336 (cit. on pp. 4, 7, 10).

[33] M. Mammarella, T. Alamo, S. Lucia, and F. Dabbene, "A probabilistic validation approach for penalty function design in stochastic model predictive control", *IFAC-PapersOnLine*, vol. 53, no. 2, pp. 11 271–11 276, Apr. 2020. DOI: 10.1016/j.ifacol.2020.12.362 (cit. on pp. 4, 69).

[34] F. Li, H. Li, and Y. He, "Stochastic model predictive control for linear systems with unbounded additive uncertainties", *Journal of the Franklin Institute*, vol. 359, no. 7, pp. 3024–3045, May 2022. DOI: 10.1016/j.jfranklin.2022.02.004 (cit. on pp. 4, 7, 10, 69).

[35] G. C. Calafiore and L. Fagiano, "Robust model predictive control via scenario optimization", *IEEE Transactions on Automatic Control*, vol. 58, no. 1, pp. 219–224, Jan. 2013. DOI: 10.1109/tac.2012.2203054 (cit. on pp. 4, 5, 10, 21, 27, 29, 30, 68, 91).

[36] G. Schildbach, L. Fagiano, C. Frei, and M. Morari, "The scenario approach for stochastic model predictive control with bounds on closed-loop constraint violations", *Automatica*, vol. 50, no. 12, pp. 3009–3018, Dec. 2014. DOI: 10.1016/j.automatica.2014.10.035 (cit. on pp. 4–7, 21, 27, 38, 55, 56, 68, 91, 106).

[37] F. Micheli and J. Lygeros, "Scenario-based stochastic mpc for systems with uncertain dynamics", in *2022 European Control Conference (ECC)*, IEEE, Jul. 2022. DOI: 10.23919/ecc55457.2022.9838080 (cit. on pp. 4, 68).

[38] M. Mammarella, A. Altamimi, M. Chamanbaz, F. Dabbene, and C. Lagoa, "Fast stochastic MPC implementation via policy learning", *IEEE Control Systems Letters*, vol. 6, pp. 3020–3025, Jun. 2022. DOI: 10.1109/lcsys.2022.3182643 (cit. on pp. 4, 7, 10).

[39] M. Cannon, B. Kouvaritakis, S. V. Raković, and Q. Cheng, "Stochastic Tubes in Model Predictive Control With Probabilistic Constraints", *IEEE Transactions on Automatic Control*, vol. 56, no. 1, pp. 194–200, Jan. 2011. DOI: 10.1109/TAC.2010.2086553 (cit. on pp. 4, 5, 10, 21).

[40] D. Q. Mayne and P. Falugi, "Stabilizing conditions for model predictive control", *International Journal of Robust and Nonlinear Control*, vol. 29, no. 4, pp. 894–903, Nov. 2018. DOI: 10.1002/rnc.4409 (cit. on pp. 4, 10, 53, 68).

[41] L. Hewing and M. N. Zeilinger, "Scenario-based probabilistic reachable sets for recursively feasible stochastic model predictive control", *IEEE Control Systems Letters*, vol. 4, no. 2, pp. 450–455, Apr. 2020. DOI: 10.1109/lcsys.2019.2949194 (cit. on pp. 4, 5, 7, 10, 21, 69).

[42] J. A. Paulson, E. A. Buehler, R. D. Braatz, and A. Mesbah, "Stochastic model predictive control with joint chance constraints", *International Journal of Control*, vol. 93, no. 1, pp. 126–139, May 2017. DOI: 10.1080/00207179.2017.1323351 (cit. on pp. 4, 5, 21, 28).

[43] M. Kögel and R. Findeisen, "Robust output feedback MPC for uncertain linear systems with reduced conservatism", *IFAC-PapersOnLine*, vol. 50, no. 1, pp. 10 685–10 690, Jul. 2017. DOI: 10.1016/j.ifacol.2017.08.2186 (cit. on p. 5).

[44] M. Lorenzen, F. Dabbene, R. Tempo, and F. Allgöwer, "Constraint-tightening and stability in stochastic model predictive control", *IEEE Transactions on Automatic Control*, vol. 62, no. 7, pp. 3165–3177, Jul. 2017. DOI: 10.1109/TAC.2016.2625048 (cit. on pp. 5, 10, 21–23, 28, 106).

[45] T. A. N. Heirung, J. A. Paulson, J. O'Leary, and A. Mesbah, "Stochastic model mredictive control - how does it work?", *Computers & Chemical Engineering*, vol. 114, pp. 158–170, Jun. 2018. DOI: 10.1016/j.compchemeng.2017.10.026 (cit. on pp. 5, 10, 21–23, 25).

[46] A. Mesbah, "Stochastic model predictive control with active uncertainty learning: A survey on dual Control", *Annual Reviews in Control*, vol. 45, pp. 107–117, 2018. DOI: 10.1016/j.arcontrol.2017.11.001 (cit. on pp. 5, 11, 21).

[47] G. Calafiore and M. C. Campi, "The scenario approach to robust control design", *IEEE Transactions on Automatic Control*, vol. 51, no. 5, pp. 742–753, May 2006. DOI: 10.1109/tac.2006.875041 (cit. on pp. 5, 28).

[48] M. C. Campi, S. Garatti, and M. Prandini, "The scenario approach for systems and control design", *Annual Reviews in Control*, vol. 33, no. 2, pp. 149–157, Dec. 2009. DOI: 10.1016/j.arcontrol.2009.07.001 (cit. on p. 5).

[49] A. Muraleedharan, H. Okuda, and T. Suzuki, "Real-time implementation of randomized model predictive control for autonomous driving", *IEEE Transactions on Intelligent Vehicles*, vol. 7, no. 1, pp. 11–20, Mar. 2022. DOI: 10.1109/tiv.2021.3062730 (cit. on p. 6).

[50] S. Polimeni, L. Meraldi, L. Moretti, S. Leva, and G. Manzolini, "Development and experimental validation of hierarchical energy management system based on stochastic model predictive control for off-grid microgrids", *Advances in Applied Energy*, vol. 2, p. 100 028, May 2021. DOI: 10.1016/j.adapen.2021.100028 (cit. on p. 6).

[51] G. C. Calafiore, "Random convex programs", *SIAM Journal on Optimization*, vol. 20, no. 6, pp. 3427–3464, Jan. 2010. DOI: 10.1137/090773490 (cit. on pp. 6, 30, 31, 55, 67, 101).

[52] M. C. Campi and S. Garatti, "A sampling-and-discarding approach to chance-constrained optimization: Feasibility and optimality", *Journal of Optimization Theory and Applications*, vol. 148, no. 2, pp. 257–280, Oct. 2010. DOI: 10.1007/s10957-010-9754-6 (cit. on pp. 6, 7, 55, 56, 67, 68).

[53] D. Bernardini and A. Bemporad, "Scenario-based model predictive control of stochastic constrained linear systems", in *Proceedings of the 48h IEEE Conference on Decision and Control (CDC) held jointly with 2009 28th Chinese Control Conference*, Shanghai, China, Dec. 2009, pp. 6333–6338. DOI: 10.1109/cdc.2009.5399917 (cit. on p. 7).

[54] A. Mesbah, I. V. Kolmanovsky, and S. D. Cairano, "Stochastic model predictive control", in *Handbook of Model Predictive Control*, 1st ed. Springer International Publishing, Sep. 2018, pp. 75–97, ISBN: 978-3-319-77488-6. DOI: 10.1007/978-3-319-77489-3_4 (cit. on pp. 7, 91).

[55] A. D. Bonzanini, J. A. Paulson, and A. Mesbah, "Safe learning-based model predictive control under state- and input-dependent uncertainty using scenario trees", in *2020 59th IEEE Conference on Decision and Control (CDC)*, Jeju, Korea (South): IEEE, Dec. 2020. DOI: 10.1109/cdc42340.2020.9304310 (cit. on pp. 7, 11).

[56] Y. Bao, K. J. Chan, A. Mesbah, and J. M. Velni, "Learning-based adaptive-scenario-tree model predictive control with improved probabilistic safety using robust bayesian neural networks", *International Journal of Robust and Nonlinear Control*, vol. 33, no. 5, pp. 3312–3333, Dec. 2022. DOI: 10.1002/rnc.6560 (cit. on pp. 7, 11).

[57] P. Velarde, L. Valverde, J. Maestre, C. Ocampo-Martinez, and C. Bordons, "On the comparison of stochastic model predictive control strategies applied to a hydrogen-based microgrid", *Journal of Power Sources*, vol. 343, pp. 161–173, Mar. 2017. DOI: 10.1016/j.jpowsour.2017.01.015 (cit. on pp. 7, 10, 106).

[58] L. Hewing, K. P. Wabersich, and M. N. Zeilinger, "Recursively feasible stochastic model predictive control using indirect feedback", *Automatica*, vol. 119, p. 109 095, Sep. 2020. DOI: 10.1016/j.automatica.2020.109095 (cit. on p. 7).

[59] M. Roser, "The world's energy problem", *Our World in Data*, Dec. 2020 (cit. on p. 8).

[60] B. L. Capehart, W. C. Turner, and W. J. Kennedy, "Guide to energy management", in 8th ed. New York, NY: Productivity Press, Mar. 2016, p. 762,

ISBN: 9781498759335. DOI: https://doi.org/10.1201/9781003151982 (cit. on p. 8).

[61] M. Stecca, L. R. Elizondo, T. B. Soeiro, P. Bauer, and P. Palensky, "A comprehensive review of the integration of battery energy storage systems into distribution networks", *IEEE Open Journal of the Industrial Electronics Society*, vol. 1, pp. 46–65, Mar. 2020. DOI: 10.1109/ojies.2020.2981832 (cit. on pp. 8, 89, 95).

[62] M. M. Rahman, A. O. Oni, E. Gemechu, and A. Kumar, "Assessment of energy storage technologies: A review", *Energy Conversion and Management*, vol. 223, p. 113 295, Nov. 2020. DOI: 10.1016/j.enconman.2020.113295 (cit. on p. 8).

[63] K. R. Pullen, "Flywheel energy storage", in *Storing Energy*, Jan. 2022, pp. 207–242. DOI: 10.1016/b978-0-12-824510-1.00035-0 (cit. on p. 8).

[64] N. Hatziargyriou, H. Asano, R. Iravani, and C. Marnay, "Microgrids", *IEEE Power and Energy Magazine*, vol. 5, no. 8, pp. 78–94, Jul. 2007. DOI: 10.1109/MPAE.2007.376583 (cit. on p. 8).

[65] A. Cagnano, E. D. Tuglie, and P. Mancarella, "Microgrids: Overview and guidelines for practical implementations and operation", *Applied Energy*, vol. 258, pp. 1–18, Jan. 2020. DOI: 10.1016/j.apenergy.2019.114039 (cit. on p. 8).

[66] J. Hu, Y. Shan, J. M. Guerrero, A. Ioinovici, K. W. Chan, and J. Rodriguez, "Model predictive control of microgrids – an overview", *Renewable and Sustainable Energy Reviews*, vol. 136, Feb. 2021. DOI: 10.1016/j.rser.2020.110422 (cit. on pp. 8, 91).

[67] O. Babayomi, Z. Zhang, T. Dragicevic, J. Hu, and J. Rodriguez, "Smart grid evolution: Predictive control of distributed energy resources: A review", *Intl. Journal of Electrical Power and Energy Systems*, vol. 147, May 2022. DOI: 10.1016/j.ijepes.2022.108812 (cit. on p. 8).

[68] V. A. Freire, L. V. R. D. Arruda, C. Bordons, and J. J. Marquez, "Optimal demand response management of a residential microgrid using model predictive control", *IEEE Access*, vol. 8, pp. 228 264–228 276, Dec. 2020. DOI: 10.1109/access.2020.3045459 (cit. on pp. 9, 91, 95).

[69] A. Nawaz, J. Wu, J. Ye, Y. Dong, and C. Long, "Distributed MPC-based energy scheduling for islanded multi-microgrid considering battery degradation and cyclic life deterioration", *Applied Energy*, vol. 329, p. 120 168, Jan. 2023. DOI: 10.1016/j.apenergy.2022.120168 (cit. on p. 9).

[70] C. Bordons, F. Garcia-Torres, and M. A. Ridao, "Uncertainties in microgrids", in *Model Predictive Control of Microgrids*, Springer International Publishing, Sep. 2019, pp. 169–190. DOI: 10.1007/978-3-030-24570-2_7 (cit. on p. 9).

[71] K. Garifi, K. Baker, B. Touri, and D. Christensen, "Stochastic model predictive control for demand response in a home energy management system", in *2018 IEEE Power and Energy Society General Meeting PESGM*, IEEE, Aug. 2018. DOI: 10.1109/pesgm.2018.8586485 (cit. on pp. 9, 106).

[72] A. Zafra-Cabeza, J. Marquez, C. Bordons, and M. A. Ridao, "An online stochastic MPC-based fault-tolerant optimization for microgrids", *Control Engineering Practice*, vol. 130, p. 105 381, Jan. 2023. DOI: 10.1016/j.conengprac.2022.105381 (cit. on p. 9).

[73] J. Lei, C. A. Hans, and P. Sopasakis, "Optimal operation of microgrids with risk-constrained state of charge", in *2021 European Control Conference (ECC)*, IEEE, Jun. 2021. DOI: 10.23919/ecc54610.2021.9655020 (cit. on p. 9).

[74] E. Kowsari, J. Zarei, R. Razavi-Far, M. Saif, T. Dragicevic, and M.-H. Khooban, "A novel stochastic predictive stabilizer for DC microgrids feeding CPLs", *IEEE Journal of Emerging and Selected Topics in Power Electronics*, vol. 9, no. 2, pp. 1222–1232, Apr. 2021. DOI: 10.1109/jestpe.2020.3008885 (cit. on p. 9).

[75] X. Wang, Y. Liu, L. Xu, J. Liu, and H. Sun, "A chance-constrained stochastic model predictive control for building integrated with renewable resources", *Electric Power Systems Research*, vol. 184, p. 106 348, Jul. 2020. DOI: 10.1016/j.epsr.2020.106348 (cit. on pp. 9, 21).

[76] Y. Zhang, F. Meng, R. Wang, W. Zhu, and X.-J. Zeng, "A stochastic MPC based approach to integrated energy management in microgrids", *Sustainable Cities and Society*, vol. 41, pp. 349–362, Aug. 2018. DOI: 10.1016/j.scs.2018.05.044 (cit. on p. 9).

[77] T. Namba, S. Funabiki, and K. Takaba, "Stochastic distributed model predictive control of microgrid with uncertain PV power prediction", *SICE Journal of Control, Measurement, and System Integration*, vol. 14, no. 1, pp. 39–50, Jan. 2021. DOI: 10.1080/18824889.2020.1863614 (cit. on p. 9).

[78] H. Zhuang, Z. Tang, and J. Zhang, "Two-stage energy management for energy storage system by using stochastic model predictive control approach", *Frontiers in Energy Research*, vol. 9, Dec. 2021. DOI: 10.3389/fenrg.2021.803615 (cit. on p. 9).

[79] M. M. Seron, G. C. Goodwin, and D. S. Carrasco, "Stochastic model predictive control: Insights and performance comparisons for linear systems", *International Journal of Robust and Nonlinear Control*, vol. 29, pp. 5038–5057, Apr. 2019, ISSN: 10498923. DOI: 10.1002/rnc.4106 (cit. on p. 10).

[80] M. Cannon, B. Kouvaritakis, and D. Ng, "Probabilistic Tubes in Linear Stochastic Model Predictive Control", *Systems & Control Letters*, vol. 58, no. 10, pp. 747–753, Oct. 2009. DOI: 10.1016/j.sysconle.2009.08.004 (cit. on pp. 10, 21).

[81] A. D. Bonzanini, D. B. Graves, and A. Mesbah, "Learning-based SMPC for reference tracking under state-dependent uncertainty: An application to atmospheric pressure plasma jets for plasma medicine", *IEEE Transactions on Control Systems Technology*, vol. 30, no. 2, pp. 611–624, Mar. 2022. DOI: 10.1109/tcst.2021.3069825 (cit. on p. 11).

[82] C. Beltran-Royo, "Two-stage stochastic mixed-integer linear programming: From scenarios to conditional scenarios", *Optimization-online*, pp. 1–30, Mar. 2018 (cit. on pp. 12, 58, 94).

[83] R. Azizipanah-Abarghooee, T. Niknam, M. Malekpour, F. Bavafa, and M. Kaji, "Optimal power flow based TU/CHP/PV/WPP coordination in view of wind speed, solar irradiance and load correlations", *Energy Conversion and Management*, vol. 96, pp. 131–145, May 2015. DOI: 10.1016/j.enconman.2014.12.070 (cit. on pp. 12, 86, 90).

[84] J. Zhang, D. Kong, Y. He, *et al.*, "Bi-layer energy optimal scheduling of regional integrated energy system considering variable correlations", *Interna-*

tional Journal of Electrical Power and Energy Systems, vol. 148, p. 108 840, Jun. 2023. DOI: 10.1016/j.ijepes.2022.108840 (cit. on pp. 12, 86, 90).

[85] A. R. Malekpour and A. Pahwa, "Stochastic networked microgrid energy management with correlated wind generators", *IEEE Transactions on Power Systems*, vol. 32, no. 5, pp. 3681–3693, Sep. 2017. DOI: 10.1109/tpwrs.2017.2650683 (cit. on pp. 12, 86, 90).

[86] C. Stene, "Analysis of correlations between energy consumption, structural specifications and climate-induced variables to increase energy efficiency in households and buildings through a prediction model", Master thesis, UiT The Arctic University of Norway, May 2021 (cit. on pp. 12, 86).

[87] A. Dobrzycki and J. Roman, "Correlation between the production of electricity by offshore wind farms and the demand for electricity in polish conditions", *Energies*, vol. 15, no. 10, pp. 1–18, May 2022. DOI: 10.3390/en15103669 (cit. on pp. 12, 86, 90).

[88] U. Maeder, F. Borrelli, and M. Morari, "Linear Offset-free Model Predictive Control", *Automatica*, vol. 45, no. 10, pp. 2214–2222, Oct. 2009. DOI: 10.1016/j.automatica.2009.06.005 (cit. on p. 17).

[89] F. Blanchini and S. Miani, *Set Theoretic Methods in Control*, 1st ed. Birkhäuser Boston, 2008, ISBN: 978-0-8176-3255-7. DOI: 10.1007/978-0-8176-4606-6 (cit. on p. 19).

[90] S. Boyd, L. El Ghaoui, E. Feron, and V. Balakrishnan, *Linear Matrix Inequalities in System and Control Theory*. Philadelphia, U.S.: Society for Industrial and Applied Mathematics, 1994, ISBN: 978-0-89871-485-2. DOI: 10.1137/1.9781611970777 (cit. on pp. 19, 33, 37, 54).

[91] M. V. Khlebnikov, B. T. Polyak, and V. M. Kuntsevich, "Optimization of Linear Systems Subject to Bounded Exogenous Disturbances: The Invariant Ellipsoid Technique", *Automation and Remote Control*, vol. 72, no. 11, pp. 2227–2275, Nov. 2011. DOI: 10.1134/s0005117911110026 (cit. on p. 19).

[92] X. Zhang, S. Grammatico, G. Schildbach, P. Goulart, and J. Lygeros, "On the sample size of randomized mpc for chance-constrained systems with application to building climate control", in *2014 European Control*

Conference (ECC), Strasbourg, France: IEEE, Jun. 2014, pp. 478–483, ISBN: 978-3-9524269-1-3. DOI: 10.1109/ecc.2014.6862498 (cit. on p. 21).

[93] S. Raimondi Cominesi, M. Farina, L. Giulioni, B. Picasso, and R. Scattolini, "A two-layer stochastic model predictive control scheme for microgrids", *IEEE Transactions on Control Systems Technology*, vol. 26, no. 1, pp. 1–13, Jan. 2018. DOI: 10.1109/tcst.2017.2657606 (cit. on p. 21).

[94] M. Y. Ramandi, N. Bigdeli, and K. Afshar, "Stochastic economic model predictive control for real-time scheduling of balance responsible parties", *International Journal of Electrical Power & Energy Systems*, vol. 118, p. 105 800, Jun. 2020. DOI: 10.1016/j.ijepes.2019.105800 (cit. on p. 21).

[95] P. Velarde, X. Tian, A. D. Sadowska, and J. M. Maestre, "Scenario-based hierarchical and distributed MPC for water resources management with dynamical uncertainty", *Water Resources Management*, vol. 33, no. 2, pp. 677–696, Nov. 2018. DOI: 10.1007/s11269-018-2130-2 (cit. on p. 21).

[96] J. Velasco, A. Liniger, X. Zhang, and J. Lygeros, "Efficient implementation of randomized MPC for miniature race cars", in *2016 European Control Conference (ECC)*, Aalborg, Denmark: IEEE, Jun. 2016, pp. 957–962, ISBN: 978-1-5090-2591-6. DOI: 10.1109/ecc.2016.7810413 (cit. on p. 21).

[97] J. L. Piovesan and H. G. Tanner, "Randomized model predictive control for robot navigation", in *2009 IEEE International Conference on Robotics and Automation*, Kobe, Japan: IEEE, May 2009, pp. 94–99, ISBN: 978-1-4244-2788-8. DOI: 10.1109/robot.2009.5152468 (cit. on p. 21).

[98] G. C. Goodwin and A. M. Medioli, "Scenario-based, closed-loop model predictive control with application to emergency vehicle scheduling", *International Journal of Control*, vol. 86, no. 8, pp. 1338–1348, Aug. 2013. DOI: 10.1080/00207179.2013.788215 (cit. on p. 21).

[99] F. A. Cuzzola, J. C. Geromel, and M. Morari, "An Improved Approach for Constrained Robust Model Predictive Control", *Automatica*, vol. 38, no. 7, pp. 1183–1189, Jul. 2002. DOI: 10.1016/s0005-1098(02)00012-2 (cit. on pp. 33, 34, 37).

[100] E. A. González Querubín, *Stochastic Model Predictive Control Toolbox. ver 1.0.4*, https://www.mathworks.com/matlabcentral/fileexchange/75803, Computer Software, Jun. 2020 (cit. on pp. 35, 116).

[101] B. Wie and D. S. Bernstein, "Benchmark problems for robust control design", *Journal of Guidance, Control, and Dynamics*, vol. 15, no. 5, pp. 1057–1059, Sep. 1992. DOI: 10.2514/3.20949 (cit. on p. 36).

[102] K. H. Johansson, B. T. Polyak, and V. M. Kuntsevich, "The Quadruple-Tank Process: A Multivariable Laboratory Process With an Adjustable Zero", *IEEE Transactions on Control Systems Technology*, vol. 8, no. 3, pp. 456–465, May 2000. DOI: 10.1109/87.845876 (cit. on p. 43).

[103] A. Numsomran, V. Tipsuwanporn, and K. Tirasesth, "Modeling of the Modified Quadruple-Tank Process", in *2008 SICE Annual Conference*, Tokyo, Japan: IEEE, Aug. 2008, pp. 818–823, ISBN: 978-4-907764-30-2. DOI: 10.1109/sice.2008.4654768 (cit. on p. 43).

[104] F. Blanchini, "Set invariance in control", *Automatica*, vol. 35, no. 11, pp. 1747–1767, Nov. 1999. DOI: 10.1016/S0005-1098(99)00113-2 (cit. on p. 53).

[105] C. Beltran-Royo, "Two-stage stochastic mixed-integer linear programming: The conditional scenario approach", *Omega*, vol. 70, pp. 31–42, Jul. 2017. DOI: 10.1016/j.omega.2016.08.010 (cit. on pp. 57, 94).

[106] C. Beltran-Royo, "Fast scenario reduction by conditional scenarios in two-stage stochastic MILP problems", *Optimization Methods and Software*, vol. 0, no. 0, pp. 1–22, Dec. 2019. DOI: 10.1080/10556788.2019.1697696 (cit. on p. 58).

[107] C. Beltran-Royo, "From scenarios to conditional scenarios in two-stage stochastic MILP problems", *International Transactions in Operational Research*, vol. 28, no. 2, pp. 660–686, Jul. 2020. DOI: 10.1111/itor.12851 (cit. on p. 58).

[108] A. J. Kleywegt, A. Shapiro, and T. Homem-de-Mello, "The sample average approximation method for stochastic discrete optimization", *SIAM Journal on Optimization*, vol. 12, no. 2, pp. 479–502, Jan. 2002. DOI: 10.1137/s1052623499363220 (cit. on p. 58).

[109] J. Dupačová, N. Gröwe-Kuska, and W. Römisch, "Scenario reduction in stochastic programming", *Mathematical Programming*, vol. 95, no. 3, Mar. 2003. DOI: 10.1007/s10107-002-0331-0 (cit. on p. 58).

[110] M. ApS, *The mosek optimization toolbox for matlab manual. version 9.0.* Sep. 2019 (cit. on pp. 70, 101).

[111] J. Löfberg, "Automatic robust convex programming", *Optimization Methods and Software*, vol. 27, no. 1, pp. 115–129, 2012. DOI: 10.1080/10556788.2010.517532 (cit. on p. 70).

[112] M. Kvasnica, B. Takács, J. Holaza, and D. Ingole, "Reachability analysis and control synthesis for uncertain linear systems in MPT", *IFAC-PapersOnLine*, vol. 48, no. 14, pp. 302–307, Oct. 2015. DOI: 10.1016/j.ifacol.2015.09.474 (cit. on p. 70).

[113] E. A. González Querubín, *Conditional Scenario-Based MPC. Version 1.0.2*, https://www.mathworks.com/matlabcentral/fileexchange/102224, Computer Software, Nov. 2021 (cit. on pp. 70, 118).

[114] I. Sansa and N. M. Bellaaj, "Forecasting and modelling of solar radiation for photovoltaic (pv) systems", in *Solar Radiation*, IntechOpen, Oct. 2021, ch. 4, pp. 1–17. DOI: 10.5772/intechopen.99499 (cit. on p. 88).

[115] M. Singh and S. Santoso, "Dynamic models for wind turbines and wind power plants", Tech. Rep., Oct. 2011, pp. 1–115. DOI: 10.2172/1028524 (cit. on p. 88).

[116] L. Luo, S. S. Abdulkareem, A. Rezvani, *et al.*, "Optimal scheduling of a renewable based microgrid considering photovoltaic system and battery energy storage under uncertainty", *Journal of Energy Storage*, vol. 28, p. 101 306, Apr. 2020. DOI: 10.1016/j.est.2020.101306 (cit. on p. 89).

[117] E. González, J. Sanchis, S. García-Nieto, and J. Salcedo, "A comparative study of stochastic model predictive controllers", *Electronics*, vol. 9, no. 12, p. 2078, Dec. 2020. DOI: 10.3390/electronics9122078 (cit. on pp. 91, 116).

[118] M. Shabani, E. Dahlquist, F. Wallin, and J. Yan, "Techno-economic impacts of battery performance models and control strategies on optimal de-

sign of a grid-connected PV system", *Energy Conversion and Management*, vol. 245, p. 114 617, Oct. 2021. DOI: 10.1016/j.enconman.2021.114617 (cit. on p. 95).

[119] H. J. Diamond, T. R. Karl, M. A. Palecki, *et al.*, "U.S. climate reference network after one decade of operations: Status and assessment", *Bulletin of the American Meteorological Society*, vol. 94, no. 4, pp. 485–498, Apr. 2013. DOI: 10.1175/bams-d-12-00170.1 (cit. on p. 101).

[120] UK Power Networks, *Smartmeter energy consumption data in london households*, https://data.london.gov.uk/dataset/smartmeter-energy-use-data-in-london-households, 2014 (cit. on p. 101).

[121] Red Eléctrica de España (REE), *Sistema de información del operador del sistema (E·SIOS)*, https://www.esios.ree.es, 2022 (cit. on p. 101).

[122] E. González, J. Sanchis, J. Salcedo, and M. Martínez, "Conditional scenario-based model predictive control", *Journal of the Franklin Institute*, vol. 360, no. 10, pp. 6880–6905, Jul. 2023. DOI: 10.1016/j.jfranklin.2023.05.012 (cit. on p. 118).

[123] E. González, J. Sanchis, J. Salcedo, and M. Martínez, "Conditional scenario-based energy management algorithm with uncertain correlated forecasts", *Journal of Energy Storage*, vol. 86, p. 111 177, May 2024. DOI: 10.1016/j.est.2024.111177 (cit. on p. 119).